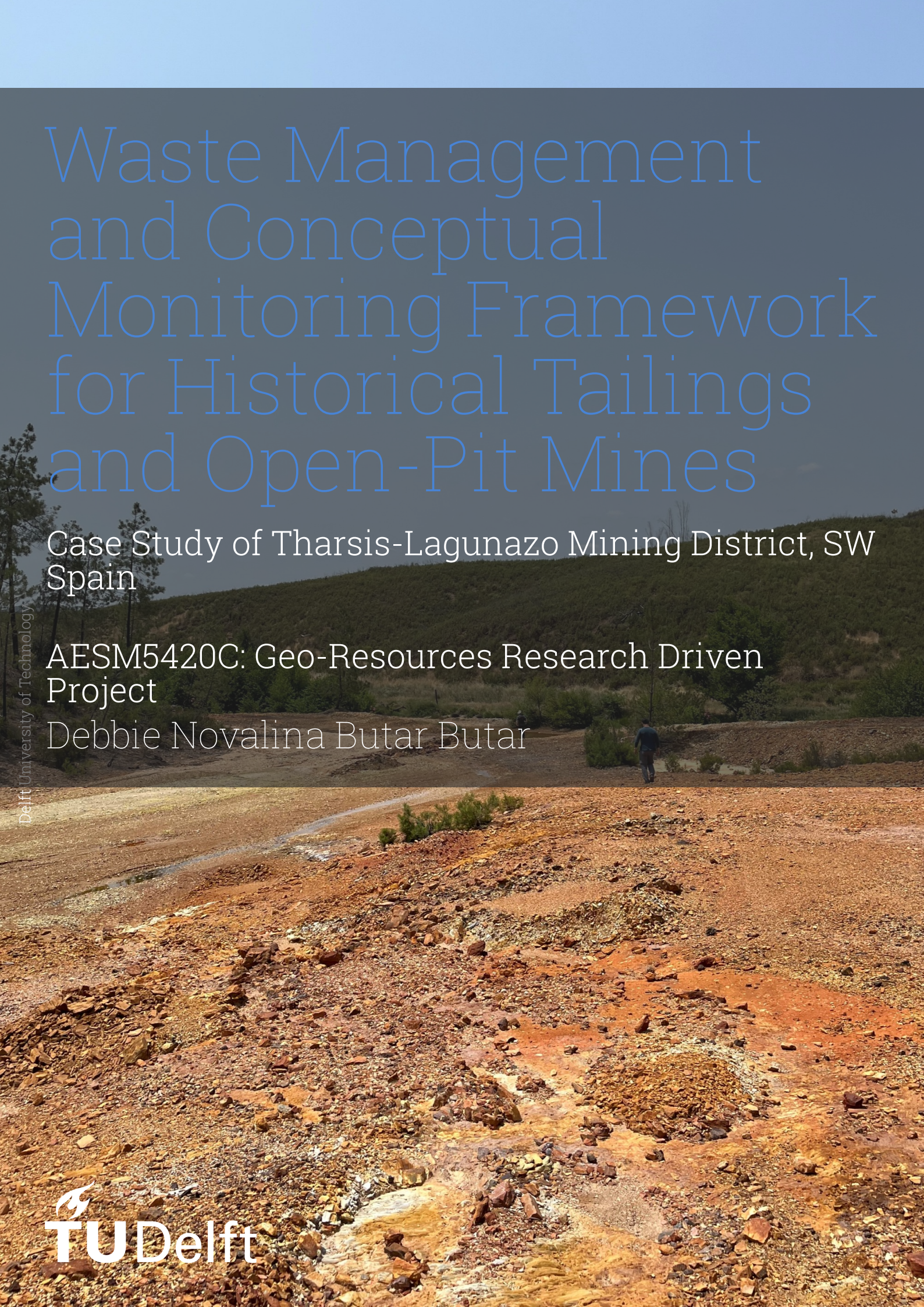
# Waste Management and Conceptual Monitoring Framework for Historical Tailings and Open-Pit Mines

## Case Study of Tharsis-Lagunazo Mining District, SW Spain

AESM5420C: Geo-Resources Research Driven Project

Debbie Novalina Butar Butar

Delft University of Technology



TU Delft

# Waste Management and Conceptual Monitoring Framework for Historical Tailings and Open-Pit Mines

## Case Study of Tharsis-Lagunazo Mining District, SW Spain

by

Debbie Novalina Butar Butar

6140467

AESM5420C

| | |
|---|---|
| Supervisor: | Dr. Feven Desta \| Dr. Mike Buxton |
| Project Duration: | August 2025 – October 2025 |
| Faculty: | Civil Engineering and Geosciences |

Cover: Mine Tailings, taken from Geo-Resources B-Module Fieldtrip, Iberian Pyrite Belt, Spain, June 2025

TU Delft

# Abstract

This study evaluates the environmental risks associated with the Tharsis-Lagunazo mining district located in the Iberian Pyrite Belt (IPB) of southwestern Spain. It primarily focuses on two key issues: acid mine drainage (AMD) and slope instability. The study proposes an integrated conceptual framework for waste management and monitoring. To achieve this, the study combines geological mapping, geochemical analysis, and hydrogeological interpretation with geotechnical slope assessments and satellite-based remote sensing. This multi-method approach effectively identifies sources of hazards, transport pathways, and sensitive environmental receptors. In addition, a multi-criteria decision analysis (MCDA) was utilized to rank critical variables for effective monitoring and site management.

Results indicate that hydrological dynamics and water chemistry are the primary controls on environmental risk. AMD generation and transport are strongly influenced by rainfall seasonality, evaporation rates, and drainage system connectivity. Key chemical indicators of AMD intensity include pH, electrical conductivity, and concentrations of Fe, Cu, and Zn. Both the Lagunazo and Mina Tharsis sites contain multiple hazard sources, such as tailings, seepage zones, and acidic pit lakes that are directly connected to downstream reservoirs. The highest contamination risks occur during rainfall events following dry periods.

Geotechnical risks are site-specific in the study area. They are mostly found at steep, weathered pit walls at Tharsis, which increase erosion and sediment delivery, while fine-grained, low-permeability tailings at Lagunazo facilitate water ponding and prolonged chemical reactions. Remote sensing proved effective for spatial screening, enabling delineation of zones affected by AMD. This integrated framework establishes clear priorities for monitoring and supports targeted rehabilitation and risk-reduction measures for abandoned mining districts, such as in Tharsis-Lagunazo.

**keywords:** *mine waste, mining, spain, tharsis, lagunazo, iberian pyrite belt*

# Contents


Preface i

Nomenclature viii

1 Introduction 1
- 1.1 Problem statement . . . 1
- 1.2 Objectives and specific objectives . . . 1
- 1.3 Research questions . . . 2
- 1.4 Report structure . . . 2

2 Literature Review 3
- 2.1 Tharsis-Lagunazo mining area . . . 3
- 2.2 Definition of Key Variables . . . 3
- 2.3 Environmental risks from tailings . . . 4
- 2.4 Remote sensing for monitoring mine waste . . . 5

3 Methodology 6
- 3.1 Study sites . . . 6
  - 3.1.1 Geology . . . 7
  - 3.1.2 Physiography of Tharsis and Lagunazo sites . . . 8
- 3.2 Data sources . . . 9
  - 3.2.1 Primary data . . . 9
  - 3.2.2 Secondary data . . . 9
- 3.3 Software and tools . . . 9

4 Results 10
- 4.1 Geology . . . 10
  - 4.1.1 Geochemical analysis . . . 10
- 4.2 Geotechnical analysis . . . 15
  - 4.2.1 Slope analysis . . . 16
  - 4.2.2 Potential local seismicity in Tharsis–Lagunazo . . . 17
  - 4.2.3 Geotechnical anomaly and risk classification . . . 17
- 4.3 Hydrogeological analysis . . . 18
  - 4.3.1 Flow frequency and seepage type in the Tharsis-Lagunazo system . . . 19
  - 4.3.2 pH of streams and receiving waters . . . 19
  - 4.3.3 Hydrogeology of Lagunazo . . . 19
  - 4.3.4 Hydrogeology of Mina Tharsis . . . 19
- 4.4 AMD risk zones . . . 20
  - 4.4.1 AMD environmental contamination risk in Lagunazo . . . 20
  - 4.4.2 AMD environmental contamination risk in Mina Tharsis . . . 20
- 4.5 Remote sensing analysis . . . 21
  - 4.5.1 Spatial and temporal changes of Tharsis Lagunazo areas (2004-2023) . . . 21
  - 4.5.2 Tailings and surface water indicators . . . 24
  - 4.5.3 Vegetation change and environmental impacts . . . 25
- 4.6 Land use management of Tharsis-Lagunazo . . . 26
- 4.7 Critical variables of Tharsis and Lagunazo . . . 26
- 4.8 Waste management and rehabilitation strategies . . . 28
  - 4.8.1 Lagunazo waste management and rehabilitation strategies . . . 28
  - 4.8.2 Tharsis waste management and rehabilitation strategies . . . 29
- 4.9 Conceptual monitoring framework for Tharsis-Lagunazo . . . 30
  - 4.9.1 Geotechnical monitoring . . . 30

4.9.2 Hydrological monitoring . . . 31
4.9.3 Geochemical monitoring . . . 31
4.9.4 Remote sensing and spatial analytics . . . 31
4.9.5 Monitoring placement . . . 31
4.9.6 Monitoring tools and deployment priority . . . 31
4.9.7 Key gaps and actions . . . 32
4.9.8 Implementation plan . . . 32

**5 Discussions** **34**
5.1 Discussions . . . 34
5.1.1 Geological, geotechnical, hydrological, and geochemical factors . . . 34
5.1.2 Effectiveness of monitoring tools . . . 34
5.1.3 Integration into a conceptual monitoring framework . . . 35
5.1.4 Environmental rehabilitation plan and implications . . . 35
5.2 Limitations . . . 36
5.3 Future recommendations . . . 36

**6 Conclusion** **37**
6.1 Main research question . . . 37
6.1.1 Sub–research question 1 . . . 37
6.1.2 Sub–research question 2 . . . 37
6.1.3 Sub–research question 3 . . . 37
6.1.4 Sub–research question 4 . . . 38

**A Geochemical Results** **44**

# List of Figures


3.1 Location of the study area showing the Mina Tharsis and Lagunazo tailings in southwestern Spain (left), and their position within Spain (right). . . . 7
3.2 Regional geology map of Lagunazo and Mina Tharsis. Source: IGME, Mapa Geologico de Espana (MAGNA 50). . . . 7
3.3 Lagunazo mine waste morphology (derived from MDT02 dataset and processed using Surfer). . . . 8
3.4 Tharsis mine waste morphology and (derived from MDT02 dataset and processed using Surfer). . . . 8

4.1 Sampling locations for XRF geochemical analysis at Lagunazo. . . . 12
4.2 Geochemical characterization of As at Lagunazo. . . . 13
4.3 Pb spatial distribution map at Lagunazo. . . . 13
4.4 Cd spatial distribution map at Lagunazo. . . . 14
4.5 Cu spatial distribution map at Lagunazo. . . . 15
4.6 Geochemical characterization of Zn at Lagunazo. . . . 15
4.7 Slope distribution in the Lagunazo tailings area, derived from DEM analysis. Steeper slopes are concentrated along ridges and mine waste dumps, while gentler slopes dominate the tailings impoundment. . . . 16
4.8 Slope map of the Mina Tharsis, showing slope classes derived from DEM analysis. Steep slopes are concentrated along pit walls and mine waste dumps, while gentler slopes characterize the surrounding terrain. . . . 17
4.9 Satellite image of the Tharsis-Lagunazo mining district (October 2004). . . . 22
4.10 Satellite image of the Tharsis-Lagunazo mining district (June 2011). . . . 22
4.11 Satellite image of the Tharsis-Lagunazo mining district (April 2013). . . . 23
4.12 Satellite image of the Tharsis-Lagunazo mining district (June 2016). . . . 23
4.13 Satellite image of the Tharsis-Lagunazo mining district (May 2019) . . . 24
4.14 Satellite image of the Tharsis-Lagunazo mining district (November 2023). . . . 24
4.15 NDWI classification map at Tharsis-Lagunazo (retrieved and analyzed from Sentinel-2 Level-2A). . . . 25
4.16 NDVI classification map at Tharsis-Lagunazo (retrieved and analyzed from Sentinel-2 Level-2A). . . . 25
4.17 Land use map of the Tharsis-Lagunazo mining district (maps retrieved and modified by author from CLC2018). . . . 26
4.18 KVG Weighted Scores and Ranking for Lagunazo and Tharsis . . . 28

A.1 Groundwater Elemental Concentrations in Huelva . . . 44
A.2 Topsoil Elemental Concentrations in Huelva . . . 44
A.3 Sediment Elemental Concentrations in Huelva . . . 45
A.4 Elemental concentrations for Lagunazo Tailings (sample LA 24-1) . . . 45
A.5 Elemental concentrations for Lagunazo Tailings (sample LA 24-2) . . . 45
A.6 Elemental concentrations for Lagunazo Tailings (sample LA 24-3) . . . 46
A.7 Elemental concentrations for Lagunazo Tailings (sample LA 24-4) . . . 46
A.8 Elemental concentrations for Lagunazo Tailings (sample LA 24-5) . . . 46
A.9 Elemental concentrations for Lagunazo Tailings (sample LA 24-6) . . . 47
A.10 Elemental concentrations for Lagunazo Tailings (sample LA 24-7) . . . 47
A.11 Elemental concentrations for Lagunazo Tailings (sample LA 24-8) . . . 47
A.12 Elemental concentrations for Lagunazo Tailings (sample LA 24-9) . . . 48
A.13 Elemental concentrations for Lagunazo Tailings (sample LA 24-10) . . . 48
A.14 Elemental concentrations for Lagunazo Tailings (sample LA 24-11) . . . 48

A.15 Elemental concentrations for Lagunazo Tailings (sample LA 24-12) . . . . . 49
A.16 Elemental concentrations for Lagunazo Tailings (sample LA 24-13) . . . . . 49
A.17 Elemental concentrations for Lagunazo Tailings (sample LA 24-14) . . . . . 49
A.18 Elemental concentrations for Lagunazo Tailings (sample LA 24-15) . . . . . 50
A.19 Elemental concentrations for Lagunazo Tailings (sample LA 24-16) . . . . . 50
A.20 Elemental concentrations for Lagunazo Tailings (sample LA 24-17) . . . . . 50
A.21 Elemental concentrations for Lagunazo Tailings (sample LA 24-18) . . . . . 51
A.22 Elemental concentrations for Lagunazo Tailings (sample LA 24-19) . . . . . 51
A.23 Elemental concentrations for Lagunazo Tailings (sample LA 24-20) . . . . . 51
A.24 Elemental concentrations for Lagunazo Tailings (sample LA 24-21) . . . . . 52
A.25 Elemental concentrations for Lagunazo Tailings (sample LA 24-22) . . . . . 52
A.26 Elemental concentrations for Lagunazo Tailings (sample LA 24-23) . . . . . 52
A.27 Elemental concentrations for Lagunazo Tailings (sample LA 24-24) . . . . . 53
A.28 Elemental concentrations for Lagunazo Tailings (sample LA 24-25) . . . . . 53
A.29 Elemental concentrations for Lagunazo Tailings (sample LA 24-26) . . . . . 53
A.30 Elemental concentrations for Lagunazo Tailings (sample LA 24-27) . . . . . 54
A.31 Elemental concentrations for Lagunazo Tailings (sample LA 24-28) . . . . . 54
A.32 Elemental concentrations for Lagunazo Tailings (sample LA 24-29) . . . . . 54
A.33 Elemental concentrations for Lagunazo Tailings (sample LA 24-30) . . . . . 55
A.34 Elemental concentrations for Lagunazo Tailings (sample LA 24-31) . . . . . 55
A.35 Elemental concentrations for Lagunazo Tailings (sample LA 24-32) . . . . . 55
A.36 Elemental concentrations for Lagunazo Tailings (sample LMW-1) . . . . . 56
A.37 Elemental concentrations for Lagunazo Tailings (sample LMW-2) . . . . . 56
A.38 Elemental concentrations for Lagunazo Tailings (sample LMW-3) . . . . . 56
A.39 Elemental concentrations for Lagunazo Tailings (sample LMW-4) . . . . . 57
A.40 Elemental concentrations for Lagunazo Tailings (sample LMW-5) . . . . . 57
A.41 Elemental concentrations for Lagunazo Tailings (sample LMW-6) . . . . . 57
A.42 Elemental concentrations for Lagunazo Tailings (sample LMW-7) . . . . . 58
A.43 Elemental concentrations for Lagunazo Tailings (sample LMW-8) . . . . . 58
A.44 Elemental concentrations for Lagunazo Tailings (sample LMW-10) . . . . . 58
A.45 Elemental concentrations for Lagunazo Tailings (sample LMW-11) . . . . . 59
A.46 Elemental concentrations for Lagunazo Tailings (sample LMW-12) . . . . . 59
A.47 Elemental concentrations for Lagunazo Tailings (sample LMW-13) . . . . . 59
A.48 Elemental concentrations for Lagunazo Tailings (sample LMW-14) . . . . . 60
A.49 Elemental concentrations for Lagunazo Tailings (sample LMW-15) . . . . . 60
A.50 Elemental concentrations for Lagunazo Tailings (sample LMW-16) . . . . . 60
A.51 Elemental concentrations for Lagunazo Tailings (sample LMW-17) . . . . . 61
A.52 Elemental concentrations for Lagunazo Tailings (sample LMW-18) . . . . . 61
A.53 Elemental concentrations for Lagunazo Tailings (sample LMW-19) . . . . . 61
A.54 Elemental concentrations for Lagunazo Tailings (sample LMW-20) . . . . . 62
A.55 Elemental concentrations for Lagunazo Tailings (sample LMW-21) . . . . . 62
A.56 Elemental concentrations for Lagunazo Tailings (sample LMW-22) . . . . . 62
A.57 Elemental concentrations for Lagunazo Tailings (sample LMW-23) . . . . . 63
A.58 Elemental concentrations for Lagunazo Tailings (sample LMW-24) . . . . . 63
A.59 Elemental concentrations for Lagunazo Tailings (sample MM-1) . . . . . 63
A.60 Elemental concentrations for Lagunazo Tailings (MM-2) . . . . . 64
A.61 Elemental concentrations for Lagunazo Tailings (MM-3) . . . . . 64
A.62 Elemental concentrations for Lagunazo Tailings (MM-4) . . . . . 64
A.63 Elemental concentrations for Lagunazo Tailings (MM-5) . . . . . 65
A.64 Elemental concentrations for Lagunazo Tailings (MM-6) . . . . . 65
A.65 Elemental concentrations for Lagunazo Tailings (MM-7) . . . . . 65
A.66 Elemental concentrations for Lagunazo Tailings (MM-8) . . . . . 66
A.67 Elemental concentrations for Lagunazo Tailings (MM-9) . . . . . 66
A.68 Elemental concentrations for Lagunazo Tailings (MM-12) . . . . . 66
A.69 Elemental concentrations for Lagunazo Tailings (MM-13) . . . . . 67
A.70 Elemental concentrations for Lagunazo Tailings (MM-14) . . . . . 67

**A.71 Elemental concentrations for Lagunazo Tailings (MM-15)** . . . . . 67
**A.72 Elemental concentrations for Lagunazo Tailings (MM-16)** . . . . . 68
**A.73 Elemental concentrations for Lagunazo Tailings (MM-17)** . . . . . 68
**A.74 Elemental concentrations for Lagunazo Tailings (MM-18)** . . . . . 68
**A.75 Elemental concentrations for Lagunazo Tailings (MM-19)** . . . . . 69
**A.76 Elemental concentrations for Lagunazo Tailings (MM-20)** . . . . . 69
**A.77 Elemental concentrations for Lagunazo Tailings (MM-21)** . . . . . 69
**A.78 Elemental concentrations for Lagunazo Tailings (MM-22)** . . . . . 70
**A.79 Elemental concentrations for Lagunazo Tailings (MM-24)** . . . . . 70
**A.80 Elemental concentrations for Lagunazo Tailings (MM-25)** . . . . . 70
**A.81 Elemental concentrations for Lagunazo Tailings (MM-26)** . . . . . 71
**A.82 Elemental concentrations for Lagunazo Tailings (MM-27)** . . . . . 71
**A.83 Elemental concentrations for Lagunazo Tailings (MM-28)** . . . . . 71
**A.84 Elemental concentrations for Lagunazo Tailings (MM-31)** . . . . . 72
**A.85 Elemental concentrations for Lagunazo Tailings (MM-32)** . . . . . 72
**A.86 Elemental concentrations for Lagunazo Tailings (MM-33)** . . . . . 72
**A.87 Elemental concentrations for Lagunazo Tailings (MM-34)** . . . . . 73
**A.88 Elemental concentrations for Lagunazo Tailings (MM-35)** . . . . . 73

# List of Tables


2.1 KVGs and KVs required for TSFs monitoring (adopted from D3.2 GAIA-TSF report) 4

4.1 Indicators and screening scores for geotechnical anomaly/risk classification (adopted from Chovan and Itasca, 2021). . . . . 18
4.2 Screening classification of geotechnical anomalies and risks in Tharsis-Lagunazo. 18
4.3 MCDA scores for Key Variables (KVs) at Lagunazo and Tharsis. . . . . 27
4.4 MCDA scores for KVGs at Lagunazo and Tharsis. . . . . 27
4.5 Surface areas and volumes of Lagunazo and Tharsis mine wastes (calculated using MDT02 datasets and the grid volume computation method). . . . . 28
4.6 Monitoring tools technology and deployment priority. . . . . 31
4.7 Monitoring tools readiness gaps and actions. . . . . 32

# Nomenclature

## Abbreviations

| Abbreviation | Definition |
|---|---|
| AMD | Acid Mine Drainage |
| CRI | Composite Risk Index |
| DEM | Digital Elevation Model |
| DTM | Digital Terrain Model |
| EC | Electrical Conductivity |
| EU | European Union |
| FoS | Factor of Safety |
| GISTM | Global Industry Standard on Tailings Management |
| ICMM | International Council on Mining and Metals |
| IDW | Inverse Distance Weighting |
| IGME | Instituto Geológico y Minero de España |
| IPB | Iberian Pyrite Belt |
| KV | Key Variables |
| KVG | Key Variable Groups |
| LiDAR | Light Detection and Ranging |
| MCDA | Multi-Criteria Decision Analysis |
| MDT | Modelo Digital del Terreno |
| MITECO | Ministerio para la Transición Ecológica y el Reto Demográfico |
| ML | Machine Learning |
| NDVI | Normalized Difference Vegetation Index |
| NDWI | Normalized Difference Water Index |
| OLD | Open Limestone Drain |
| TSF | Tailings Storage Facilities |
| XRF | X-ray Fluorescence |
| WHO | World Health Organization |

## Elemental symbols

| Element | Definition |
|---|---|
| Ag | Silver |
| As | Arsenic |
| Au | Gold |
| Cd | Cadmium |
| Cr | Chromium |
| Cu | Copper |
| Fe | Iron |
| Hg | Mercury |
| Mn | Manganese |
| Mo | Molybdenum |
| Ni | Nickel |
| Pb | Lead |
| Zn | Zinc |

# 1

# Introduction

## 1.1. Problem statement

The Tharsis-Lagunazo mining area is located in Huelva Province, southwestern Spain, within the Spanish part of the Iberian Pyrite Belt (IPB). The IPB extends across southern Spain and Portugal and is recognized for its rich Volcanogenic Massive Sulfide (VMS) deposits containing pyrite, chalcopyrite, sphalerite, and galena. Mining in the Tharsis-Lagunazo district began during Roman times and expanded significantly in the 19th and 20th centuries due to the growing demand for copper and sulfur. Early mining focused on gossan ores, the oxidized caps of massive sulfide bodies, which also contain valuable amounts of gold and silver [77, 83, 84].

Centuries of mining have left behind extensive environmental impacts, including large tailings deposits, waste rock piles, and open pits. These materials remain exposed to air and water, leading to ongoing Acid Mine Drainage (AMD) formation. The presence of mine heaps, gossan, and slag deposits has created a rugged landscape with acidic soils and high concentrations of metals and sulfates. These conditions vary seasonally, influenced by rainfall, evaporation, and temperature changes.

The Tharsis mine is among the largest and most environmentally affected sites in the IPB. Of its five open pits, four are now flooded with acidic water [84]. The total area disturbed by mining covers about 394 hectares, including tailings, pit lakes, waste heaps, and surrounding soils. Since the closure of mining operations in 2001, the lack of environmental controls has led to a decline in water quality and increased contamination. Recent studies show that AMD in the Tharsis region changes with the seasons, with higher concentrations of iron, aluminum, and sulfates during dry periods and lower levels during the wet season [53].

These environmental problems continue to threaten nearby ecosystems, surface waters, and groundwater. Understanding how these impacts evolve spatially and temporally is essential for designing effective monitoring systems and supporting future rehabilitation or re-mining in the area.

## 1.2. Objectives and specific objectives

This study is guided by the following objectives:

1. Identify the geological, geotechnical, hydrological, and geochemical factors that play the most important roles in determining environmental risks in the Tharsis-Lagunazo district.
2. Evaluate how effectively different monitoring tools, such as in-situ sensors, remote sensing data, and geochemical surveys, can detect and track these risks, and assess their readiness for application at Tharsis–Lagunazo.
3. Integrate field observations, laboratory analyses, and satellite-based data into a conceptual monitoring framework that supports waste management and long-term environmental rehabilitation planning.

4. Develop a phased plan for environmental rehabilitation, outlining short-, medium-, and long-term actions that align with monitoring results.

## 1.3. Research questions

**Main research question:**

*How can a conceptual monitoring framework improve the understanding of environmental risks, guide cost-effective management decisions, and support phased rehabilitation in the Tharsis–Lagunazo mining area?*

To address the main research question, the following sub-research questions are formulated:

1. Which key factors (geological, geotechnical, hydrological, and geochemical) have the greatest influence on environmental risks at Lagunazo and Mina Tharsis?
2. How suitable and ready are different monitoring tools for detecting and tracking these factors, and how can they be combined into an integrated monitoring system?
3. How can field observations, laboratory analyses, and satellite-based data be integrated into a conceptual monitoring framework that supports waste management and long-term environmental rehabilitation planning?
4. How can rehabilitation activities be prioritized and phased over time based on environmental risk levels?

## 1.4. Report structure

This report is structured into six main chapters, each addressing a specific aspect of the study.

**Chapter 1: Introduction** presents an overview of the study, including the problem statement, objectives, and research questions. It also outlines the report's structure to guide the reader through the following chapters.

**Chapter 2: Literature review** provides the background and theoretical foundation of the study. It introduces the Tharsis–Lagunazo mining area, defines the Key Variable Groups (KVGs) relevant to Tailings Storage Facility (TSF) monitoring, and discusses the main environmental risks associated with mine tailings. The chapter also reviews current applications of remote sensing techniques in mine waste monitoring.

**Chapter 3: Methodology** explains the approach and procedures used in the study. It describes the study sites, data sources, and the software tools applied for analysis. This chapter also outlines the methods used to process and interpret geological, geotechnical, hydrogeological, and remote sensing data.

**Chapter 4: Results** presents the main findings of the study. It includes analyses of geological, geotechnical, hydrogeological, and AMD conditions in the Tharsis–Lagunazo area. The chapter further discusses remote sensing results, land use characteristics, critical monitoring variables, and proposed waste management and rehabilitation strategies. It introduces a conceptual monitoring framework and recommendations for monitoring placement, tools, and implementation.

**Chapter 5: Discussion** interprets the results in relation to the research objectives and existing literature. It highlights key insights, discusses study limitations, and provides practical recommendations for improving TSF monitoring and management.

**Chapter 6: Conclusion** summarizes the main findings and provides answers to the research questions.

# 2

# Literature Review

## 2.1. Tharsis-Lagunazo mining area

The Tharsis–Lagunazo mining district is located in Huelva Province, southwestern Spain, within the central part of IPB. The IPB extends across southern Spain and Portugal and hosts numerous polymetallic deposits rich in pyrite, chalcopyrite, sphalerite, and galena [69, 78]. Mining in the Tharsis-Lagunazo area began in Roman times and peaked during the 19th and 20th centuries, producing large amounts of copper and sulfur-bearing minerals [44]. Centuries of mining have left behind extensive environmental legacies, including open pits, waste rock piles, and tailings deposits.

The area lies within environmentally sensitive watersheds with interconnected surface-water systems and shallow aquifers, which increase the risk of contaminant dispersion into nearby ecosystems and agricultural land. The oxidation of sulfide-rich tailings and waste materials has generated AMD, leading to persistent metal contamination in soils and waters [8, 73]. Studies show that drainage from the Tharsis mine contains high concentrations of iron (Fe), copper (Cu), zinc (Zn), and sulfate ($SO_4^{2-}$), with strong seasonal variability driven by rainfall and evaporation cycles [58]. The persistence of AMD decades after mine closure highlights the long-term reactivity of mine waste in the IPB.

Climatic and geomorphological factors further influence contamination processes. The Mediterranean climate promotes alternating oxidation and flushing cycles that enhance metal mobility [72]. At Lagunazo, flat terrain and low-permeability tailings favor ponding and slow drainage, while Tharsis shows steep slopes, erodible pit walls, and acidic pit lakes. These contrasting conditions create distinct environmental risks that require site-specific management and monitoring strategies.

The Tharsis–Lagunazo district, therefore, presents both a challenge and an opportunity for applying integrated mine rehabilitation practices. Combining remote sensing, geochemical, and hydrological data allows for better characterization of contamination pathways and environmental changes. Remote sensing tools such as Sentinel-1 and Sentinel-2 provide valuable information on surface water, vegetation stress, and terrain changes, while geochemical surveys help track AMD and metal dispersion. Together, these methods support a more detailed understanding of environmental dynamics and can guide sustainable remediation planning. This integrated approach aligns with current European strategies promoting digital monitoring and adaptive mine closure management [23, 66].

## 2.2. Definition of Key Variables

This study adopts the Key Variables (KVs) defined in the D3.2 report of the GAIA-TSF Key Variable Definition Analysis. Each variable is organized into Key Variable Groups (KVGs) according to its characteristics.

The classification of KVGs was based on stakeholder priorities, aligned with industry standards and best practices. Four KVGs were identified as the primary parameters for developing a monitoring system for TSFs: KVG1 (Geological and Geomorphological), KVG2 (Hydro-Meteorological), KVG3

(Geotechnical), and KVG4 (Socio-Environmental). The detailed KVGs and their corresponding KVs are presented in **Table 2.1**.

**Table 2.1:** KVGs and KVs required for TSFs monitoring (adopted from D3.2 GAIA-TSF report)

| | |
|---|---|
| **KVG 1: Geological & Geomorphological** | GEO.1 Seismic ground movement<br>GEO.2 Topographic uplift/subsidence<br>GEO.3 Slope stability<br>GEO.4 Channel migration |
| **KVG 2: Hydro-Meteorological** | HM.1 Water level/phreatic surface<br>HM.2 Evaporation<br>HM.3 Temperature<br>HM.4 Wind direction/speed<br>HM.5 Rainfall<br>HM.6 Extreme weather events |
| **KVG 3: Geotechnical** | GT.1 Pore-pressure/uplift<br>GT.2 Internal movement/sliding<br>GT.3 Siltation<br>GT.4 Bulk density<br>GT.5 Permeability/porosity<br>GT.6 Thermal properties<br>GT.7 Cohesion and friction angle<br>GT.8 Wall thickness and height<br>GT.9 Construction material quality<br>GT.10 Cracks and fractures<br>GT.11 Maintenance history |
| **KVG 4: Socio-Environmental** | SE.1 Water quality<br>SE.2 Geochemistry and mineralogy<br>SE.3 Air pollution<br>SE.4 Biodiversity<br>SE.5 Anthropogenic activities<br>SE.6 Public health<br>SE.7 Community awareness |

The identification and classification of KVGs is fundamental for the effective monitoring and management of TSFs. Each KVG represents a clear domain of physical, environmental, and operational parameters that collectively define the stability and performance of a tailings system. By categorizing variables into KVGs, we can systematically identify and prioritize the most critical factors, and therefore enable targeted monitoring strategies and risk mitigation measures to each site's characteristics and conditions.

## 2.3. Environmental risks from tailings

Previous studies confirmed with field observation in Lagunazo and Tharsis reveal them to comprise different sources of mine waste. At Lagunazo, it consists of tailings, slag, and waste rock, while in Mina Tharsis it consists of waste dumps, tailings, slag heaps with residual metals, and AMD. The exposure of the waste to the effect of interaction with rainwater poses threats to the surrounding environment.

Tailings and waste from sulfide-rich mining, particularly in open-pit operations, often generate AMD. AMD is acidic water formed when sulfide minerals (mainly pyrite) are exposed to oxygen and water. This process lowers pH levels and mobilizes hazardous metals, such as iron (Fe), copper (Cu), arsenic (As), cadmium (Cd), and zinc (Zn), which can pollute soil, surface water, and groundwater systems [82].

The severity of AMD impacts lies in its persistence in the environment. Once started, AMD generation can continue for decades after mining ceases, unless effective mitigation measures are taken. AMD is widely recognized as one of the most serious and long-lasting environmental legacies of mining. It causes not only ecological degradation, but also risks to agriculture and human health in downstream communities. For example, AMD have been linked to biodiversity loss in rivers, contamination of drinking water supplies, and soil degradation in mining regions across Europe [62].

In addition to chemical contamination, untreated tailings can also pose physical risks. These include dust emissions during dry seasons, slope instabilities, and the potential for catastrophic dam failures.

One major example in Spain is the Aznalcollar accident in 1998, which released millions of cubic meters of acidic sludge into the Donana National Park in southern Spain [32]. These risks highlight the need for systematic monitoring approaches that can address both chemical and physical hazards associated with historical mine waste.

## 2.4. Remote sensing for monitoring mine waste

Remote sensing technology provides a broad, efficient, and non-invasive means of observing and monitoring mine-affected areas. In areas like Tharsis-Lagunazo with a long history of mining, remote sensing technology can be used to analyze spatial and temporal changes of the area, in accordance with mining-related activities and land-cover changes, as well as their implication for the environment.

Remote sensing technology, such as airborne and satellite hyperspectral imagery, has been successfully used to detect mineralogical changes on tailings surfaces, enabling the estimation of acid-generating potential and mapping of contamination zones. These techniques also support seasonal monitoring of environmental indicators, such as moisture distribution, vegetation stress, and secondary mineral precipitates. These are factors that are relevant in semi-arid regions impacted by historical mining [70].

Recent advances in multi-scale approaches have strengthened the role of remote sensing in AMD studies. By utilizing high-resolution data combined with satellite imagery, we can capture both local details and regional trends, thereby enhancing our ability to detect AMD seeps, vegetation anomalies, and changes in water quality. In addition, the spatial resolution of the sensors used greatly influences monitoring effectiveness, with high-resolution data proving essential in complex mine waste environments [13].

Furthermore, integration of optical, thermal, and radar datasets has expanded monitoring capabilities. For example, radar interferometry (e.g., InSAR) can be applied to detect ground deformation in tailings dams, while multispectral vegetation indices, such as Normalized Difference Vegetation Index (NDVI), Normalized Difference Water Index (NDWI), can indicate contamination through stress signals in surrounding ecosystems [67]. These multi-source approaches make remote sensing a powerful tool for long-term environmental monitoring of legacy mining areas.

# 3

# Methodology

The methodological framework integrates study site selection, geospatial and analytical software, and multi-source datasets to enable a comprehensive assessment of the spatial and temporal changes in mine wastes at Tharsis-Lagunazo, and their impact on the surrounding environment.

## 3.1. Study sites

The study area is located within the Tharsis-Lagunazo mining district in Huelva Province, southwestern Spain (see **Figure 3.1**). This region includes the Lagunazo tailings deposit, the open-pit mines of the Tharsis mining complex, and the surrounding land and water systems. The total study area covers approximately 42.3 $km^2$.

The Tharsis-Lagunazo district features a diverse landscape of land uses and surface conditions, including active and abandoned mine sites, waste storage areas, natural vegetation, agricultural land, and water bodies. These characteristics make it an appropriate area for assessing environmental risks, developing monitoring strategies, and supporting rehabilitation planning related to historical mining activities.

The study area was selected to capture the main environmental and geotechnical features of the Tharsis-Lagunazo mining district. It includes the Lagunazo tailings deposit, several abandoned open pits at Tharsis that now form acidic pit lakes, and nearby reservoirs and agricultural land. This boundary was selected to ensure that the study encompasses the primary mine wastes and the potential extent of AMD generation, the pathways of metal transport through water bodies, and the surrounding land-use systems affected by mining. The area is large enough to capture the full range of mining-related impacts while remaining manageable for detailed spatial, geochemical, and remote-sensing analyses.

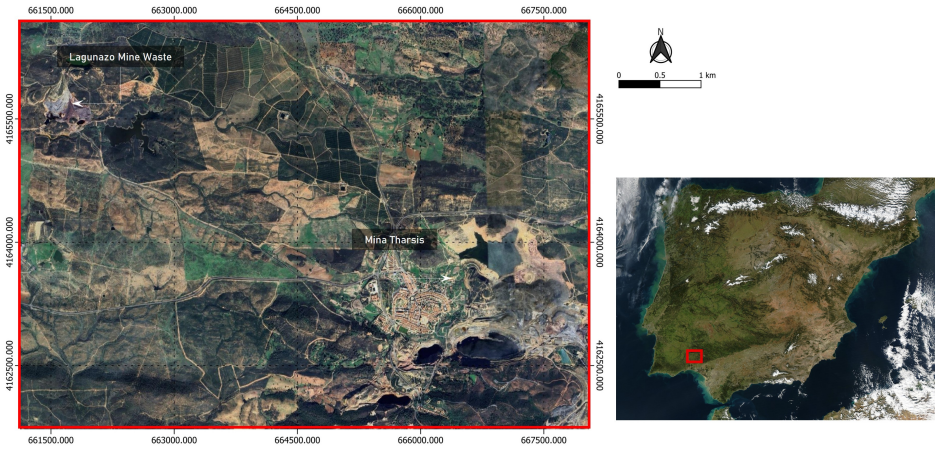



**Figure 3.1:** Location of the study area showing the Mina Tharsis and Lagunazo tailings in southwestern Spain (left), and their position within Spain (right).

### 3.1.1. Geology

The Tharsis-Lagunazo mining district lies within the central part of the IPB, one of the largest volcanic-sedimentary massive sulfide provinces in the world. The IPB is composed mainly of Devonian to Carboniferous volcanic and sedimentary rocks, dominated by felsic to intermediate volcanic sequences and associated shales. These rocks host numerous VMS deposits that contain pyrite, chalcopyrite, sphalerite, and galena. The stratigraphy is cut by dense sets of faults and thrusts that localize ore bodies and control present-day drainage (see **Figure 3.2**).

Local geology of Tharsis-Lagunazo is characterized by thick gossan layers formed by the oxidation of massive sulfides, underlain by mineralized horizons rich in pyrite and chalcopyrite. The bedrock consists primarily of volcaniclastics, shales, and tuffs that have undergone hydrothermal alteration associated with mineralization. The combination of these geological formations contributes to AMD generation and metal mobilization, underscoring the importance of geological understanding for environmental monitoring and risk assessment in this region.

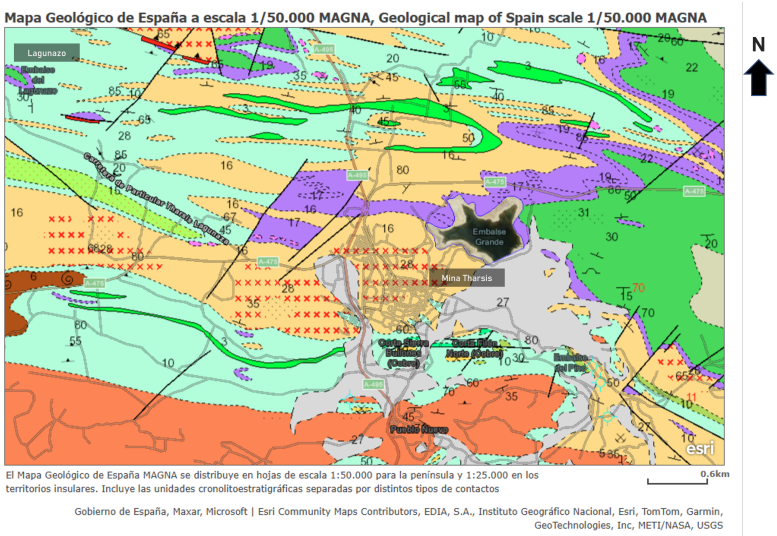



**Figure 3.2:** Regional geology map of Lagunazo and Mina Tharsis. Source: IGME, Mapa Geologico de Espana (MAGNA 50).

### 3.1.2. Physiography of Tharsis and Lagunazo sites

The Tharsis-Lagunazo district is situated in IPB, a region characterized by low to moderate relief, formed on Paleozoic metasediments and VMS deposits. The present-day landscape has been significantly altered by mining, with large excavations, waste dumps, and tailings deposits transforming the natural terrain [59, 64].

The Lagunazo tailings are located in the northwestern part of the study area, on relatively flat, gently undulating ground. This physiographic setting made it suitable for the long-term accumulation of fine-grained tailings, slag, and waste rock. The flat topography promotes the persistence of these deposits and favors chronic seepage of AMD into nearby water bodies such as the Embalse de Lagunazo. The tailings also extend close to agricultural land, thereby increasing the risk of soil and surface water contamination.

In contrast, the Tharsis mining area, located to the southeast, exhibits a more irregular topography, characterized by large open pits (e.g., Corta Filon Norte and Filon Centro) and extensive waste dumps. The abandoned pits have been filled with water, forming acidic pit lakes that act as long-term reservoirs of metals and acidity. Waste dumps located on elevated ground contribute episodic runoff to a dense drainage channel network that connects directly to downstream reservoirs, such as Embalse del Pino and Embalse Grande. This physiographic setting enhances the mobility of contaminants, especially during heavy rainfall or seasonal mixing events.

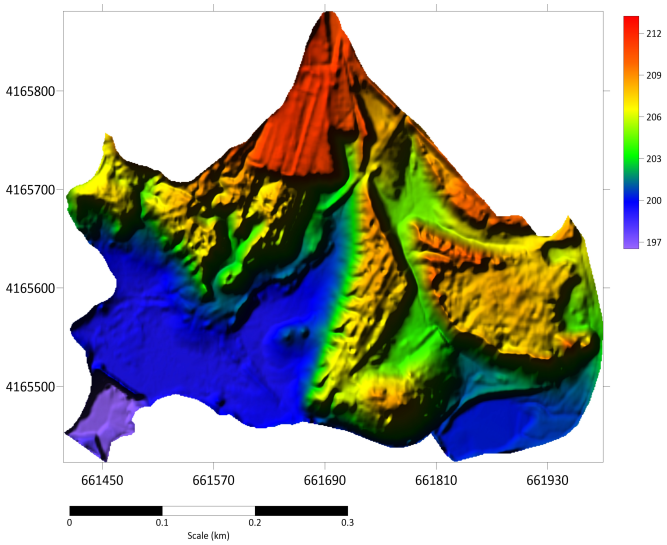



**Figure 3.3:** Lagunazo mine waste morphology (derived from MDT02 dataset and processed using Surfer).

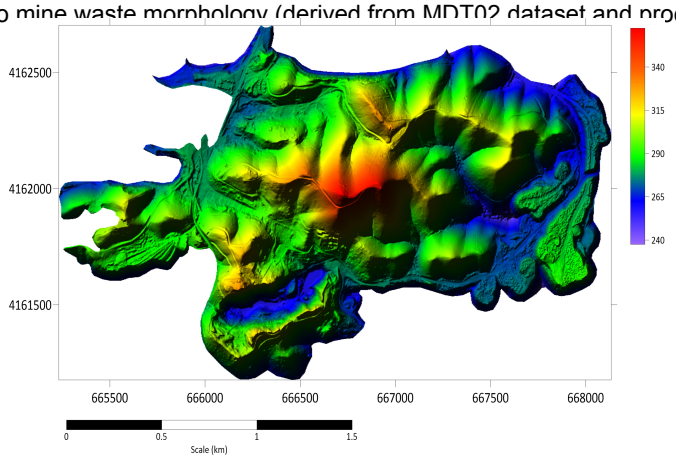



**Figure 3.4:** Tharsis mine waste morphology and (derived from MDT02 dataset and processed using Surfer).

The physiography explains the different contamination pathways in the district. Lagunazo represents a flat terrain system dominated by continuous seepage from tailings, while Tharsis illustrates a pit

dump system where episodic runoff and lake overflows drive contamination pulses. These contrasting settings would highlight the dual role of physiography in controlling AMD risks in the area.

## 3.2. Data sources

This study integrates multiple datasets to support a comprehensive environmental and geotechnical assessment of the Tharsis-Lagunazo site. The datasets are classified into two main categories: primary and secondary data, based on their source and method of acquisition.

### 3.2.1. Primary data

Primary data in this study were obtained from tailings samples collected during from previous fieldwork campaigns at Lagunazo site, including elemental analyses (pXRF) by the Resource Engineering Section conducted in 2023 and 2024.

### 3.2.2. Secondary data

Secondary data were collected from national and institutional databases to support geological, geochemical, and environmental analyses.

- **Sentinel-2 Level-2A:** Multispectral optical imagery with 10 m spatial resolution was used for surface characterization and for calculating vegetation and water-related indices such as NDVI and NDWI. Data were accessed through the Copernicus Open Access Hub [25].
- **Sentinel-1 SAR:** Synthetic Aperture Radar (SAR) imagery was employed to detect ground surface deformation and variations in moisture conditions, complementing optical observations. Data were obtained from the Copernicus Open Access Hub [24].
- **Landsat series:** Landsat-8 and Landsat-9 imagery (30 m spatial resolution) were used to analyze long-term land cover and environmental changes from 2004 to 2023. These data were acquired from the USGS EarthExplorer platform [81].
- **Geochemical datasets:** Data provided by the Geological and Mining Institute of Spain (IGME) include geochemical reference information for soils, sediments, and water in the Tharsis–Lagunazo area. These datasets were used to evaluate contamination risks and support environmental interpretation. Data are accessible via IGME's geochemical portal [29].
- **Digital Elevation Model (DEM):** Modelo Digital del Terreno (MDT02) from the Instituto Geografico Nacional (IGN) was used to analyze surface morphology, hydrological patterns, and volumetric relationships. Data were obtained from the IGN download center [36].
- **Thematic maps:** Topographic and land-use maps were obtained from the Ministry for the Ecological Transition and the Demographic Challenge (MITECO). These datasets provide essential spatial context for baseline characterization and environmental monitoring. Data are accessible through the MITECO geographic portal [52].
- **CORINE Land Cover (CLC):** The 2018 CLC dataset was used to map land use and assess environmental and land management conditions. It provides harmonized land cover and land use information at a scale of 1:100,000, updated every six years. Data are available from the Centro Nacional de Informacion Geografica (CNIG) [12].

## 3.3. Software and tools

Software and tools were used in this study to process and visualize results obtained from primary and secondary data.

- **QGIS Desktop 3.42.2:** Used for spatial visualization of geological, morphological, hydrological, and geotechnical data. The Processing Toolbox, including the SAGA NextGen Terrain Analysis module, was applied for hydrological analysis (e.g., Fill Sinks (Wang & Liu), Strahler Order, and Channel Network and Drainage Basins).
- **Visual Studio Code:** Used for Python-based programming, geochemical data visualization, and spatial interpolation map generation.
- **Google Earth:** Used for preliminary demarcation of the study area and plotting of the samples.

# 4

# Results

The following sections present the main results of this study. It presents the physical, geological, hydrological, and geochemical conditions of the Tharsis-Lagunazo district, with a focus on identifying key processes, environmental risk factors, waste management, a preliminary economic assessment, and the phasing of implementation. Each section highlights the most relevant findings that guide the later discussion on environmental impacts and rehabilitation strategies.

## 4.1. Geology

The regional and local geology of Tharsis-Lagunazo, as described in **subsection 3.1.1**, showed that sulfide mineralization is widespread and pyrite–rich, with chalcopyrite, sphalerite, and galena hosted mainly in fine–grained siliciclastic and volcanic units. Carbonate rocks are scarce across both sites. This lithological assemblage implies very low natural acid-neutralizing capacity.

From a risk perspective, these results indicate a high susceptibility to AMD, as exposure of pyrite to oxygen and water readily generates acidity and mobilizes iron (Fe), copper (Cu), zinc (Zn), and lead (Pb). With limited buffering and short hydrological pathways, dissolved metals can be transported from mine wastes toward nearby receptors, notably Embalse Grande, Embalse del Pino, and Embalse del Lagunazo.

### 4.1.1. Geochemical analysis

We utilized geochemical data from regional surveys and site-specific XRF measurements to assess the distribution of harmful elements. The results reveal contrasting patterns between relatively safe groundwater and enriched soils, sediments, and tailings, indicating key contamination hotspots and environmental risks.

#### Regional geochemistry

We reviewed regional geochemical data from IGME for this study as an initial assessment. Because of the scale difference between this project and the IGME survey, only 3 sample points from the publicly available IGME dataset fall within the Huelva region.

Although the sample locations lie outside the Tharsis-Lagunazo study area, the results closely resemble the pXRF analyses of the primary data, showing elevated concentrations of several harmful elements. Therefore, these data can serve as proxy indicators for mapping the spatial extent of environmental contamination resulting from a long history of mining activities and for illustrating how such activities can produce extensive environmental impacts even at considerable distances.

**Water geochemistry** The groundwater analysis results (see **Appendix A**) indicate that the concentrations of trace metals, including cadmium (Cd), chromium (Cr), copper (Cu), manganese (Mn), and lead (Pb), are generally below or close to the maximum allowable limits set by the European Union (EU) and the World Health Organization (WHO) for drinking water quality.

We used the threshold values from EU Drinking Water Directive [26] and WHO [86] standards. From

these standards, the permissible limits for these elements are: Cd (5 µg/L), Cr (25 µg/L), Cu (2000 µg/L), Mn (50 µg/L), and Pb (5 µg/L). For this study, threshold zones were defined as 80–100% of the regulatory limit to visualize potential risk ranges for each element. As shown in the plots, all measured concentrations fall well below these limits, except for Mn in one sample, which approaches the upper threshold zone.

The relatively low concentrations observed across most samples suggest that groundwater quality in the Huelva region remains within acceptable environmental standards, despite the area's proximity to the IPB, which has a long history of intensive mining. This observation is consistent with previous hydrogeochemical studies reporting that groundwater in the IPB is generally less affected by metal contamination than surface waters, which are more directly influenced by AMD processes [58, 73]. The attenuation in groundwater is largely attributed to geochemical buffering, dilution, and the presence of confining layers that limit the downward migration of acidic leachates.

Localized exceedances, particularly of Mn and Pb, may occur near legacy mine waste deposits or along preferential groundwater flow paths where sulfide mineral oxidation continues. Such areas are more vulnerable to episodic contamination driven by seasonal rainfall, water-table fluctuations, and waste oxidation processes [8]. Continuous groundwater monitoring is therefore recommended to detect potential changes in trace metal concentrations and to assess long-term trends related to hydrological or climatic variations.

The results confirm that while AMD severely impacts surface water systems within the IPB, the regional groundwater quality remains largely below contamination thresholds. However, sustained observation is essential to prevent potential deterioration and to inform rehabilitation and water management strategies in mining-affected areas.

**Topsoil and sediment geochemistry** In contrast to the water data, both soil and sediments (see **Appendix A**) exhibit significantly elevated concentrations of heavy metals, such as Cr, Cu, Pb, and Ni. In some samples, concentrations almost approach threshold zones, although they often remain below the regulatory threshold for agricultural soils.

These patterns reflect the dual influence of natural geological enrichment from VMS deposits and the strong implication of historical mining activity across the IPB. Multiple geochemical surveys in the region have demonstrated that soils and sediments near abandoned mines contain anomalously high levels of trace metals, often several times higher than regional background values [27, 50].

In sediment samples, Pb and Zn exhibit elevated concentrations, reflecting their mobility under acidic conditions and their persistence in mine tailings. These results suggest that even if soils and sediments are relatively uncontaminated, they continue to act as reservoirs of metal pollution and potential long-term sources of environmental risk.

**Environmental implications** The presence of Cr in topsoil and sediment may harm the environment [42]. However, for Cr, only Cr(VI) is carcinogenic, whereas Cr(III) is an essential trace element for humans [19]. The elemental data retrieved from IGME does not state the Cr phase.

Both phases are characterized by low solubility, meaning that if leaching of chromium occurs, it may be associated with oxidation into the hexavalent state, depending on the redox potential and pH [43]. This reaction is highly relevant for environmental issues, because trivalent chromium is an essential trace element for plants, whereas hexavalent chromium is carcinogenic and phytotoxic [3].

The contrasting patterns between relatively safe water and highly enriched soils and sediments illustrate the importance of considering geochemical partitioning and metal mobility in the IPB. Metals stored in soils are partly immobilized by adsorption onto mineral surfaces. Yet, their mobility may increase under acidic or reducing conditions, potentially leading to leaching into groundwater or bioaccumulation in crops and vegetation [55]. This risk is exacerbated by the limited buffering capacity of local soils, which are often affected by sulfide oxidation and low pH.

Soil contamination represents a more immediate ecological and agricultural concern, while water risks remain more localized. Effective environmental management in the IPB, therefore, requires strategies that stabilize contaminated soils and mitigate AMD generation, such as alkaline amendments, organic matter addition, and passive remediation systems that have proven successful in some parts of IPB [46]. Integrating these approaches with ongoing monitoring programs would reduce the risk of heavy

metals transfer from soils to water systems and contribute to the sustainable rehabilitation of this mining-impacted region.

### XRF analysis

Samples used for the XRF analysis were obtained from tailings and AMD water collected during the 2023 and 2024 field campaigns. The sampling locations are shown in **Figure 4.1**, and detailed analytical results and plots are provided in **Appendix A**.

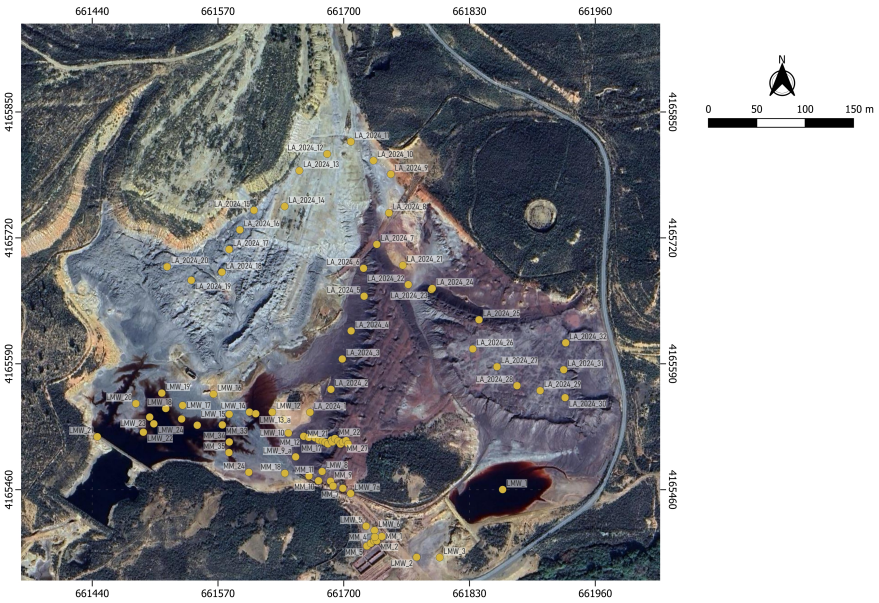
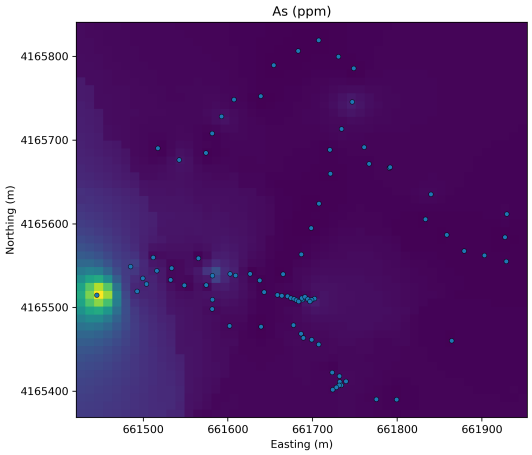



**Figure 4.1:** Sampling locations for XRF geochemical analysis at Lagunazo.

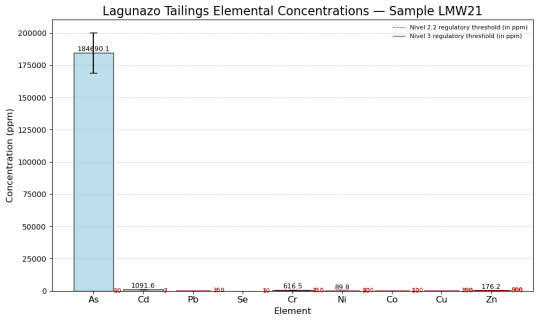
A total of 84 samples were analyzed to map the spatial distribution of elemental concentrations and to produce variance maps relevant to environmental risk assessment. XRF analysis detected varying concentrations of As, Cd, Pb, Cu, and Zn across the study area. However, similar analyses were not performed for the Tharsis site due to the unavailability of samples. The spatial interpolation was carried out using the Inverse Distance Weighting (IDW) method with a power parameter of 2. The observed elevated concentrations and spatial distribution patterns of the analyzed metals are discussed in the following sections.

**As** As occurs naturally in rocks and soils, but it becomes hazardous when it contaminates water or sediments. Long-term exposure can cause skin problems, cancers, heart disease, and harm to child development [22, 87]. As can also build up in plants and animals, moving through food chains.

At Lagunazo, As appears to be the highest at the southwestern side of the mine waste, as highlighted by sample LMW21, which is located close to the AMD. Concentrations drop away from this point, implying the affected area is relatively small. The main risks are direct contact with contaminated fines and short-range movement in shallow water near this location (see **Figure 4.2a**).




**(a)** As spatial distribution map at Lagunazo.




**(b)** Sample LMW21 at Lagunazo with corresponding environmental safe limit.

**Figure 4.2:** Geochemical characterization of As at Lagunazo.

**Pb** Pb is highly toxic and has no beneficial role in the body. High levels in water, soil, or dust can damage the brain and nervous system, and can also harm kidneys and blood pressure [11, 88]. Pb stays in soil and sediments for long periods and can enter food chains. In acidic pH conditions (see **subsection 4.3.2**), Pb mobility increases significantly, making it more soluble in water and increasing the environmental risks associated with Pb contamination, as it can spread more easily throughout the surrounding environment.

At Lagunazo, Pb appears in several locations across the tailings pile, especially in the northwest to central-south parts. Pb tends to bind to particles, so sediment transport is likely to dominate movement rather than dissolved flow. Dust control and sediment management are therefore necessary (see **Figure 4.3**).

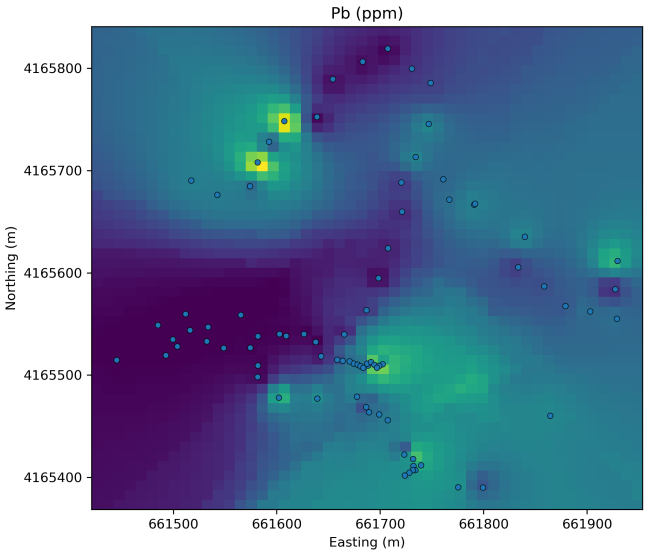



**Figure 4.3:** Pb spatial distribution map at Lagunazo.

**Cd** Cd is not essential for life and is toxic even at low concentration. It can accumulate in crops, damaging kidneys and bones, and is a known human carcinogen [5, 80]. In aquatic systems, high levels of Cd can harm fish and invertebrates.

Highest Cd concentrations are observed in the south-central part of the site, near sample MM10 and MM11. Because Cd is more mobile in acidic conditions typical of sulfide tailings, there is a risk of short-

distance transport in runoff around this location. Local containment, runoff interception, and surface sealing would help limit the spread of pollutants. Under acidic pH conditions (see **subsection 4.3.2**), Cd mobility is enhanced, leading to increased Cd solubility and bioavailability in the environment. The higher solubility can elevate the risk of plant uptake and promote Cd mobility in the surrounding soil, as well as in surface and groundwater (see **Figure 4.4**).

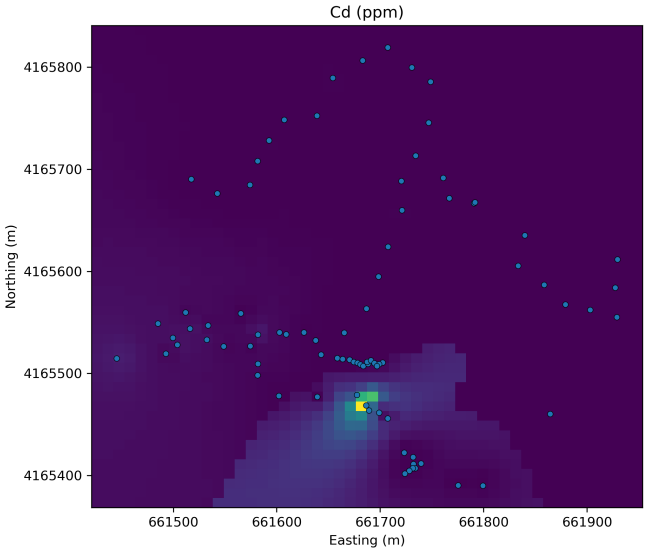



**Figure 4.4:** Cd spatial distribution map at Lagunazo.

**Cu** Cu is essential in small amounts but toxic at high concentrations. Excess copper in water or sediments can harm aquatic life and reduce biodiversity. In humans, long-term exposure may damage the liver or kidneys [17]. Under acidic environment (see **subsection 4.3.2**), Cu mobility is enhanced, leading to increased Cu solubility and bioavailability in the environment. The higher solubility can elevate the risk of plant uptake and promote Cu mobility in the surrounding environments.

At Lagunazo, Cu shows the broadest area of elevated values, extending from the central to the eastern parts of the waste. Cu appears dispersed along shallow surfaces, and the affected area is moderate to large. Although Cu is often less mobile in water than Cd or Zn, its wide distribution increases the likelihood of soil and vegetation impacts. Environmental controls should focus on runoff management and stabilizing fine materials across this location (see **Figure 4.5**).

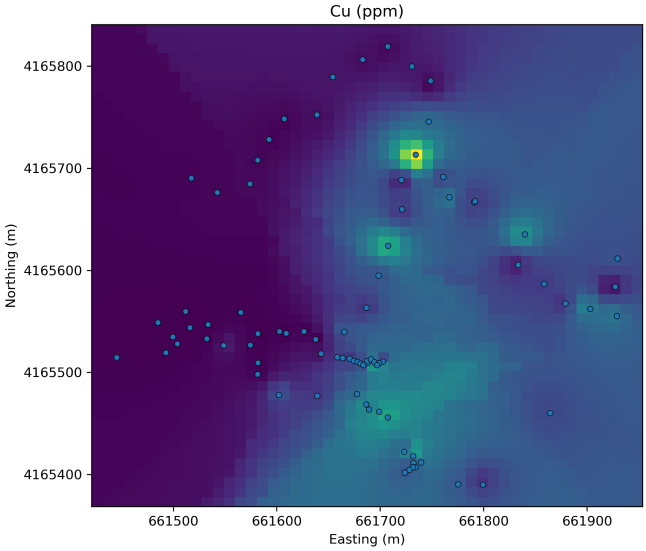
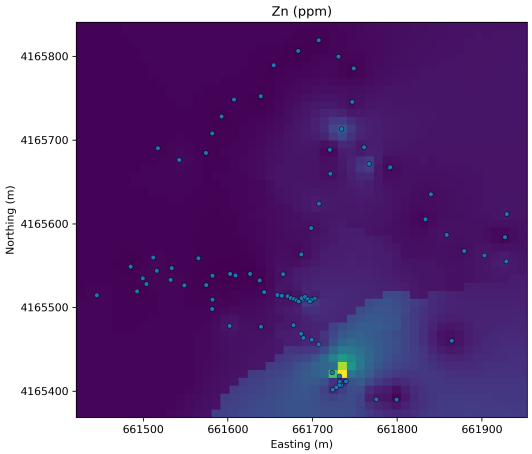


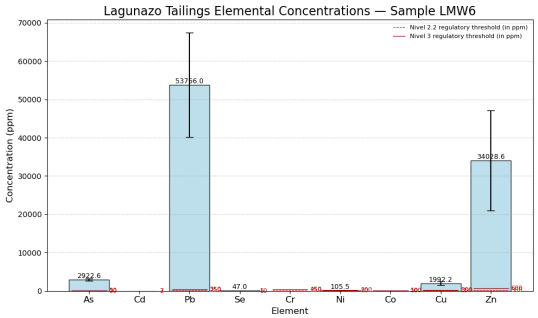

**Figure 4.5:** Cu spatial distribution map at Lagunazo.

**Zn** Zn is an essential nutrient, but it can be harmful in excess. High Zn in water or soil can harm plants, fish, and aquatic invertebrates, and may upset metal balance in the human body [2, 57, 90]. In acidic environments (see **subsection 4.3.2**), Zn mobility increases, making it more soluble in water and increasing the environmental risks associated with Zn contamination, as it can spread more easily throughout the surrounding environment.

Zn is elevated in the southern zone, with the highest values near sample LMW6. Similar to Cd, Zn can move in acidic waters, so the primary concern is dissolved transport during the rainy season, with potential effects on nearby soils and small drainage paths. Monitoring downgradient from this zone is recommended (see **Figure 4.6a**).




**(a)** Zn spatial distribution map at Lagunazo.




**(b)** Sample LMW6 at Lagunazo with corresponding environmental safe limit.

**Figure 4.6:** Geochemical characterization of Zn at Lagunazo.

## 4.2. Geotechnical analysis

We evaluated the geotechnical conditions to understand slope stability and the potential accumulation of AMD in tailings and pit areas. The results identify zones most vulnerable to erosion, flooding, and contamination, providing a basis for targeted risk management. However, the calculation of the Factor of Safety (FoS) is outside the scope of this study due to the absence of the required parameter data.

### 4.2.1. Slope analysis

Slope analysis provides insight into terrain stability and water flow patterns. The results distinguish between the relatively flat surfaces of the Lagunazo tailings and the steep pit walls of Mina Tharsis, showing how slope conditions affect erosion, drainage, and AMD risks.

#### Lagunazo

The slope map of the Lagunazo tailings indicates a dominantly flat surface. Most of the deposit shows flat to very gentle slopes (0–2°), with large areas remaining below 5°. Localized steeper zones (>10°) occur along the outer boundaries of tailings, at contacts with ground (see **Figure 4.7**).

The flat central surface favors water ponding and slow drainage in the tailings pile. This increases the likelihood of infiltration into sulfide-rich materials and, therefore, the potential for AMD generation [6, 38]. In contrast, the steeper margins of the tailing piles are more susceptible to sediment erosion (gullying) during intense rainfall. These edges can act as channels for transporting fine sediments and dissolved metals away from the tailings deposit.

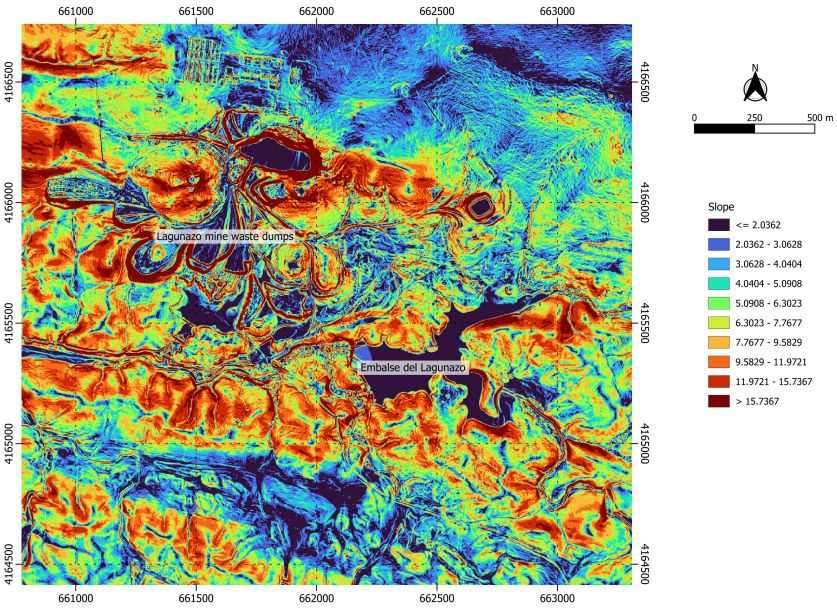



**Figure 4.7:** Slope distribution in the Lagunazo tailings area, derived from DEM analysis. Steeper slopes are concentrated along ridges and mine waste dumps, while gentler slopes dominate the tailings impoundment.

#### Mina Tharsis

The slope map of the Mina Tharsis shows three main slope classes: (1) Very steep slopes (>15.7°), which form rings along the pit walls at Corta Filon Norte and Corta Filon Centro. These slopes are related to excavated benches and cut faces. (2) Moderate slopes (6-12°), which occur around the pits and along access benches and haul roads, acting as transition zones to the surrounding terrain. (3) Flat to gently sloping surfaces ($\leq$2°), which correspond to water bodies and sedimented floors inside the pits, as well as the surfaces of Embalse Grande and Embalse del Pino (see **Figure 4.8**).

The steep pit walls concentrate runoff toward the pit lakes, which are known to be acidic and metal-rich [71]. This setting favors the rapid erosion of exposed faces and the transportation of sediment and contaminants to the lakes, thereby enhancing their role as long-term AMD sources in Mina Tharsis [30]. The waste dump area in the southeast shows extensive steep and very steep slopes (>12°), indicating high susceptibility to gullying erosion. Moderate slopes surrounding the pits can also provide pathways that connect eroding dumps to nearby reservoirs, increasing the risk of sediment and metal transport toward Embalse del Pino and Embalse Grande [54].

Compared with the Lagunazo mine waste, Mina Tharsis presents stronger contrasts between very steep pit walls and flat pit lakes. The dominant risks here are (i) slope instability and erosion along the pit walls and dump fronts, and (ii) the persistence of contaminated waters within the pit lakes. Stabilization

and drainage control, therefore, should be prioritized, particularly on steep faces. Erosion control on dump slopes as well as monitoring of inflows and water levels in the pit lakes and adjacent reservoirs are also highly recommended [6, 30, 71].

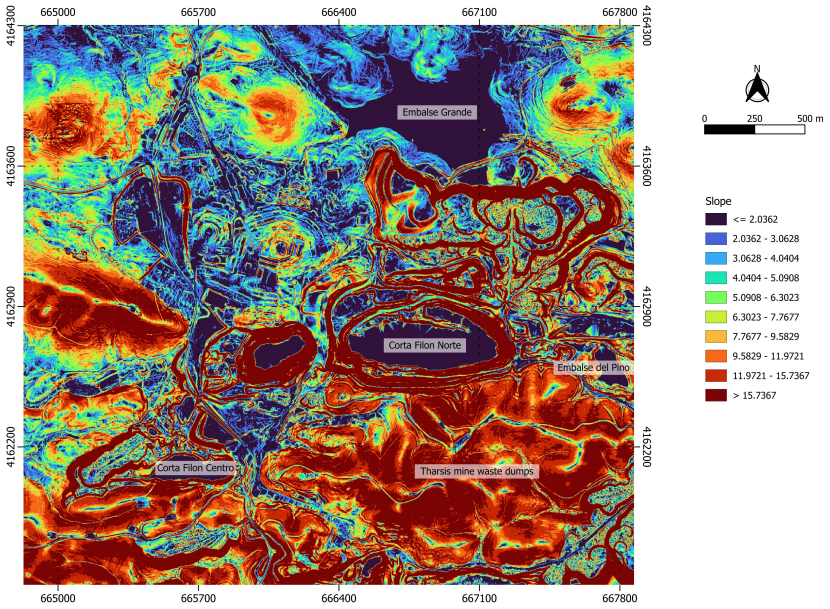



**Figure 4.8:** Slope map of the Mina Tharsis, showing slope classes derived from DEM analysis. Steep slopes are concentrated along pit walls and mine waste dumps, while gentler slopes characterize the surrounding terrain.

### 4.2.2. Potential local seismicity in Tharsis–Lagunazo

Although the Tharsis-Lagunazo district lies in a relatively low seismic hazard zone compared with eastern Andalusia, it is influenced by regional sources associated with the Azores-Gibraltar plate boundary and the Gulf of Cadiz.

Historically large events (e.g., the 1755 Lisbon earthquake and tsunami, and the 1969 Cape St. Vincent earthquake) produced felt intensities and some damage in the Huelva-Cadiz coast, underscoring that infrequent but significant shaking is possible in the broader area [4, 16, 75].

Spain's official seismic hazard updates indicate non-negligible peak ground accelerations for the province at standard code return periods, even if lower than those in Granada–Murcia [1, 35]. Regional Probabilistic Seismic Hazard Assessment (PSHA) studies for Andalusia also account for Atlantic sources (Gulf of Cadiz) in addition to intraplate seismicity [4, 20].

The tailings and mine wastes in Lagunazo and Mina Tharsis can increase local risks during an earthquake. These materials were often deposited without strong engineering control and may have uneven composition and low strength. During ground shaking, they could move, crack, or, in some cases, lose strength and behave like a fluid. This may cause small slope failures or allow contaminated water or sediments to spread into nearby streams.

Even though the overall seismic hazard in the area is low, the condition of these tailings makes them more sensitive to shaking, so they should be carefully studied and monitored as part of local risk assessments.

### 4.2.3. Geotechnical anomaly and risk classification

Adopted by geotechnical risk assessment studies by Chovan and Itasca [14, 41] for designing geotechnical risk assessment for TSFs using Composite Risk Index (CRI) analysis, we utilized indicators and classes, as outlined in **subsection 4.2.3**, to investigate the geotechnical anomalies and risks in Tharsis-Lagunazo. The aim is to map anomalies and risks at Tharsis and Lagunazo, and to provide a clear, field-ready framework for prioritizing inspections and works.

### Indicators and classes

We combined simple terrain, hydrological, and condition indicators into a CRI,

$$R = \frac{\sum_i w_i \, s_i}{\sum_i w_i},$$

where $s_i \in [0, 3]$ is the score per indicator (0=none, 3=severe) and $w_i$ is its weight. **Table 4.1** lists the indicators and scoring thresholds derived from the DEM, remote sensing, and monitoring layers introduced in **Section 4.2** and **subsection 4.2.1**.

**Table 4.1:** Indicators and screening scores for geotechnical anomaly/risk classification (adopted from Chovan and Itasca, 2021).

| Indicator | How to derive | Score (0-3) |
|---|---|---|
| Slope angle | DEM derived slope (°) | 0: $< 2$; 1: 2–6; 2: 6–12; 3: $> 12$ ($> 16$ for pit walls) |
| Flow concentration | Flow accumulation / Strahler order | 0: negligible; 1: minor rills; 2: channelized; 3: main drain or toe line |
| Distance to water | Distance to pit lake/reservoir/pond | 0: $> 250$ m; 1: 100–250 m; 2: 30–100 m; 3: $< 30$ m |
| Surface wetness | NDWI/imagery wet patches | 0: none; 1: occasional; 2: seasonal; 3: persistent |
| Cover integrity (tailings) | Cracks, bare spots, dust | 0: intact; 1: minor; 2: patchy; 3: widespread |
| Material reactivity | Sulfide/slag vs. soil cover | 0: inert soils; 1: mixed; 2: waste rock; 3: sulfide rich tailings/benches |
| Hydrochemistry (water) | pH/EC at nearest outlet | 0: pH$>6$; 1: 5–6; 2: 4–5; 3: $<4$ [6, 71] |

Risk classes are then defined as: **Low** ($R < 0.8$), **Moderate** ($0.8 \leq R < 1.5$), **High** ($1.5 \leq R < 2.2$), and **Very High** ($R \geq 2.2$). We could refine these boundaries with local statistics as monitoring data accumulate.

### Classification by area and recommended actions

**Table 4.2:** Screening classification of geotechnical anomalies and risks in Tharsis-Lagunazo.

| Location | Area | Anomalies | Risk |
|---|---|---|---|
| **Lagunazo** | | | |
| | Central tailings plateau | Ponding; slow drainage; AMD generation | Moderate |
| | Outer margins & outlet channel | Gullying/erosion; export of fines/metals | High–Very High |
| | Contacts with natural ground | Local seepage and rilling | Moderate |
| **Tharsis** | | | |
| | Pit walls (Corta Filon Norte/Centro) | Bench erosion, rockfalls, rapid runoff | Very High |
| | Mine waste dumps (SE sector) | Steep erodible faces; gullying | High |
| | Pit lake shorelines | Wave erosion; acidic outflows; stratification pulses | High |
| | Reservoir inflows (Embalse Grande / Embalse del Pino) | Sediment delivery; metal loads | Moderate |

From the analysis above, we can see that Lagunazo shows low structural hazard but **Moderate to Very High** risk where tailings intersect drainage paths. For this case, source control and polishing treatment are therefore essential [6, 38]. Steep pit walls and reactive waters dominate Tharsis and thus, slopes and pit lake margins are classified as having a **High to Very High** risk, requiring priority stabilization and water-management measures [30, 54, 71].

## 4.3. Hydrogeological analysis

This section presents the drainage characteristics and hydrological pathways that connect mine wastes to water pondings and surface water bodies. The results show how short flow paths and dense stream networks increase the risk of contaminant transport during rainfall events.

The hydrogeological setting at Lagunazo is strongly influenced by its steep catchments in the north and east, particularly at the border, where a reddish slag pile is located. Short flow paths between tailings piles and the dam reservoir enable the rapid transport of contaminated runoff during rainfall events, particularly during the wet season.

Dissolved metals and acidic waters can quickly reach the Embalse del Lagunazo, where processes such as iron precipitation and sediment accumulation not only temporarily store contaminants but also provide a long-term solution to this issue. Still, they may also be released later under changing redox conditions.

### 4.3.1. Flow frequency and seepage type in the Tharsis-Lagunazo system

Hydrological observations in the Tharsis district show that mine leachate from the large waste dumps and pit walls discharges continuously throughout the year. For Tharsis, the leachate flow has been documented as constant in all seasons [74]. This perennial AMD baseflow sustains acidic runoff and seepage to local streams (e.g., the Meca-Odiel network), which is then modulated by a Mediterranean climate with sharp wet-dry contrasts. Superimposed on the continuous baseflow are episodic discharge during and after rainfall events and during seasonal mixing/overturn of pit lakes, which mobilize freshly weathered products and redistribute metal-rich, acidic waters to channels and downstream reservoirs [54, 65, 71]. In short, we could classify the system as perennial and continuous AMD seepage, with strong episodic amplifications driven by rainfall and lake stratification dynamics.

### 4.3.2. pH of streams and receiving waters

Across the Tharsis-Lagunazo area, AMD-affected streams typically exhibit pH $< 3$ close to mine sources. Along the Odiel system, pH commonly drops from near-neutral headwaters to $\sim$3.5 after receiving mine inflows [31, 74]. Pit lakes in Tharsis (e.g., Filon Norte, Filon Centro, Sierra Bullones) are persistently acidic, with typical ranges pH $\sim$2.2–3.6 [71]. The downstream reservoir, which is a major receiver of AMD loads from the Tharsis area, has evolved to pH $\sim$3–5 (often near $\sim$3.5) with high dissolved metal levels [8, 79]. In contrast, local agricultural reservoirs that (e.g., Embalse Grande and Embalse de Lagunazo) exhibit near-neutral conditions. In contrast, Embalse del Pino, adjacent to Tharsis, records acidic values. Previous UAV and Sentinel-2 surveys report an overall pH span from $\sim$0.01 (acidic hotspots) to $\sim$7.8 (neutral waters) across these water bodies [39, 40].

### 4.3.3. Hydrogeology of Lagunazo

The Lagunazo site features several mine waste dump piles situated within a catchment characterized by a dense network of small streams. These channels converge rapidly toward the Embalse del Lagunazo, creating short pathways between waste material and the reservoir. This connectivity means that rainfall events can quickly mobilize acid and dissolved metals from the tailings piles. The high drainage density increases the potential for dissolution at the beginning of the wet season, that is, when salts and oxidation products accumulated during the dry months are suddenly transported into the streams.

Once contaminated water enters the reservoir, dissolved iron can precipitate as iron oxyhydroxides. This process not only can temporarily remove metals from the water but also contributes to further acidification. Over the long term, sediments enriched in metals may become secondary sources of contamination, particularly under anoxic conditions. As a result, the reservoir acts as both a trap and a potential source of pollutants to downstream areas.

Previous field observation at Lagunazo showed clear water in one of the small streams. This can likely occur even under AMD influence because iron precipitates are often removed from the water column and retained on the streambed. After short aeration, dissolved Fe(II) oxidizes to Fe(III) and hydrolyzes to form different phases (mainly schwertmannite, jarosite, and goethite). These flocs settle rapidly and coat gravels and biofilms, so the bed turns orange–brown while the flowing water remains visually clear. This clear water behaviour is well-documented in AMD systems of IPB and reflects fast settling kinetics, short residence times, and trapping of particulates along rough channel substrates [6, 71].

### 4.3.4. Hydrogeology of Mina Tharsis

The Mina Tharsis is well known for producing severe AMD. The area contains both large pit lakes (e.g., Corta Filon Norte and Corta Filon Centro) and waste dumps, all of which are connected to nearby reservoirs (Embalse del Pino and Embalse Grande) through a dense channel network. The short distance between upstream and downstream results in minimal natural dilution, making the reservoirs highly vulnerable to contamination.

Hydrogeological studies indicate that the pit lakes exhibit strong stratification, with acidic, metal-rich deep waters that can mix upward during seasonal turnover or extreme weather events. Overflow and

seepage from the lakes, combined with runoff from surrounding dumps, contribute large contaminant loads to the drainage system. Consequently, the reservoirs downstream receive both continuous and episodic inputs of acidic and metal-rich waters, with high concentrations of iron, aluminum, and trace metals in surface waters and sediments [60, 63]. These processes highlight the importance of integrated hydrogeological monitoring in understanding lake stratification, drainage connectivity, and the seasonal dynamics of contaminant release.

## 4.4. AMD risk zones

By integrating geological, hydrological, and geotechnical findings, we can identify specific areas of high AMD risk. The results highlight the primary contamination sources at both Lagunazo and Mina Tharsis as well as their potential to affect nearby reservoirs and downstream water systems.

In these areas, water infiltration promotes the oxidation of pyrite-rich waste, producing acidic leachates with high concentrations of pyrite-associated metals, such as Fe, Cu, and Zn. Such processes are well documented in the Mina Tharsis and throughout the IPB [7]. Seasonal studies in the region have shown that AMD intensity often increases after rainfall events, when drainage from waste piles and pit lakes delivers contaminated waters to the environment [55].

### 4.4.1. AMD environmental contamination risk in Lagunazo

Lagunazo tailings are located on a hillside where several small streams bypass them. These streams join and flow downslope toward the Embalse del Lagunazo reservoir. Small ponds or collection areas exist below the tailings, but the drainage network can bypass them, especially during heavy rainfall. The reservoir has shallow backwaters that can trap fine sediment and retain water for extended periods, increasing the likelihood of dissolved metals spreading [30].

The primary AMD sources in this area are the exposed surfaces of the tailings, seepage at the base of the waste dumps, and acidic ponds or pits near the tailings. During dry months, metal-rich salts form on the surface of the waste. During the wet season, the initial phase of rainfall events (i.e., the first flush) leads to the wash-off of accumulated pollutants, such as metals, from surfaces and their transport into receiving water bodies. This process often results in elevated concentrations of metal(loid)s, increasing the risk of environmental contamination and metal leaching into groundwater and sediments.

Embalse del Lagunazo is the most vulnerable receptor. It may experience low pH and high concentrations of sulfate, iron, copper, zinc, and aluminum, which is similar to other pit lakes and reservoirs in the Mina Tharsis [71]. Downstream rivers linked to the Odiel system could also be affected, as previous research has shown that AMD in this region can travel long distances and reach coastal wetlands near Huelva [58]. Wetlands and soils around the reservoir may store iron precipitates and adsorbed metals that could later be released back into the water under changing chemical conditions [6].

Seasonal changes strongly influence the contamination risk. In the dry season, water in ponds becomes more concentrated, and salts accumulate on the tailings. The first rains in the wet season are likely to cause the largest AMD discharge. During the wet season, continued seepage and possible overflow from ponds or pits may keep acidic water flowing into the drainage network [30, 55].

Terrain features show that the Lagunazo tailings are well connected hydrologically to Embalse del Lagunazo. This connection enables rapid transport of acidic, metal-rich water to the reservoir and downstream channels during storms. Without measures to intercept or treat runoff, the area represents a significant seasonal risk for AMD contamination. Similar studies in the IPB have highlighted the importance of controlling surface water flow and using passive treatment systems to reduce these impacts [6, 46].

### 4.4.2. AMD environmental contamination risk in Mina Tharsis

The drainage system in Mina Tharsis consists of many short and steep streams draining old open pits, waste piles, and tailings toward nearby reservoirs, such as Embalse Grande and Embalse del Pino. This landscape allows rainwater to flow quickly from mine wastes into surface waters. Because the IPB is rich in sulfide minerals, these minerals can react with air and water, producing acidic water that dissolves metals such as Fe, Cu, Zn, and Pb. Similar AMD has been reported in rivers downstream of Tharsis, such as the Odiel and Tinto [58].

AMD sources at Tharsis include exposed tailings and waste piles where metal-rich salts form during

dry months, seepage at the base of waste slopes, and acidic pit lakes such as Corta Filon Norte and Corta Filon Centro. When it rains, these salts dissolve, causing short but intense acidic and metal-rich pulses. During the wet season, seepage and possible pit or pond overflow can keep acidic water flowing [55]. Acidic pit lakes in this region have very low pH and high sulfate and iron concentrations, acting as long-term contamination sources [71].

The drainage network connects these sources directly to Embalse Grande and Embalse del Pino. These reservoirs have low-gradient margins and backwaters, where fine sediments and dissolved metals can settle or persist for long periods, thereby increasing contamination risks downstream [30]. Remote sensing studies in the IPB also show that streams crossing oxidized mine waste can transport AMD signals over broad areas [70]. Riparian zones and wetlands near the reservoirs may trap iron-rich precipitates that adsorb metals, but could rerelease them when water chemistry changes [6].

The Mina Tharsis has a high risk of AMD contamination. Rapid runoff from steep terrain, multiple contamination sources, and direct connections to reservoirs and streams create seasonal risks. The most significant contamination events are expected during the autumn rains, followed by steady acidic flows during winter. Previous studies recommend controlling runoff and using passive treatment systems, such as open limestone channels or alkaline drains, to limit the spread of AMD [6, 46].

We could also best describe the pit lake fluctuations in Tharsis as episodic rather than depositional changes. Episodic variations are generally driven by rainfall, runoff, and seasonal mixing events, which can rapidly release acidic, metal-rich waters into connected drainage systems [59, 63]. In contrast, depositional processes mainly influence long-term sediment chemistry but do not control short-term water-level dynamics.

## 4.5. Remote sensing analysis

We analyzed satellite images over the years (2004-2023) to capture spatial and temporal changes in the extent of tailings, water bodies, and vegetated areas at Tharsis-Lagunazo. To produce maps with spatial NDVI and NDWI values, data were gathered from Copernicus using Sentinel-2 L2A from January 1st, 2020, to a recent date (September 23rd, 2025). In this study, NDVI and NDWI were used to map water, vegetation, and signs of impact around the Tharsis-Lagunazo area. These simple indicators help identify where mine waste may be affecting nearby land and water, and they support mapping zones likely influenced by AMD.

### 4.5.1. Spatial and temporal changes of Tharsis Lagunazo areas (2004-2023)

**October 2004** The landscape shows a clear separation of mining areas. We can see that the Lagunazo tailings appear compact with sharp boundaries and limited surface moisture. Open pits at Tharsis (e.g., Corta Filon Norte and Centro) contain only shallow pit lakes. Reservoirs are present but relatively small, and vegetation cover is sparse and discontinuous across the district. The satellite image during this period represents low water extent, minimal revegetation, and a geomorphology dominated by exposed waste and pit benches.




**Figure 4.9:** Satellite image of the Tharsis-Lagunazo mining district (October 2004).

**June 2011** Pit lake levels have decreased, which may indicate lower water levels due to intense evaporation in summer.

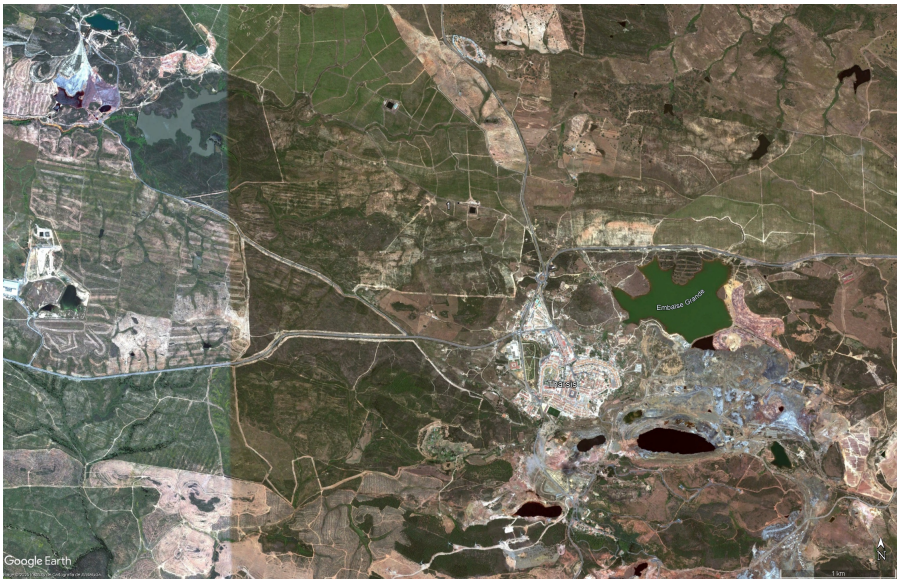



**Figure 4.10:** Satellite image of the Tharsis-Lagunazo mining district (June 2011).

**April 2013** Tailings surfaces are generally stable. Embalse del Lagunazo and Embalse Grande have reduced areal extents compared to 2011, while pit lakes appear deeper (darker tones) and occupy a larger portion of the pit voids. Vegetation increases around the site, particularly on low-slope surfaces and near impoundments. Overall, the spatial signal suggests a transition from surface runoff dominance to more sustained water retention within the pits.




**Figure 4.11:** Satellite image of the Tharsis-Lagunazo mining district (April 2013).

**June 2016** Tailings remain stable without lateral expansion, probably due to the absence of rain in the summer period. Vegetation forms larger patches around the pits and along drainage lines, indicating improved soil moisture conditions and reduced surface disturbance.




**Figure 4.12:** Satellite image of the Tharsis-Lagunazo mining district (June 2016).

**May 2019** Tailings remain stable, with minimal surface changes. The Embalse del Lagunazo is smaller than in earlier years, whereas pit lakes are larger and display darker tones, consistent with greater depth or higher suspended material. Many pits are nearly complete, and water occupies most of the excavated footprints. Vegetation is dense and widespread, especially on gentle slopes and around the reservoirs. Advanced natural revegetation can also be seen in this period.




**Figure 4.13:** Satellite image of the Tharsis-Lagunazo mining district (May 2019)

**November 2023** During this period, we observe that tailings remain stable but appear saturated in some areas, with no new expansion fronts emerging. Embalse del Lagunazo is at or near full capacity, and Embalse Grande is stable. Tharsis' open pits function effectively as lakes, with water occupying entire voids. Vegetation reaches its widest distribution and densest stages.

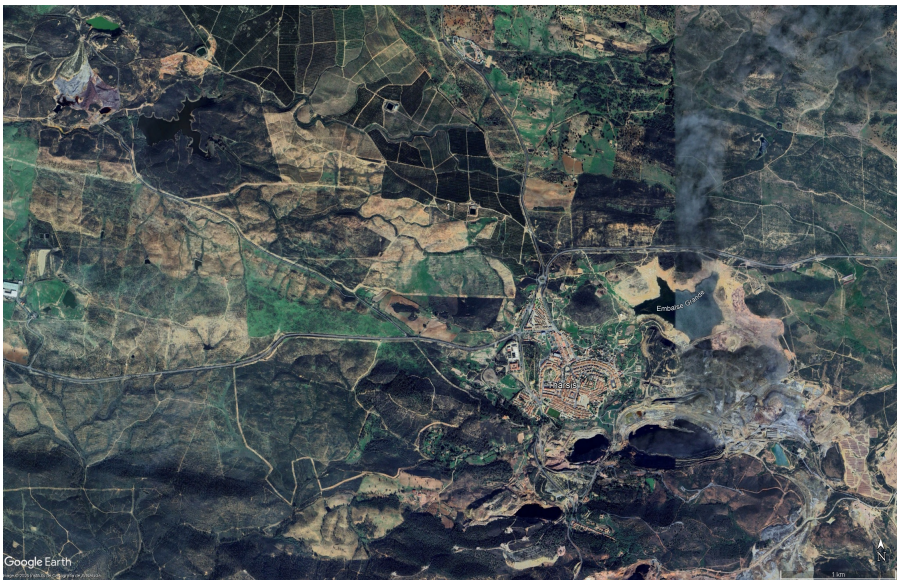



**Figure 4.14:** Satellite image of the Tharsis-Lagunazo mining district (November 2023).

Over 19 years (2004-2023), we could see that the water level in the pit lakes in Tharsis has experienced long term level changes. These increases are superimposed on significant seasonal fluctuations, where water levels rise during wet winter and autumn months due to precipitation and fall during the dry summer due to evaporation.

### 4.5.2. Tailings and surface water indicators

NDWI can highlight water and wet ground. As shown in **Figure 4.15**, the reservoirs and pit bonds at Tharsis-Lagunazo show strong positive NDWI and thus confirm open water. Most tailings and waste piles exhibit a negative NDWI value, indicating they are in dry conditions. Small areas with low NDVI but positive NDWI, located on or just below the tailings, indicate wet spots, ponding, or seepage. We

can also consider these locations as priority sites for AMD generation and transport. If narrow lines of positive NDWI lead downslope from waste toward reservoirs or rivers, they may indicate runoff paths and potential inputs to surface waters. During the wet season, these wet areas often expand. Repeating the analysis over time may help track short-term contamination risks.

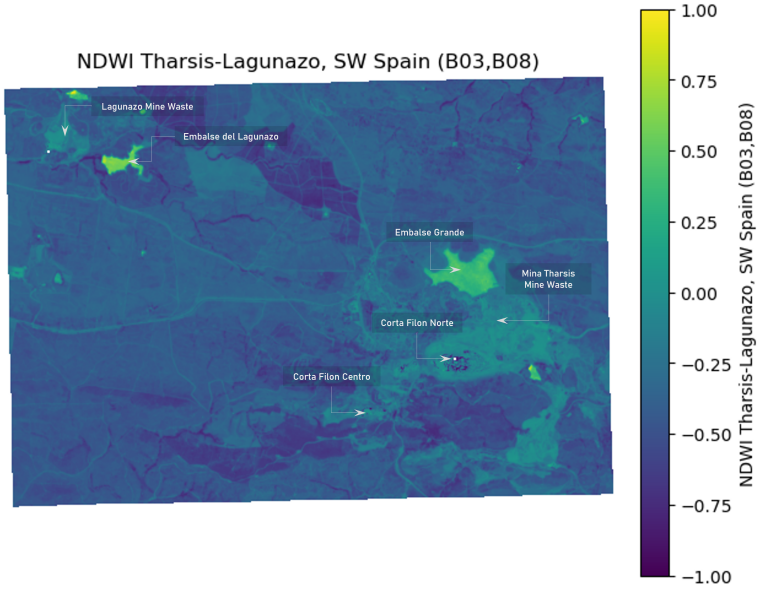



**Figure 4.15:** NDWI classification map at Tharsis-Lagunazo (retrieved and analyzed from Sentinel-2 Level-2A).

### 4.5.3. Vegetation change and environmental impacts

NDVI separates healthy vegetation from the ground. As shown in **Figure 4.16**, the vegetated areas around the site exhibit moderate to high NDVI values, indicating good vegetation cover. On the other hand, tailings and pit benches exhibit low NDVI values, suggesting that these areas have little to no vegetation.

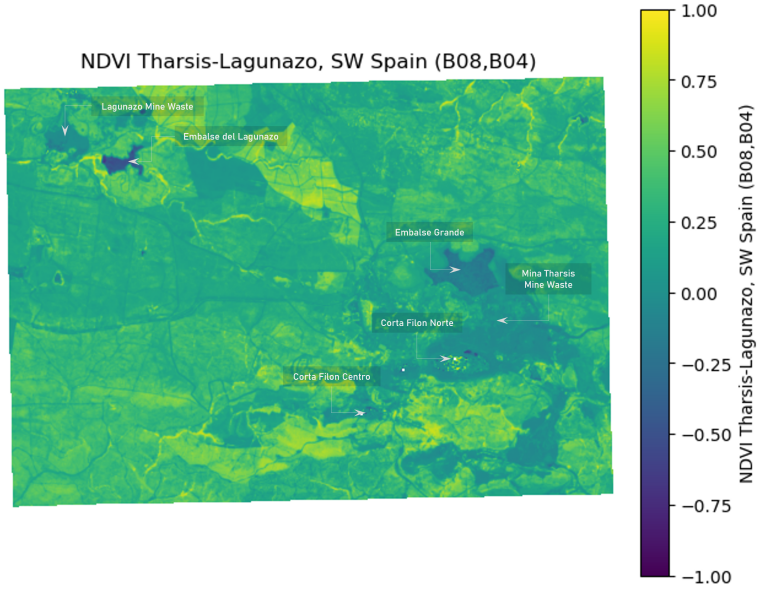



**Figure 4.16:** NDVI classification map at Tharsis-Lagunazo (retrieved and analyzed from Sentinel-2 Level-2A).

When combined, the indices indicate that high NDVI and low NDWI indicate healthy vegetation, while low NDVI and positive NDWI indicate open water or wet tailings. Conversely, low NDVI and NDWI

values indicate dry and bare mine waste. These classes will help to guide management actions, such as stabilizing dry and erodible tailings, controlling waste at seepage and ponding points, and monitoring areas where vegetation is not recovering, which may signal ongoing environmental impact.

## 4.6. Land use management of Tharsis-Lagunazo

The land-use map shows that mining areas are located very close to agricultural land. This close contact creates serious environmental risks. Croplands and orchards that rely on rainfall are directly next to disturbed mining zones, making them vulnerable to AMD, heavy metal contamination, and sediment runoff (see **Figure 4.17**).

Nearby water bodies, such as pit lakes and reservoirs, make this problem worse. They can carry pollutants downstream into farmland and irrigation systems. To protect agricultural production, it is important to manage water carefully and create buffer zones between mine waste areas and cultivated fields.

Around the mining zones, patches of natural and semi-natural vegetation still remain, but these areas are fragmented and often degraded. Meadows, scrubland, and mixed woodland-shrub areas provide some ecological protection, while small patches of broad-leaved and coniferous forests remain near Tharsis. These habitats are valuable for biodiversity and can support environmental restoration, although they face threats from erosion, poor soils, and contamination.

We can see that the land-use pattern in Tharsis-Lagunazo shows a landscape in which mining, agriculture, and natural ecosystems are closely connected. Therefore rehabilitation efforts should aim to stabilize mine waste, restore vegetation, and improve water quality. Creating wetlands, sediment ponds, and vegetated buffer zones can help control pollution, while reforestation can strengthen habitat connections and reduce fragmentation.

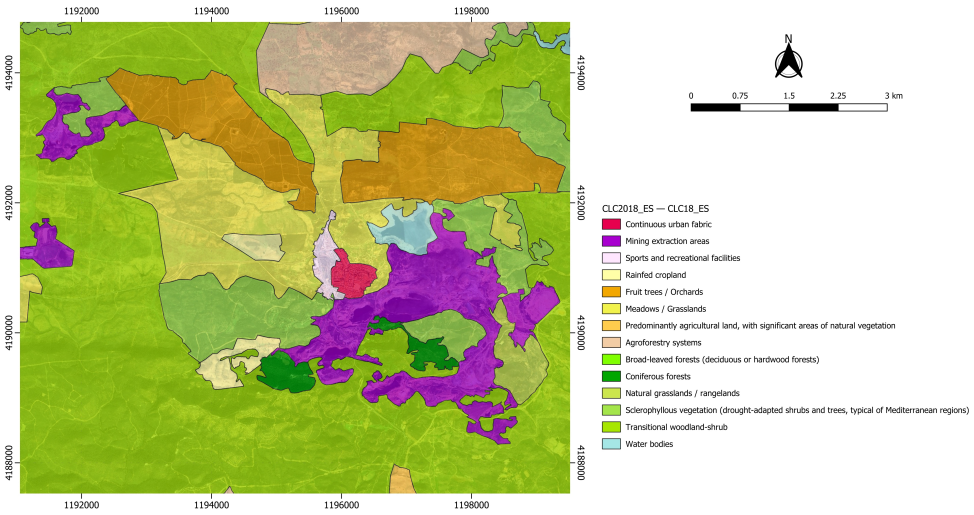



**Figure 4.17:** Land use map of the Tharsis-Lagunazo mining district (maps retrieved and modified by author from CLC2018).

## 4.7. Critical variables of Tharsis and Lagunazo

To map the critical variables for Tharsis and Lagunazo, we combined geological, hydrological, geotechnical, and geochemical findings. We later scored each KV and KVG in **Table 2.1** using four criteria: Hazard Severity, Pathway Connectivity, Temporal Dynamics, and Implementability. We then used a Multi-Criteria Decision Analysis (MCDA) to rank the variables for Lagunazo and Tharsis. We decided on these four criteria as the basis for scoring in the context of Tharsis-Lagunazo, given their suitability and urgency.

1. **Hazard severity**: measures the potential scale of damage from mine waste instability or contamination at Tharsis–Lagunazo, ranging from localized erosion to large-scale slope failure or acid

drainage.

2. **Pathway connectivity**: measures the degree to which contaminants or geotechnical hazards can move through waste piles, drainage channels, or the Embalse del Lagunazo reservoir into the wider environment.
3. **Temporal dynamics**: measures how the risks evolve, for example, with rainfall events, seasonal water level changes, or the long-term weathering of mine waste.
4. **Implementability (TRL)**: measures the maturity and field readiness of the proposed monitoring or remediation technologies for application at Tharsis-Lagunazo.

For each variable, the four scores were weighted and summed to obtain a final weighted score. We presented the detailed weights and final scores for KVs and KVGs in Table 4.3 and Table 4.4, respectively.

**Table 4.3:** MCDA scores for Key Variables (KVs) at Lagunazo and Tharsis.

| Variable | Site | Level | C1 Hazard Severity | C2 Pathway Connectivity | C3 Temporal Dynamics | C4 Implementability (TRL) | Weighted Score |
|---|---|---|---|---|---|---|---|
| HM.1 Water level / pond stage | Lagunazo | KV | 4 | 5 | 5 | 5 | 4.65 |
| HM.5 Rainfall | Lagunazo | KV | 4 | 5 | 5 | 5 | 4.65 |
| SE.2 Geochemistry & mineralogy | Lagunazo | KV | 5 | 4 | 4 | 5 | 4.55 |
| SE.1 Water quality | Lagunazo | KV | 5 | 4 | 4 | 4 | 4.35 |
| HM.6 Extreme weather events | Lagunazo | KV | 4 | 4 | 5 | 4 | 4.20 |
| GEO.4 Channel migration | Lagunazo | KV | 3 | 4 | 3 | 3 | 3.25 |
| GEO.3 Slope stability | Lagunazo | KV | 3 | 3 | 3 | 4 | 3.20 |
| GT.5 Permeability/porosity | Lagunazo | KV | 3 | 3 | 3 | 3 | 3.00 |
| GT.10 Cracks and fractures | Lagunazo | KV | 3 | 3 | 3 | 3 | 3.00 |
| GT.2 Internal movement/sliding | Lagunazo | KV | 2 | 2 | 2 | 3 | 2.20 |
| HM.1 Water level at pit lake | Tharsis | KV | 5 | 5 | 5 | 5 | 5.00 |
| HM.5 Rainfall | Tharsis | KV | 5 | 5 | 5 | 5 | 5.00 |
| SE.1 Water quality | Tharsis | KV | 5 | 5 | 4 | 4 | 4.60 |
| HM.6 Extreme weather events | Tharsis | KV | 4 | 4 | 5 | 4 | 4.20 |
| GEO.3 / GT.7 Slope stability | Tharsis | KV | 4 | 4 | 4 | 4 | 4.00 |
| GT.5 Permeability/porosity | Tharsis | KV | 3 | 4 | 3 | 3 | 3.25 |
| GEO.4 Channel migration | Tharsis | KV | 3 | 4 | 3 | 3 | 3.25 |
| GT.10 Cracks and fractures | Tharsis | KV | 3 | 3 | 3 | 3 | 3.00 |
| GT.2 Internal movement/sliding | Tharsis | KV | 3 | 3 | 3 | 3 | 3.00 |
| GT.6 Thermal properties | Tharsis | KV | 2 | 2 | 2 | 2 | 2.00 |

**Table 4.4:** MCDA scores for KVGs at Lagunazo and Tharsis.

| Variable | Site | Level | Criteria (1–5) | | | | Weighted Score |
|---|---|---|---|---|---|---|---|
| | | | C1 Hazard Severity | C2 Pathway Connectivity | C3 Temporal Dynamics | C4 Implementation (TRL) | |
| Socio-Environmental (water quality, geochemistry) | Lagunazo | KVG | 5 | 4 | 4 | 5 | 4.55 |
| Hydro-Meteorological (runoff, water level, rainfall) | Lagunazo | KVG | 4 | 5 | 5 | 4 | 4.45 |
| Geological & Geomorphological (topography, channels) | Lagunazo | KVG | 3 | 4 | 3 | 4 | 3.45 |
| Geotechnical (slopes, erosion edges) | Lagunazo | KVG | 3 | 3 | 3 | 4 | 3.20 |
| Hydro-Meteorological (pit-lake hydrology, rainfall) | Tharsis | KVG | 5 | 5 | 5 | 4 | 4.80 |
| Socio-Environmental (water quality at pit lakes & outlets) | Tharsis | KVG | 5 | 5 | 4 | 4 | 4.60 |
| Geotechnical (steep benches, erosion) | Tharsis | KVG | 4 | 4 | 4 | 4 | 4.00 |
| Geological & Geomorphological | Tharsis | KVG | 3 | 4 | 3 | 4 | 3.45 |

After weighing and ranking all KVs and KVGs for Lagunazo and Tharsis using MCDA, we found that the two sites have different priorities. These priority variables guide the conceptual monitoring framework

for each site. As shown in **Figure 4.18**, at Lagunazo, the highest-ranked KVG is Socio-Environmental (particularly water quality and geochemistry). In contrast, Geotechnical (slopes and erosion edges) ranks lowest. At Tharsis, Hydro-Meteorological factors (particularly pit lake hydrology and rainfall) rank highest, whereas Geological & Geomorphological is the lowest-ranked KVG.

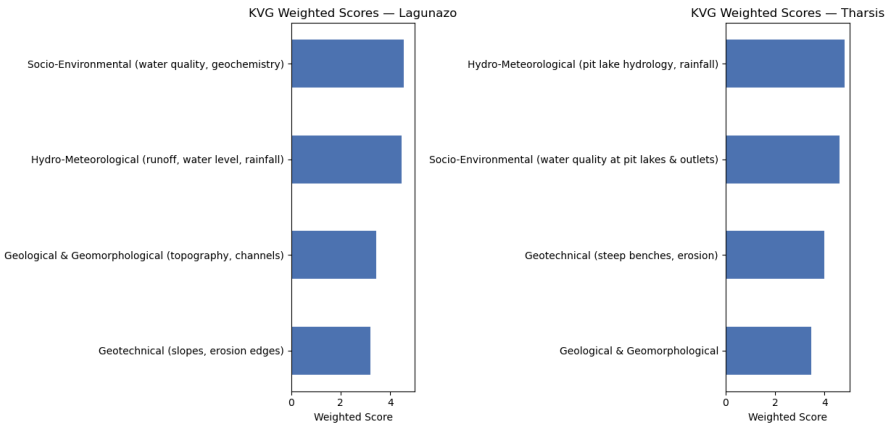



**Figure 4.18:** KVG Weighted Scores and Ranking for Lagunazo and Tharsis

## 4.8. Waste management and rehabilitation strategies

Based on the identified risks, we outlined potential strategies for waste management and site rehabilitation for Tharsis-Lagunazo. The results presented in this section suggest specific measures for Lagunazo and Mina Tharsis, including geochemical monitoring, revegetation, engineering, and adaptive management.

To better calculate and determine the most effective waste management strategies at Tharsis-Lagunazo, we first estimated the mine waste volumes for Tharsis and Lagunazo from the MDT02 datasets. We used Surfer software with grid volume computations. The parameters and calculated volume for both areas are presented in **Table 4.5**.

**Table 4.5:** Surface areas and volumes of Lagunazo and Tharsis mine wastes (calculated using MDT02 datasets and the grid volume computation method).

| Area | Lower surface, Z (m) | Surface area ($m^2$) | Volume ($m^3$) |
|---|---|---|---|
| Lagunazo | 197 | 158,219 | 1,257,231 |
| Tharsis | 275 | 1,919,186 | 35,383,402 |

### 4.8.1. Lagunazo waste management and rehabilitation strategies

The Lagunazo tailings occupy an area of about 158,219 $m^2$ (15.8 ha) and have an estimated volume of 1.26 million $m^3$ (see **Table 4.5**), with the lowest surface located around 197 m a.s.l. Because the deposit is relatively small, it is suitable for a single, well-drained cover system combined with focused monitoring. As an initial plan, a 0.5 m growth or neutralization layer could be placed across the entire surface, requiring approximately 0.08 million $m^3$ of cover material.

#### Chemical monitoring

As indicated in **subsection 4.1.1**, As concentrations are highest in the southwest near the AMD source. We can implement diversion of upslope runoff using lined drains and collect contaminated flows for treatment. Filtration systems can be applied for arsenic removal [**56**]. We can seal hotspot surfaces with compacted clay or geosynthetics and apply a limestone-amended soil layer, to bring the pH at circumneutral levels, where As mobility is lowest and the oxidized As species can adsorb onto Fe- or Al- oxides, thereby inhibiting its mobility.

Pb is concentrated mainly in the north–central and southern zones. To manage these areas, we can apply an inert soil cover amended with lime and phosphate to immobilize Pb and reduce dust. We can

also implement shallow-rooted vegetation and small sediment traps within drainage channels to limit Pb transport [9, 37]. The desired conditions for promoting Pb immobilization occur at circumneutral to slightly alkaline pH (6-8) and under moderately oxidizing to slightly reducing redox (Eh) conditions. Under these conditions, Pb is immobilized through precipitation and /or adsorption onto mineral surfaces (such as Fe/Al oxides or clays).

Cd shows elevated levels in the south-central area, where high acidity enhances its mobility. We can raise the pH using limestone or dolomite and, where necessary, implement a reactive limestone layer beneath the cover to capture Cd. Additionally, we can route runoff through small wetlands or sulfate-reducing bioreactors to promote either in the form of Cd carbonated or through co-precipitation with Fe-oxides [37].

Cu is more widespread across the central and eastern zones. We can reshape the surface to ensure positive drainage, divert clean water away from the deposit, and construct lined sediment ponds. Implementing a uniform evapotranspiration cover and Cu-tolerant vegetation can further stabilize these areas.

Zn concentrations are highest near LMW6 in the south. We can apply similar measures to those for Cd, such as compacted covers, limestone drains, and reinforced swales, to prevent the transport of dissolved Zn during storm events.

#### Revegetation and soil function

We can grade the surface and implement a low-permeability cover with a neutralized growth layer. In Pb-rich zones, lime and phosphate amendments can be applied to reduce bioavailability [9]. Fast-growing grasses can be established for initial erosion control, followed by shallow-rooted shrubs for long-term stabilization. Deep-rooted species should be avoided on steep slopes to protect liner integrity. Through these measures, we can reduce dust, slow surface runoff, and enhance soil moisture retention.

#### Monitoring and adaptive management

Routine monitoring analyses can include pH, EC, and dissolved metals (such as As, Cd, Cu, and Zn) at drains, treatment units, and the sediment pond, as well as dust monitoring for Pb at site boundaries. If monitoring results indicate continued contamination or underperformance of the cover, we can adapt management by thickening the cover, adding reactive materials, or upgrading drainage systems.

### 4.8.2. Tharsis waste management and rehabilitation strategies

The Tharsis site is much larger, covering about 1,919,186 $m^2$ (191.9 ha) with an estimated 35.38 million $m^3$ of waste (see **Table 4.5**) and the lowest surface lies around 275 m a.s.l. Because of its size, steep pit walls, permeable rocks, and pit lakes, managing water flow is the main priority. The first steps should focus on separating clean water from contaminated areas and protecting downstream environments. A complete 0.5 m cover would need about 0.96 million $m^3$ of material, therefore a gradual, phased approach should be used to manage rehabilitation efficiently.

#### Water management

We can implement source separation of clean and contact water by constructing diversion channels and lined drains upslope of pits and dumps to prevent runoff from reaching sulfide-rich zones. Captured contact water can be conveyed through lined ditches at slope toes, while cutoff trenches can be applied in permeable sediments to intercept seepage [89]. We can begin with the most reactive or high-flow sub-catchments.

#### Pit lakes

As pit lakes are persistent AMD sources in the IPB [10], we can apply submerged limestone beds to create a circumneutral pH level and install baffles to slow circulation and improve treatment efficiency. Reinforced spillways can be implemented to prevent uncontrolled discharges during extreme rainfall events. Flooding, by raising the water table is also proven to be an effective measure to create a reducing (low redox) environment, thereby decreasing the mobility of certain metals (e.g., Fe, Mn, Zn, Cd, Pb, Cu, As, Ni) that are otherwise mobile under oxidizing and acidic conditions. This approach can promote the immobilization of these metals by inducing changes in speciation, precipitation, and sulfide formation.

#### Pit slope stabilization

We can stabilize steep pit walls by regrading to gentler slopes with berms or benches, reinforcing erodible faces with rock armoring, and adding water bars to break flow paths [47]. We can also apply low-permeability capping systems, such as clay or geosynthetic covers, to limit infiltration. Implementation should proceed in phases, beginning with the most erosion-prone sectors.

#### Passive treatment systems

We can apply passive treatment units, such as open limestone drains and constructed wetlands, to neutralize acidity and remove metals from baseflows [28]. These systems can be complemented with active or modular treatment units during storm events, guided by flow monitoring data.

#### Reservoir protection

To protect Embalse Grande and Embalse del Pino, we can implement forebays, vegetated buffer zones, low berms, and rock-lined inflows to reduce sediment and AMD transport [49]. We can prioritize implementation along the shortest and steepest flow paths first.

#### Revegetation

We can establish fast-growing grasses for initial stabilization, followed by native, metal-tolerant shrubs to control erosion and reduce dust emissions. Deep-rooted trees should be avoided in areas with liners or drains to prevent damage [85]. Vegetation establishment can be sequenced following completion of hydrological control works.

#### Monitoring management

For the $\sim$192 ha footprint, we can scale the monitoring network to include water-quality measurements at pit-lake outlets, drains, and reservoir inlets, with a higher sampling frequency during wet seasons. We can monitor rainfall, surface flows, and lake levels, and perform routine slope inspections. Remote sensing indices such as NDWI and NDVI can be applied to detect wet zones and assess vegetation health [18]. The results can guide the phasing and optimization of rehabilitation works.

Lagunazo and Tharsis, therefore, need different emphases. At Lagunazo (15.8 ha; $1.26 \times 10^6\ \mathrm{m}^3$), actions focus on localized contaminant control, dust suppression, and a single, continuous cover with tight drainage. At Tharsis (191.9 ha; $3.538 \times 10^7\ \mathrm{m}^3$), the scale and hydrology dominate: staged water separation, pit-lake management, slope stabilization, and downstream protection are prioritized, followed by progressive capping and revegetation. Both sites require shallow-rooted vegetation and continuous monitoring, but the density and phasing reflect their very different sizes and risks.

## 4.9. Conceptual monitoring framework for Tharsis-Lagunazo

This section presents a monitoring framework that integrates geological, geotechnical, hydrological, and geochemical methods to enhance risk detection and support long-term site management. We could also recommend similar integrated approaches for abandoned mine sites in the IPB, where AMD, unstable slopes, and pit lakes remain persistent hazards [60, 68]. The framework also incorporates an assessment of monitoring technologies using TRL, which supports the selection of tools and planning of future implementation [48]. We linked monitoring strategies to the critical risks identified in this study, as summarized in **Section 4.8**.

### 4.9.1. Geotechnical monitoring

At Mina Tharsis, slope instability and erosion of pit walls require regular monitoring. UAV photogrammetry provides high-resolution mapping of erosion features and bench degradation after rainfall, and has proven effective for low-cost slope monitoring in mining environments [45]. Where access allows, tilt sensors or crack gauges should be installed on critical benches and dump faces to monitor their condition. At Lagunazo, routine topographic surveys of tailings crests and toes will help verify the stability of regraded surfaces and the integrity of cover, especially in zones steeper than $12^\circ$, where gullying is likely to initiate.

### 4.9.2. Hydrological monitoring

Hydrological monitoring is crucial for tracking flow paths and water balances. Each subcatchment should include one rain gauge, one flow logger in the main ditch, and a staff gauge at the nearest pond, pit lake, or reservoir inflow. We can equip toe drains and lined channels with V-notch weirs or flumes for event-based flow measurement, which are standard in mine water studies [89]. In pit lakes such as Corta Filon Norte and Filon Centro, continuous water level recording and seasonal profiles of temperature and conductivity are recommended to assess stratification and seasonal mixing patterns [10].

### 4.9.3. Geochemical monitoring

We can deploy field sondes (pH, EC, temperature) at ditches, pit lake outlets, and reservoir inflows. Samples are collected during both the wet and dry seasons, and then analyzed for major ions and dissolved metals to quantify loads and calibrate sensors. At Lagunazo, pXRF provides rapid assessment of tailings and sediment contamination, particularly for elements such as As, Cd, and Zn, which can be identified as local hotspots [49].

### 4.9.4. Remote sensing and spatial analytics

Remote sensing provides cost-effective coverage for spatially extensive areas. Sentinel-2 time series of NDVI and NDWI can detect wet spots, seepage lines, and vegetation recovery on reworked surfaces [18]. Sentinel-1 InSAR should be used to monitor millimeter-scale deformation at waste piles and tailings facilities, which is increasingly applied in mine waste monitoring [15].

### 4.9.5. Monitoring placement

Monitoring priorities differ between Tharsis and Lagunazo. At Tharsis, pit lakes (for water levels and profiles), toe drains below steep benches, and main ditches leading to Embalse Grande and Embalse del Pino (flow, pH, EC) should be monitored, along with reservoir inflows for pH, EC, and turbidity. At Lagunazo, monitoring should focus on the tailings toe and outlet to Embalse del Lagunazo (flow, pH, EC), supported by targeted pXRF measurements for As, Cd, and Zn hotspots.

### 4.9.6. Monitoring tools and deployment priority

Based on the conceptual monitoring framework provided above (see **Section 4.9**) and the KVs identified (see **Section 4.7**), monitoring tools were prioritized by relevance and feasibility. We evaluated each tool using TRL to reflect implementation maturity, and summarized the selected deployment locations in **Table 4.6**.

**Table 4.6:** Monitoring tools technology and deployment priority.

| Tool | Purpose | Location | TRL | Priority |
|---|---|---|---|---|
| Staff gauges | Track pond levels | Tharsis pit lakes and reservoirs | 9 | High |
| Multiparameter sondes | Continuous AMD signals | Tharsis ditches and toe drains, Lagunazo outlet | 9 | High |
| Weirs and flow loggers | Flow for load estimates | Toe drains, main ditches and outlets | 9 | High |
| Grab samples | Calibrate and validate sensors | All sensor points | 9 | High |
| Field pXRF measurements | Map As, Cd, Zn hotspots (as shown in maps in **subsection 4.1.1**) | Lagunazo tailings, bank sediments | 8–9 | Medium-High |
| UAV photogrammetry | 3D erosion (gully) mapping | Tharsis benches, Lagunazo margins | 8 | Medium |
| Crack monitoring/tilt sensors | Open pit benches and waste dump | Tharsis steep faces | 7–8 | Medium |
| Sentinel-2 NDVI/NDWI | Wet spots, vegetation cover | Both sites | 9 | Medium |
| Sentinel-1 InSAR | Slow surface motion | Waste dumps and embankments | 7–8 | Medium |
| Data platform (QA/QC and alerting systems) | Integrate data and alarms | All | 6–7 | Medium |

### 4.9.7. Key gaps and actions

Most monitoring activities demonstrate high feasibility, as indicated by the high TRLs in Table 4.6. However, several implementation gaps remain. To ensure consistent operation and maintain data quality, we propose targeted actions to address these gaps. A summary of the identified gaps and corresponding actions is provided in Table 4.7.

**Table 4.7:** Monitoring tools readiness gaps and actions.

| Gap | Action | TRL |
|---|---|---|
| Probe fouling | Monthly maintenance and calibration, keep spare probe at critical sites | 9 |
| Debris affects flow ratings | Debris racks or cages, rechecking rating curves after big rains | 9 |
| InSAR decorrelation | Use seasonal stacks (time series sets of interferogram) | 7–8 |
| UAV access after big rains | Clear flight plan | 8 |
| Data scattered across tools | Set up a basic QA/QC dashboard with alarms | 6–7 |

### 4.9.8. Implementation plan

#### Priority actions

**Lagunazo** For the priority actions, we can install a reactive cover on the main tailings area (about 12–15 ha) to reduce infiltration and dust, collect contact water with toe drains, and route it to a small lined sediment pond for settling. At the outlet, we then construct one passive wetland/bioreactor cell to polish Cd-Zn before discharging it to the Embalse del Lagunazo. These steps give immediate source control, lower metal loads and suspended solids, and are straightforward to build and operate.

**Tharsis** For the priority actions, we can build diversion channels and lined toe ditches (about 2–3 km) to separate clean runoff and safely convey contact water, and add a cutoff trench where seepage emerges. We can armour the most erodible benches (about 10,000 $m^2$) to reduce erosion. Along the pit-lake margins, we can install short segments of Open Limestone Drains (OLDs), approximately 0.6–1.0 km, to help neutralize acidity.

OLD is a passive treatment system used to reduce the acidity of mine water. It consists of a shallow channel filled with crushed limestone through which acidic water flows. As the water passes over the limestone, chemical reactions occur that neutralize the acidity and increase the pH by dissolving calcium carbonate ($CaCO_3$).

This process also helps to reduce the concentration of dissolved metals such as iron and aluminum. OLDs are simple, low-cost, and effective for mildly acidic waters, but their performance decreases when water contains high levels of iron or aluminum, which can form coatings on the limestone and reduce its reactivity. Therefore, they are best used as a first or supportive treatment step rather than a standalone long-term solution [33, 76].

Finally, we can provide vegetated buffer strips and rock-lined inflows at Embalse Grande and Embalse del Pino. Together, these steps reduce inflows to pit lakes, improve water quality, and strengthen slope stability.

**Monitoring (both sites)** For the priority actions, we can equip pit lakes and reservoir inlets with staff gauges and multiparameter sondes (pH, EC, temperature), install one flow logger per main ditch, and carry out wet-season grab sampling with targeted field pXRF transects on tailings. These steps provide continuous level and quality data, quantify flows, and quickly identify metal hotspots, supporting compliance tracking and adaptive management.

#### Phasing

**Phase I (0-6 months)** For the implementation phasing, we can start with actions that deliver avoided costs from Year 1. This includes cutting clean water off sulfide surfaces, sealing 2-3 hotspot patches at Lagunazo, building a small lined sediment pond, armouring one or two critical benches, and installing the core monitoring instruments (staff gauges, sondes, and one flow logger per main ditch).

**Phase II (6-24 months)** For Phase II, we can extend lined ditches and add the cutoff trench at Tharsis, place the reactive cover over the main Lagunazo footprint, construct one wetland/bioreactor cell,

install short OLD segments, and improve reservoir inflows and buffer strips. This consolidates hydraulic separation and source control, allowing avoided costs to grow year-on-year in line with the economic analysis.

**Phase III (Years 2-5)** For Phase III, we can focus on staged implementation in the highest-risk areas: complete the priority diversions and toe ditches at Tharsis, armor the most erodible benches, and extend vegetation cover where it yields the best return. Monitoring data are used to verify performance. By the end of this phase, the benefit stream should be clearly established.

**Phase IV (Years 5-7)** Based on monitoring evidence, we can expand covers and buffers where benefits are strongest, add a secondary wetland cell if needed, retire temporary works, and optimize the monitoring network.

**Phase V (Years 7-10)** For the last phase, we can complete any remaining hotspot treatments justified by monitoring, shift to steady-state maintenance and adaptive monitoring, and formalize long-term asset management (including periodic remote-sensing/InSAR checks). The objective is to hold water-quality and stability gains and maintain a reliable benefit stream over the remaining asset life.

### Expected outcomes

This 10-year plan is expected to deliver measurable environmental and economic benefits. At the Lagunazo outlet and reservoir inlets, we aim for a pH increase of about one unit and a 30–50% reduction in dissolved Cu, Zn, and Cd within the first two years compared to 2024 levels. These improvements should remain stable over time. At Tharsis, we aim to prevent pit-lake overflows through lined ditches that minimize erosion. Visible reduction in bench rilling should occur by Years 2–3, with stable slopes maintained through Year 10. On treated areas, vegetation cover should reach at least 70% after one year and 85% after two years, maintained long term through routine care.

# 5

# Discussions

## 5.1. Discussions

### 5.1.1. Geological, geotechnical, hydrological, and geochemical factors

Hydrological and geochemical factors are the main controls on environmental risk in the Tharsis–Lagunazo district. The MCDA results highlight rainfall, evaporation, pond level, and drainage quality as key environmental drivers, while pH, electrical conductivity, and Fe–Cu–Zn concentrations are strong indicators of AMD. The high weighting of hydrological parameters reflects the region's climate, where strong seasonality in rainfall leads to alternating wet and dry cycles that influence oxidation-reduction reactions, metal mobilization, and surface runoff.

During intense precipitation events, rapid infiltration and surface runoff can transport oxidized sulfides and metal-rich sediments into adjacent water bodies. On the other hand, during dry periods, evaporation concentrates dissolved metals and sulfates, enhancing the potential for secondary mineral precipitation, such as jarosite. These geochemical dynamics are amplified by poor drainage and limited vegetation cover in Tharsis-Lagunazo.

Geotechnical and geological conditions add site-specific risks in Tharsis-Lagunazo. In Tharsis, steep and weathered pit walls composed of heavily weathered schists and gossanized materials are prone to erosion and instability, particularly along benches and fractures exposed to rainfall. Such instability increases sediment transport and turbidity in nearby ponds, indirectly contributing to AMD dispersion by increasing reactive surface area. In contrast, flat terrain in Lagunazo, supported with the fine-grained, low-permeability nature of its tailings promote water ponding and therefore restrict oxygen diffusion.

The predominance of hydrological and hydrochemical processes aligns with the Global Industry Standard on Tailings Management (GISTM), which prioritizes water balance management and geotechnical integrity as center of risk reduction [34]. Long-term management should therefore focus on enhancing drainage capacity, minimizing surface ponding, and tracking seasonal variations in pH and metal concentrations to assess AMD generation potential and containment performance.

### 5.1.2. Effectiveness of monitoring tools

Integrating in-situ sensors, geochemical surveys, and remote sensing datasets provided complementary insights into the interactions governing each site behaviour. Field measurements of pH, EC, and water levels captured rapid hydrochemical responses following rainfall events, which are key indicators of AMD activation within the tailings surface. These short-term variations reflect the balance between oxidizing conditions during dry phases and flushing events during wet seasons.

Remote sensing significantly expanded spatial and temporal coverage beyond what regular field methods alone could achieve. Sentinel-2 NDWI could effectively delineate ponding zones, while NDVI could detect vegetation stress patterns, which may reflect underlying salinity or toxicity, and Sentinel-1 SAR backscatter and coherence data were sensitive to variations in surface roughness and dielectric properties, highlighting potential deformation or moisture-related subsidence. DEMs, when added with

UAV-derived orthomosaics could reveal fine-scale erosional gullies, sediment accumulation zones, and cracks on pit walls, the features which are often invisible to medium-resolution satellite sensors.

This approach reflects current international best practice for post-mining environmental management. Comparable multi-sensor monitoring frameworks in Australia and Canada demonstrate how combining geospatial data with geochemical and hydrological information supports evidence-based mine closure strategies [51, 66]. Furthermore, the integration of open-access Sentinel data, supported with UAV and ground observations also aligns with EU recommendations for transparent, scalable, and cost-effective monitoring of mine waste facilities [23]. The results here we presented demonstrate that freely available satellite data, when processed and validated with in-situ measurements, can provide a robust foundation for continuous and long-term surveillance of legacy tailings sites.

### 5.1.3. Integration into a conceptual monitoring framework

Integrating field, laboratory, and satellite datasets provided a comprehensive understanding of hydrological and geochemical dynamics within the district. The combination of NDWI time-series analysis, water-quality data, and DEM-based hydrological modelling proved particularly effective in identifying persistent ponding zones associated with acidic drainage outlets. The spatial overlap between remotely detected moisture anomalies and high-EC field measurements reinforces the reliability of satellite-derived indicators as proxides for environmental risk.

This cross-validation supports the importance of remote-sensing, when properly calibrated with ground observations, can act as early-warning tools for AMD activation or infrastructure deterioration at Tharsis-Lagunazo. For instance, a sudden increase in NDWI without corresponding rainfall could indicate seepage, while declining NDVI values in previously stable zones may suggest increasing toxicity or salinization. Embedding these indicators in an operational monitoring system could enable near real-time risk detection and prompt management responses.

The proposed framework also aligns with GISTM's decision-making principles by emphasizing redundancy, transparency, and adaptive management. Field campaigns and laboratory analyses refine the calibration of remote indicators, while continuous satellite monitoring ensures temporal consistency. Comparable multi-source frameworks have also been implemented in Chile and Scandinavia, where real-time data integration supports AMD management, slope stability monitoring, and progressive ecological recovery assessment [21]. These cases demonstrate that harmonizing heterogeneous datasets within a unified geospatial framework enhances monitoring efficiency and strengthens long-term closure planning.

### 5.1.4. Environmental rehabilitation plan and implications

The proposed rehabilitation plan prioritized water management, slope stabilization, and progressive revegetation, which are main components that form the foundation of sustainable mine closure. At Lagunazo, interventions should focus on enhancing drainage and applying shallow reactive covers (e.g., limestone-rich or organic layers) to reduce infiltration and metal leaching. These covers could promote neutralization and limit-sulfide oxidation, which can complement natural evapotranspiration processes to minimize pond formation.

At Tharsis, stabilization of pit walls and regulation of pit-lake levels are critical. Slope reshaping combined with geotechnical reinforcement (e.g., gabion structures or terracing), can reduce erosion and improve long-term stability. Vegetation restoration along pit margins not only mitigrates erosion but also fosters ecosystem recovery and gradually re-establishes soil structure.

This phased and risk-based strategy is consistent with adaptive closure approaches applied in the Pilbara mine (Australia), northern Sweden, and Chile, where rehabilitation progresses in parallel with continuous monitoring [21, 51, 61]. Similarly, the monitoring tools proposed, such as Sentinel satellites, UAV mapping, and in-situ sensors are technically accessible, cost-efficient, and scalable. The staged implementation approach allows incremental investment while maintaining performance feedback for evaluation, to ensure that management remains both adaptive and economically sustainable. From the results we have combined with the best practices, we can conclude that the framework we propose represents a feasible and science-based for managing and rehabilitating legacy tailings, not only within the IPB but could also be implemented to other mining regions facing similar hydrogeochemical

challenges.

## 5.2. Limitations

The geochemical dataset used in this study was limited to Lagunazo, as no contemporary sampling data were available for Mina Tharsis. This restricts direct spatial comparison and may underrepresent localized heterogeneity within the district. In addition, coarse resolution also limits the detection of small-scale hydrochemical gradients. As a result, the derived geochemical risk assessments for Tharsis only rely on indirect evidence from remote sensing and hydrological proxies.

Hydrological estimates were primarily derived from surface models and assumed water levels, without accounting for potential subsurface seepage through fractured or porous materials beneath Tharsis. As a result, hidden preferential flow paths and subsurface drainage may remain uncharacterized. Moreover, the absence of continuous monitoring during the wet season introduces uncertainty in capturing short-lived but critical AMD discharge that typically occur immediately after rainfall. Remote sensing analysis, despite being effective, also face intrinsic limitations, such as cloud cover, mixed pixel effects in narrow ponds, and temporal gaps between acquisitions.

## 5.3. Future recommendations

Future research should prioritize the collection of higher resolution and more frequent data to strengthen the reliability and predictive capacity of the monitoring framework. Expanding the spatial coverage of geochemical and hydrological measurements, particularly across Tharsis, would refine spatial interpolation models and improve calibration of satellite-based indices. Seasonal sampling during both wet and dry periods would capture AMD events and probably clarify the timing of metal mobilization processes.

The integration of Sentinel-2 NDWI with higher-resolution optical or radar imagery (e.g., WorldView or TerraSAR-X) could enhance the detection of small water bodies. Incorporating InSAR-derived ground deformation maps alongside NDWI time series would further clarify the interactions between surface hydrology, tailings consolidation, and potential subsidence mechanisms.

Expanding the framework to other legacy sites within the IPB or another mining districts with similar risks would test the transferability of the indicators across varying lithological and climatic settings. Incorporating Machine Learning (ML) algorithms for automated classification of water bodies, vegetation stress, or anomalous zones could further optimize large-scale monitoring and reduce manual interpretation biases.

Coupling satellite observations with UAV-based surveys and ground-based sensors would bridge the spatial and temporal gaps, enabling multi-scale, and real-time data assimilation. This integrated approach can be useful for the development of early warning systems, which is capable of detecting hydrological and geochemical anomalies, by supporting safer, more transparent, and more sustainable management of TSF.

# 6

# Conclusion

## 6.1. Main research question

*How can a conceptual monitoring framework improve the understanding of environmental risks, guide cost-effective management decisions, and support phased rehabilitation in the Tharsis–Lagunazo mining area?*

This study demonstrates that integrating geochemical, geotechnical, hydrological, and remote-sensing data into a single risk-based monitoring framework can significantly enhance the early detection of AMD risks and support effective rehabilitation.

At Lagunazo, the framework focuses on controlling contamination sources and regularly monitoring water quality at the outlet to Embalse del Lagunazo. At Tharsis, it prioritizes separating clean and contaminated water, monitoring pit-lake levels and quality, and maintaining slope stability. Simple decision tools, such as the CRI and MCDA, help direct investments to the most effective actions, supporting adaptive and cost-efficient rehabilitation over a 10-year period.

### 6.1.1. Sub−research question 1

*Which factors have the greatest influence on environmental risks at Lagunazo and Mina Tharsis?*

Risk drivers vary by site. At Lagunazo, risks are mainly linked to water quality, short hydrological flow paths, and flat tailings surfaces that promote ponding and infiltration. Margins contribute to fine and metal transport during storms. At Tharsis, hydro-meteorological conditions dominate, followed by geotechnical instability on steep benches and dump faces. Acidic pit lakes act as long-term contamination sources, with periodic mixing and storm events intensifying releases.

### 6.1.2. Sub−research question 2

*How suitable and ready are different monitoring tools for detecting and tracking these factors, and how can they be combined into an integrated system?*

High-TRL tools such as staff gauges, sondes, weirs, and pXRF units are ready for immediate use, providing reliable baselines for AMD load and hotspot detection. Medium-TRL tools including UAV photogrammetry, crack and tilt sensors, and Sentinel- 2 data improve spatial coverage and track erosion, wet areas, and vegetation.

### 6.1.3. Sub−research question 3

*How can field observations, laboratory analyses, and satellite-based data be integrated into a conceptual monitoring framework that supports waste management and long-term environmental rehabilitation planning?*

Field, laboratory, and satellite datasets can be effectively integrated into a monitoring framework by linking hydrological, geochemical, and remote-sensing indicators. The results show that NDWI and

DEM-based analyses, when validated with water quality and in situ data, reliably identify ponding zones and AMD-affected areas. This integration improves early detection of environmental change. The proposed framework also aligns with international standards for mine closure, providing a practical basis for long-term monitoring and rehabilitation planning in legacy tailings sites.

### 6.1.4. Sub−research question 4

*How can rehabilitation activities be prioritized and phased over time based on environmental risk levels?*

A five-phase plan is proposed to reduce AMD and stabilize site conditions over time. **Phase I** separates clean water from sulfide areas, seals hotspots, and installs key monitoring tools. **Phase II** extends lined ditches and trenches at Tharsis, adds a reactive cover and polishing cell at Lagunazo, and places limestone drains near pit-lake edges. **Phase III** completes diversions and toe drains, reinforces slopes, and continues surface capping and revegetation. **Phase IV** expands the best-performing covers, improves monitoring, and removes temporary works. **Phase V** treats any remaining hotspots and shifts to long-term maintenance supported by remote sensing.

Expected results include about a one-unit increase in pH, a significant drop in dissolved Cu, Zn, and Cd, less visible erosion by Years 2–3, and massive vegetation cover after two growing seasons.

# Bibliography


[1] *Actualización de mapas de peligrosidad sísmica de españa 2012* (tech. rep.). (2017). Instituto Geográfico Nacional (IGN). https://www.ign.es/web/libros-digitales/peligrosidad-sismica2012

[2] Australian Industrial Chemicals Introduction Scheme. (2024). Zinc environmental hazards [Accessed: 2025-08-29]. https://www.industrialchemicals.gov.au/sites/default/files/2024-04/EVA00143%20-%20Draft%20Evaluation%20Statement.pdf

[3] Barceloux, D. (1999). Chromium. *Journal of Toxicology: Clinical Toxicology*, *37*(2), 173–194. https://doi.org/10.1081/CLT-100102418

[4] Benito, B., Navarro, M., Gaspar-Escribano, J., Vidal, F., Góngora, A., García-Rodríguez, M., & Martínez-Solares, J. (2009). Seismic hazard in andalusia region (southern spain). *Proceedings of SISMOSAN Project*. https://grupos.topografia.upm.es/sismo/data/Paper-sismosan-Almeria_JRG.pdf

[5] *Cadmium toxicity in the environment* [Frontiers in Environmental Science; Accessed: 2025-08-29]. (2022). https://www.frontiersin.org/articles/10.3389/fenvs.2022.949581/full

[6] Canovas, C. R., Macias, F., Basallote, M. D., Olias, M., Nieto, J. M., & Perez-Lopez, R. (2021). Metal(loid) release from sulfide-rich wastes to the environment: The case of the iberian pyrite belt (sw spain). *Current Opinion in Environmental Science & Health*, *20*, 100240. https://doi.org/10.1016/j.coesh.2021.100240

[7] Canovas, C. R., Olias, M., Nieto, J. M., Sarmiento, A. M., & Ceron, J. C. (2021). Hydrogeochemical characteristics of acid mine drainage in the iberian pyrite belt: Lessons learned from decades of studies. *Journal of Environmental Management*, *277*, 111383. https://doi.org/10.1016/j.jenvman.2020.111383

[8] Cánovas, C. R., Olías, M., Macías, F., Torres, E., Miguel, E. G. S., Galván, L., Ayora, C., & Nieto, J. M. (2016). Water acidification trends in a reservoir of the iberian pyrite belt (sw spain). *Science of the Total Environment*, *541*, 400–411. https://doi.org/10.1016/j.scitotenv.2015.09.070

[9] Cao, X., et al. (2008). Immobilization of lead in contaminated soils by phosphate amendments. *Environmental Science and Pollution Research*, *15*(5), 459–466. https://doi.org/10.1065/espr2007.05.416

[10] Castro, J., & Ayora, C. (2015). Acid mine drainage in the iberian pyrite belt: An overview and remediation strategies. *Journal of Geochemical Exploration*, *154*, 4–11.

[11] Centers for Disease Control and Prevention. (2024). *Soil contamination and lead* [Accessed: 2025-08-29]. https://www.cdc.gov/lead-prevention/prevention/soil.html

[12] Centro Nacional de Información Geográfica (CNIG). (2025). Corine land cover (clc) 2018 dataset [Accessed: October 2025].

[13] Chalkley, R., Crane, R. A., Eyre, M., Hicks, K., Jackson, K.-M., & Hudson-Edwards, K. A. (2023). A multi-scale feasibility study into acid mine drainage (amd) monitoring using same-day observations. *Remote Sensing*, *15*(1), 76. https://doi.org/10.3390/rs15010076

[14] Chovan, K. M., Julien, M. R., Ingabire, E.-P., James, M., Masengo, E., Lépine, T., & Lavoie, P. (2021). A risk assessment tool for tailings storage facilities [Early access / ahead of print at time of publication]. *Canadian Geotechnical Journal*. https://doi.org/10.1139/cgj-2020-0329

[15] Cigna, F., & Tapete, D. (2019). Satellite insar monitoring of mining-induced subsidence: Recent results and future prospects. *International Journal of Applied Earth Observation and Geoinformation*, *82*, 101930.

[16] Consorcio de Compensación de Seguros. (n.d.). Earthquake of 28 february 1969, sw cape of saint vincent: Effects in huelva and cádiz. https://www.consorsegurosdigital.com/en/numero-04/in-depth/earthquakes-in-spain-recent-activity-in-the-alboran-sea-en/

[17] *Copper toxicity in aquatic systems* [Frontiers in Environmental Science; Accessed: 2025-08-29]. (2022). https://www.frontiersin.org/articles/10.3389/fenvs.2022.949581/full

[18] Coppin, P., Jonckheere, I., Nackaerts, K., Muys, B., & Lambin, E. (2004). Review: Digital change detection in ecosystem monitoring: A review. *International Journal of Remote Sensing*, *25*(9), 1565–1596.
[19] Costa, M. (1997). Toxicity and carcinogenicity of cr(vi) in animal models and humans. *Critical Reviews in Toxicology*, *27*(5), 431–442. https://doi.org/10.3109/10408449709078442
[20] Crespo, M. J., et al. (2014). Seismic hazard of the iberian peninsula. *Natural Hazards and Earth System Sciences*, *14*, 1309–1323. https://nhess.copernicus.org/articles/14/1309/2014/nhess-14-1309-2014.pdf
[21] Edraki, M., Tornos, F., & Arvidsson, R. (2022). Adaptive and sustainable mine closure: Lessons from chilean and scandinavian case studies. *Journal of Cleaner Production*, *369*, 133419. https://doi.org/10.1016/j.jclepro.2022.133419
[22] *Environmental impacts of arsenic: A review* [Frontiers in Environmental Science; Accessed: 2025-08-29]. (2022). https://www.frontiersin.org/articles/10.3389/fenvs.2022.949581/full
[23] European Commission. (2021). Mine waste and extractive waste management in the european union – report on best practices. https://ec.europa.eu/environment/waste/mining/
[24] European Space Agency (ESA). (2025a). Copernicus open access hub – sentinel-1 sar imagery [Accessed: October 2025].
[25] European Space Agency (ESA). (2025b). Copernicus open access hub – sentinel-2 level-2a imagery [Accessed: October 2025].
[26] European Union. (2020). Directive (eu) 2020/2184 on the quality of water intended for human consumption [Official Journal of the European Union, L 435, 23.12.2020].
[27] Fernandez-Caliani, J. C., Barba-Barragan, A., Gonzalez, I., & Cantano, M. (2008). Heavy metal pollution in soils around the abandoned mine sites of the iberian pyrite belt (southwest spain). *Water, Air, & Soil Pollution*, *200*(1–4), 211–226. https://doi.org/10.1007/s11270-008-9907-2
[28] Gazea, B., Adam, K., & Kontopoulos, A. (1996). Review of passive systems for the treatment of acid mine drainage. *Minerals Engineering*, *9*(1), 23–42.
[29] Geological and Mining Institute of Spain (IGME). (2025). Igme geochemical database portal [Accessed: October 2025].
[30] Gonzalez, R. M., Olias, M., Macias, F., Canovas, C. R., & Fernandez de Villaran, R. (2018). Hydrological characterization and prediction of flood levels of acidic pit lakes in the tharsis mines, iberian pyrite belt. *Journal of Hydrology*, *566*, 807–817. https://doi.org/10.1016/j.jhydrol.2018.09.046
[31] Grande, J. A., Luís, A. T., Córdoba, F., Leiva, M., Dávila, J. M., Fortes, J. C., Santisteban, M., da Silva, E. F., & Sarmiento, A. M. (2021). Odiel river (sw spain), a singular scenario affected by acid mine drainage (amd): Graphical and statistical models to assess diatoms and water hydrogeochemistry interactions. *International Journal of Environmental Research and Public Health*, *18*(16), 8454. https://doi.org/10.3390/ijerph18168454
[32] Grimalt, J. O., Ferrer, M., & Macpherson, E. (1999). The donana disaster: Heavy metal contamination of a world heritage wetland. *Science of the Total Environment*, *242*(1–3), 13–30.
[33] Hedin, R. S., Nairn, R. W., & Kleinmann, R. L. P. (1994). *Passive treatment of coal mine drainage*. U.S. Bureau of Mines.
[34] ICMM, UNEP, & PRI. (2020). Global industry standard on tailings management.
[35] Instituto Geográfico Nacional (IGN). (2015). Peligrosidad sísmica de españa: Pga (10% en 50 años, periodo de retorno 475 años), suelo tipo roca. https://www.ign.es/web/resources/sismologia/PGA_475_DINA1_Web_Espanol.pdf
[36] Instituto Geográfico Nacional (IGN). (2025). Centro de descargas – modelo digital del terreno (mdt02) [Accessed: October 2025].
[37] Interstate Technology & Regulatory Council. (2020). Mining waste treatment technology selection [Accessed: 2025-09-18].
[38] Isgro, M. A., Basallote, M. D., & Barbero, L. (2022). Unmanned aerial system-based multispectral water quality monitoring in the iberian pyrite belt (sw spain). *Mine Water and the Environment*, *41*, 30–41. https://doi.org/10.1007/s10230-021-00837-4
[39] Isgró, M. A., Basallote, M. D., & Barbero, L. (2022a). Comparison of uas and sentinel-2 multispectral imagery for water quality monitoring: A case study for acid mine drainage affected areas (sw spain) [Reports neutral agricultural reservoirs (e.g., EG, EL) and acidic water bodies in Thar-

sis; overall range pH ∼0.01–7.76]. *Remote Sensing*, *14*(16), 4053. https://doi.org/10.3390/rs14164053

[40] Isgró, M. A., Basallote, M. D., & Barbero, L. (2022b). Unmanned aerial system–based multispectral water quality monitoring in the iberian pyrite belt (sw spain). *Mine Water and the Environment*, *41*, 30–41. https://doi.org/10.1007/s10230-021-00837-4

[41] Itasca International Inc. (2021). *Proposing a geotechnical risk index (gri)* (tech. rep.) (Technical application note / white paper). Itasca International Inc. https://itasca-int.objects.frb.io/assets/docs/about/documents/software/applications/Geotechnical-Risk-Index-reviewed.pdf

[42] Jaishankar, M., Tseten, T., Anbalagan, N., Mathew, B., & Beeregowda, K. (2014). Toxicity, mechanism and health effects of some heavy metals. *Interdisciplinary Toxicology*, *7*(2), 60–72. https://doi.org/10.2478/intox-2014-0009

[43] Karaouglu, M., Zor, c., & Uugurlu, M. (2010). Biosorption of cr(iii) from solutions using vineyard pruning waste. *Chemical Engineering Journal*, *159*, 98–106. https://doi.org/10.1016/j.cej.2010.02.047

[44] Leistel, J. M., Marcoux, E., Thiéblemont, D., & et al. (1998). The volcanic-hosted massive sulphide deposits of the iberian pyrite belt: Review and preface to the special issue. *Mineralium Deposita*, *33*(1-2), 2–30. https://doi.org/10.1007/s001260050130

[45] Lucieer, A., de Jong, S. M., & Turner, D. (2014). Uav-based photogrammetry for mapping and monitoring of landslides. *Earth Surface Processes and Landforms*, *39*(1), 92–97.

[46] Macias, F., Perez-Lopez, R., Caraballo, M. A., Nieto, J. M., Ayora, C., & Castillo, J. (2017). Passive treatment of acid mine drainage using open limestone channels: A case study in the iberian pyrite belt (sw spain). *Water*, *9*(6), 415. https://doi.org/10.3390/w9060415

[47] Macklin, M. G., et al. (2006). A review of the environmental impacts of metal mining and the potential for natural recovery. *Earth-Science Reviews*, *79*(1-2), 1–25.

[48] Mankins, J. C. (2009). Technology readiness assessments: A retrospective. *AIAA SPACE 2009 Conference & Exposition*, 1–11.

[49] Martin, A. J., et al. (2014). Hydrochemical characteristics and seasonal influence on the water quality of a reservoir affected by acid mine drainage (iberian pyrite belt, sw spain). *Environmental Science and Pollution Research*, *21*(10), 6306–6321.

[50] Martin-Mendez, I., Galan, E., Romero-Baena, A. J., & Valverde, J. (2023). Soil geochemistry and geochemical baselines in the iberian pyrite belt: Implications for environmental assessment. *Mineral Economics*, *36*(1), 53–68. https://doi.org/10.1007/s41513-023-00210-0

[51] McCullough, C. D. (2020). *Mine closure and completion: Environmental management handbook*. CSIRO Publishing.

[52] Ministerio para la Transición Ecológica y el Reto Demográfico (MITECO). (2025). Miteco geographic portal – environmental and land-use maps [Accessed: October 2025].

[53] Moreno-Gonzalez, R., Isgro, V., & Sanchez-Espana, J. (2022). Seasonal dynamics of mine pit lakes in the iberian pyrite belt: Implications for water quality and management. *Science of the Total Environment*, *826*, 154146. https://doi.org/10.1016/j.scitotenv.2022.154146

[54] Moreno-Gonzalez, R., Macias, F., Olias, M., & Ruiz Canovas, C. (2022). Temporal evolution of acid mine drainage (amd) leachates from the abandoned tharsis mine (iberian pyrite belt, spain). *Environmental Pollution*, *295*, 118697. https://doi.org/10.1016/j.envpol.2021.118697

[55] Moreno-Gonzalez, R., Ruiz-Canovas, C., Olias, M., & Macias, F. (2020). Seasonal variability of extremely metal-rich acid mine drainages from the tharsis mines (sw spain). *Environmental Pollution*, *259*, 113829. https://doi.org/10.1016/j.envpol.2019.113829

[56] Muller, D., et al. (2021). High-efficiency arsenic removal by electrocoagulation with iron dosage. *Water*, *13*(5), 687. https://doi.org/10.3390/w13050687

[57] National Center for Biotechnology Information. (2022). Zinc toxicity and health effects [Accessed: 2025-08-29]. https://www.ncbi.nlm.nih.gov/books/NBK554548/

[58] Nieto, J. M., Sarmiento, A. M., Olias, M., Canovas, C. R., Riba, I., Kalman, J., & Delvalls, T. A. (2013). Acid mine drainage in the iberian pyrite belt: Overview and environmental impacts. *Environmental Science and Pollution Research*, *20*(11), 7524–7541. https://doi.org/10.1007/s11356-013-1634-7

[59] Nieto, J. M., Sarmiento, A. M., Olías, M., Cánovas, C. R., & Riba, I. (2007a). Acid mine drainage in the iberian pyrite belt: An overview with special emphasis on current environmental problems. *Mine Water and the Environment*, *26*(4), 267–275. https://doi.org/10.1007/s10230-007-0027-9

[60] Nieto, J. M., et al. (2007b). Acid mine drainage in the iberian pyrite belt: An overview and field trip guide. *Macla*, *7*, 22–33.
[61] Nordic Mining Research Network. (2022). Sustainable mine closure practices in the nordic region. https://nordicminingnetwork.org/sustainable-closure
[62] Nordstrom, D. K. (2011). Mine waters: Acidic to circumneutral. *Elements*, *7*(6), 393–398.
[63] Olías, M., Cánovas, C. R., Macías, F., & Basallote, M. D. (2013). Water quality and distribution of trace elements in the tharsis mines (iberian pyrite belt, sw spain). *Applied Geochemistry*, *28*, 123–135. https://doi.org/10.1016/j.apgeochem.2012.10.010
[64] Olías, M., Nieto, J. M., Sarmiento, A. M., Cánovas, C. R., & Delgado, J. (2006). Seasonal water quality variations in a river affected by acid mine drainage: The odiel river (south west spain). *Science of the Total Environment*, *333*(1-3), 267–281. https://doi.org/10.1016/j.scitotenv.2004.12.036
[65] Olías, M., Nieto, J. M., Sarmiento, A. M., & Cánovas, C. R. (2004). Seasonal water quality variations in a river affected by acid mine drainage: The odiel river (south west spain). *Science of the Total Environment*, *333*, 267–281. https://doi.org/10.1016/j.scitotenv.2004.05.012
[66] Parbhakar-Fox, A., McCullough, C. D., & Edraki, M. (2022). Advances in mine rehabilitation monitoring and closure planning in australia. *Environmental Earth Sciences*, *81*(7), 1–18. https://doi.org/10.1007/s12665-022-10371-4
[67] Parbhakar-Fox, A., & Lottermoser, B. (2020). Remote sensing for mine waste monitoring: A review. *Remote Sensing*, *12*(6), 981.
[68] Perez-Lopez, R., Nieto, J. M., & de la Rosa, J. D. (2011). Acid mine drainage in the iberian pyrite belt: An overview with special emphasis on current remediation strategies. *Hydrometallurgy*, *104*(3-4), 278–284.
[69] Relvas, J. M. R. S., Barriga, F. J. A. S., Ferreira, A., & et al. (2001). Hydrothermal alteration and mineralization in the neves corvo volcanic-hosted massive sulfide deposit, iberian pyrite belt, portugal. *Mineralium Deposita*, *36*, 416–434. https://doi.org/10.1007/s001260100178
[70] Riaza, A., Buzzi, J., Garcia-Melendez, E., Carrere, V., & Muller, A. (2011). Monitoring the extent of contamination from acid mine drainage in the iberian pyrite belt (sw spain) using hyperspectral imagery. *Remote Sensing*, *3*(10), 2166–2186. https://doi.org/10.3390/rs3102166
[71] Sanchez-Espana, J., Lopez Pamo, E., Santofimia, E., & Diez Ercilla, M. (2008). The acidic mine pit lakes of the iberian pyrite belt: An approach to their physical limnology and hydrogeochemistry. *Applied Geochemistry*, *23*(5), 1260–1287. https://doi.org/10.1016/j.apgeochem.2007.12.036
[72] Santos, A., Olías, M., & Nieto, J. M. (2020). Climatic influence on acid mine drainage generation and metal mobility in the iberian pyrite belt, sw spain. *Science of the Total Environment*, *717*, 137171. https://doi.org/10.1016/j.scitotenv.2020.137171
[73] Sarmiento, A. M., Nieto, J. M., Olias, M., & Cánovas, C. R. (2009). Hydrochemical characteristics and seasonal influence on the pollution by acid mine drainage in the odiel river (iberian pyrite belt, sw spain). *Applied Geochemistry*, *24*(5), 697–714. https://doi.org/10.1016/j.apgeochem.2008.12.025
[74] Sarmiento, A. M., Nieto, J. M., Olías, M., Cánovas, C. R., et al. (2006). Environmental impact of mining activities in the odiel watershed (sw spain) [Includes statement that Tharsis leachate flow is constant year-round]. *Proceedings of the 7th International Conference on Acid Rock Drainage (ICARD)*, 1850–1863. https://doi.org/10.21000/JASMR060218501851
[75] Silva, S., et al. (2017). Micro-seismicity in the gulf of cádiz: Is there a link between... *Tectonophysics*. https://ui.adsabs.harvard.edu/abs/2017Tectp.717..226S/abstract
[76] Skousen, J., Sexstone, A., & Ziemkiewicz, P. (2000). *Acid mine drainage control and treatment*. West Virginia University Extension Service.
[77] Taylor, R. J., et al. (1999). The iberian pyrite belt—a review. *Ore Geology Reviews*, *14*(1–3), 1–28.
[78] Tornos, F. (2006). Environment of formation and styles of volcanogenic massive sulfides: The iberian pyrite belt. *Ore Geology Reviews*, *28*(3), 259–307. https://doi.org/10.1016/j.oregeorev.2004.12.005
[79] Torres, E., Ayora, C., Cánovas, C. R., García-Robledo, E., Galván, L., & Sarmiento, A. M. (2016). Oxycline formation induced by fe(ii) oxidation in a water reservoir affected by acid mine drainage [Reports Sancho Reservoir pH near 3.5]. *Environmental Science and Pollution Research*, *23*, 12725–12739. https://doi.org/10.1007/s11356-016-6489-6

[80] *Toxicity of cadmium to aquatic life* [Accessed: 2025-08-29]. (2023). https://pmc.ncbi.nlm.nih.gov/articles/PMC10258679/
[81] United States Geological Survey (USGS). (2025). Usgs earthexplorer – landsat series imagery [Accessed: October 2025].
[82] Wikipedia contributors. (2025a). *Acid mine drainage* [Accessed: 2025-08-29]. https://en.wikipedia.org/wiki/Acid_mine_drainage
[83] Wikipedia contributors. (2025b). *Tharsis-la zarza mining basin* [Accessed: 2025-08-29]. https://en.wikipedia.org/wiki/Tharsis-La_Zarza_mining_basin
[84] Woldai, T., & Fabbri, A. G. (2002). The impact of mining on the environment: A case study from the tharsis–lagunazo mining area, province huelva, sw spain. In A. G. Fabbri, G. Gaal, & R. B. McCammon (Eds.), *Deposit and geoenvironmental models for resource exploitation and environmental security* (pp. 345–364, Vol. 80). Kluwer Academic Publishers. https://doi.org/10.1007/978-94-010-0303-2_17
[85] Wong, M. H. (2003). Ecological restoration of mine degraded soils, with emphasis on metal contaminated soils. *Chemosphere*, *50*(6), 775–780.
[86] World Health Organization. (2017). *Guidelines for drinking-water quality, fourth edition incorporating the first addendum*. https://www.who.int/publications/i/item/9789241549950
[87] World Health Organization. (2023a). Arsenic [Accessed: 2025-08-29]. https://www.who.int/news-room/fact-sheets/detail/arsenic
[88] World Health Organization. (2023b). Lead poisoning and health [Accessed: 2025-08-29]. https://www.who.int/news-room/fact-sheets/detail/lead-poisoning-and-health
[89] Younger, P. L., Banwart, S. A., & Hedin, R. S. (2002). Mine water: Hydrology, pollution, remediation. *Kluwer Academic Publishers*.
[90] *Zinc toxicity to aquatic life* [Accessed: 2025-08-29]. (2023). https://pmc.ncbi.nlm.nih.gov/articles/PMC10258679/

# A

# Geochemical Results

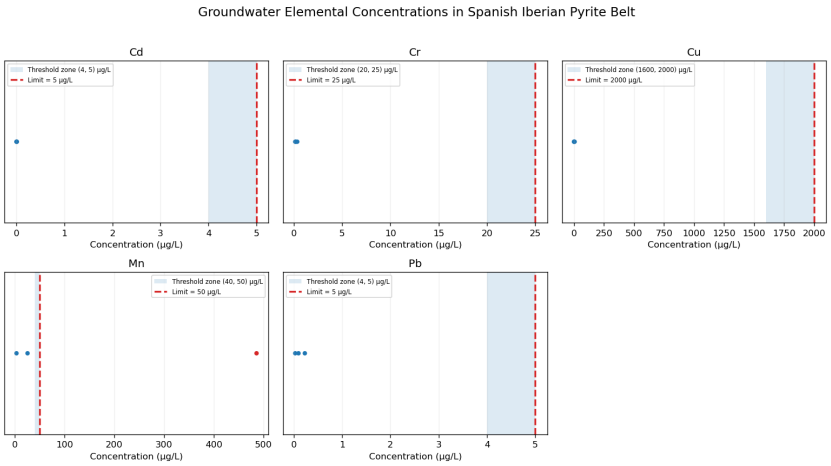



**Figure A.1:** Groundwater Elemental Concentrations in Huelva

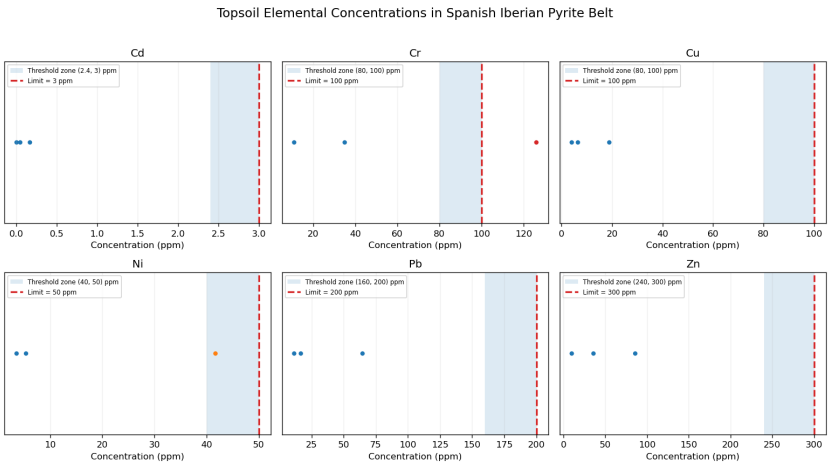



**Figure A.2:** Topsoil Elemental Concentrations in Huelva

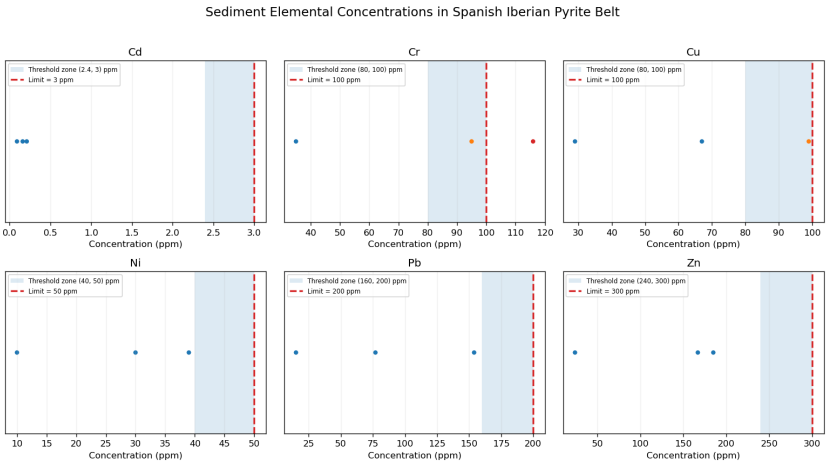



**Figure A.3:** Sediment Elemental Concentrations in Huelva

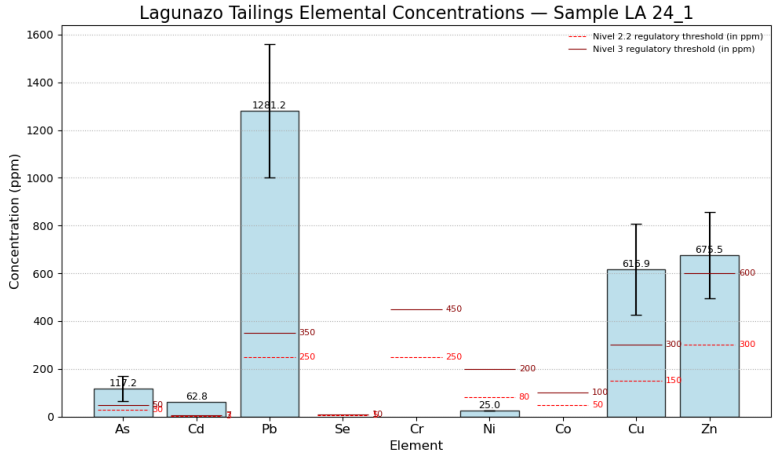



**Figure A.4:** Elemental concentrations for Lagunazo Tailings (sample LA 24-1)

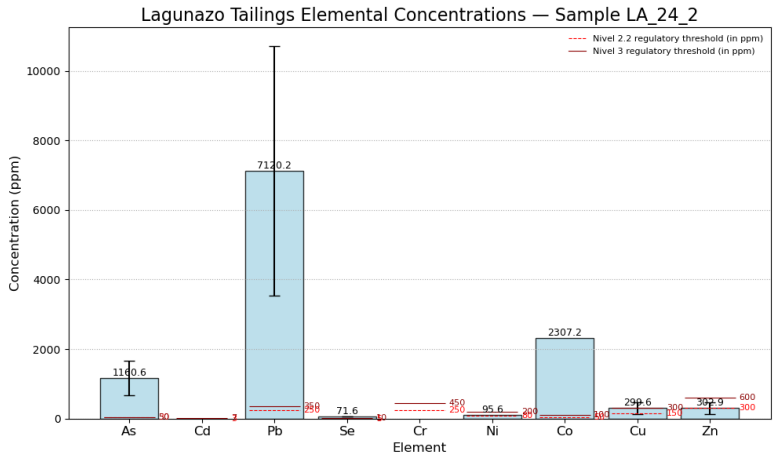



**Figure A.5:** Elemental concentrations for Lagunazo Tailings (sample LA 24-2)

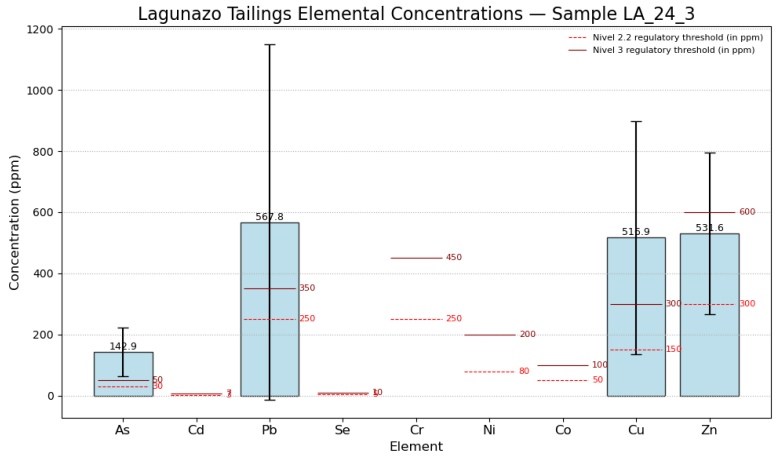



**Figure A.6:** Elemental concentrations for Lagunazo Tailings (sample LA 24-3)

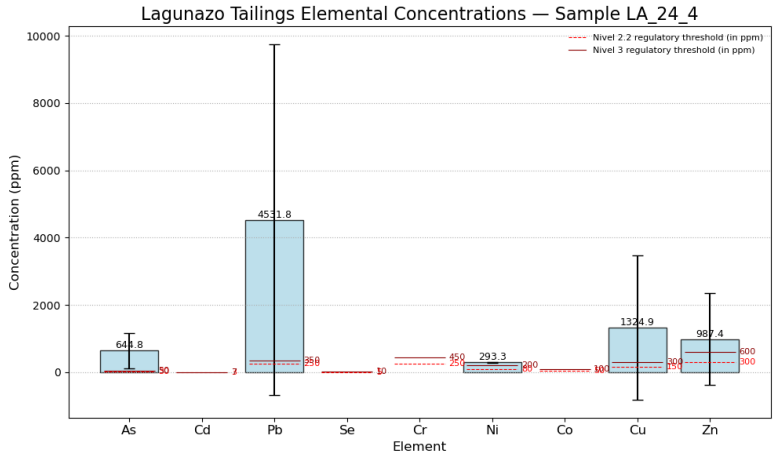



**Figure A.7:** Elemental concentrations for Lagunazo Tailings (sample LA 24-4)

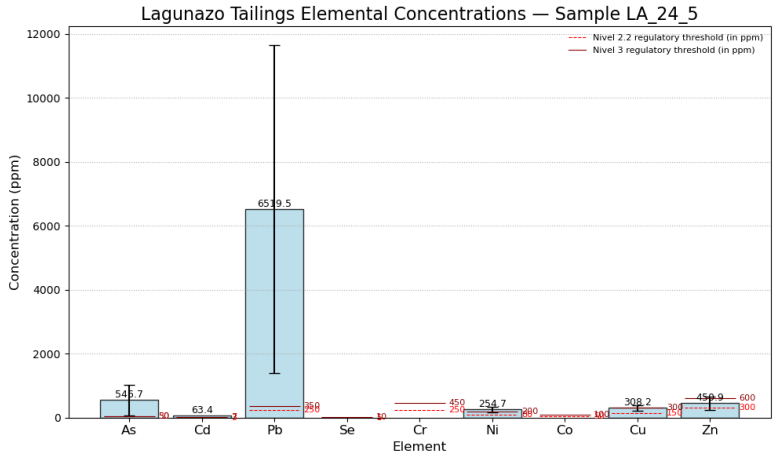



**Figure A.8:** Elemental concentrations for Lagunazo Tailings (sample LA 24-5)

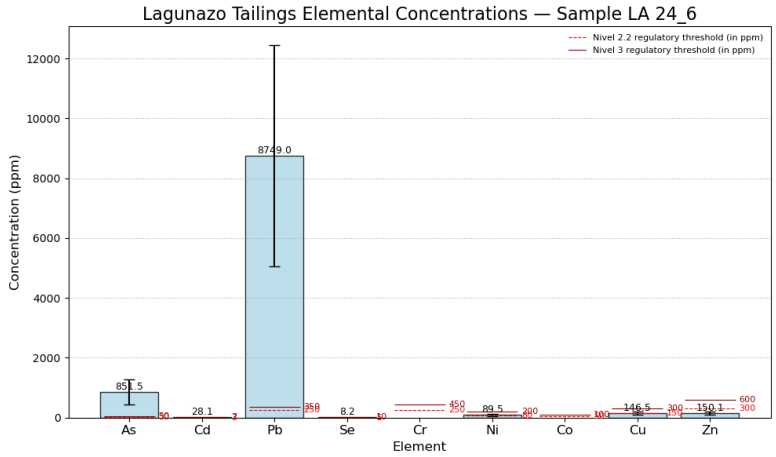



**Figure A.9:** Elemental concentrations for Lagunazo Tailings (sample LA 24-6)

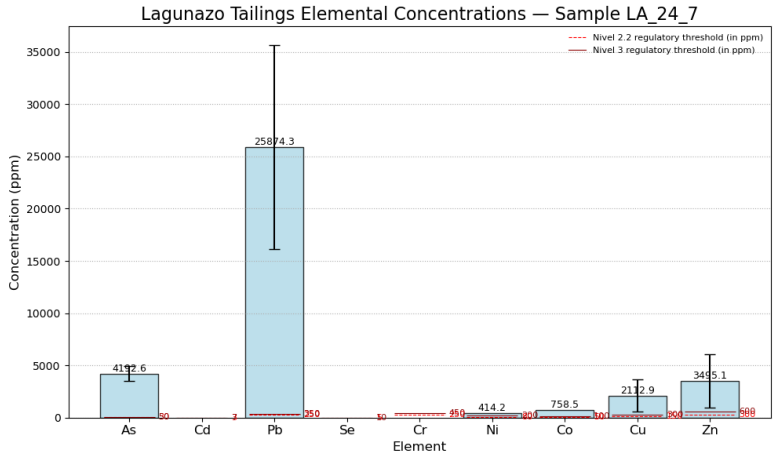



**Figure A.10:** Elemental concentrations for Lagunazo Tailings (sample LA 24-7)

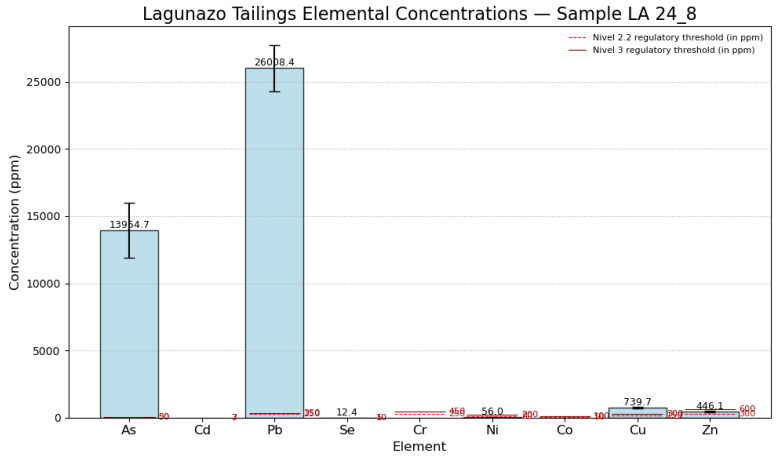



**Figure A.11:** Elemental concentrations for Lagunazo Tailings (sample LA 24-8)

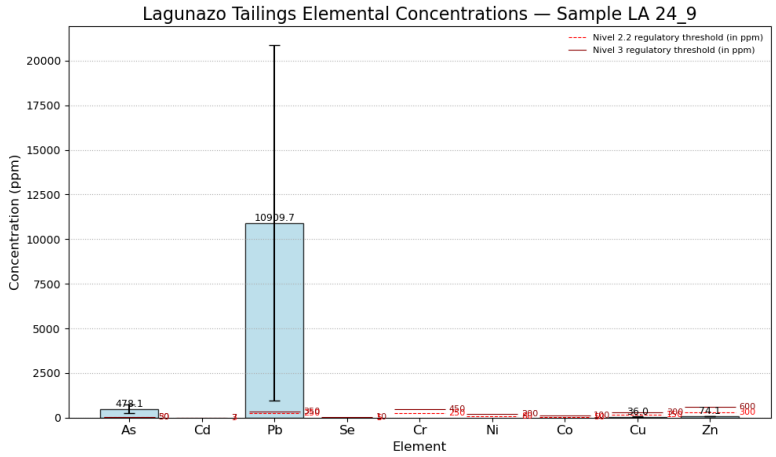



**Figure A.12:** Elemental concentrations for Lagunazo Tailings (sample LA 24-9)

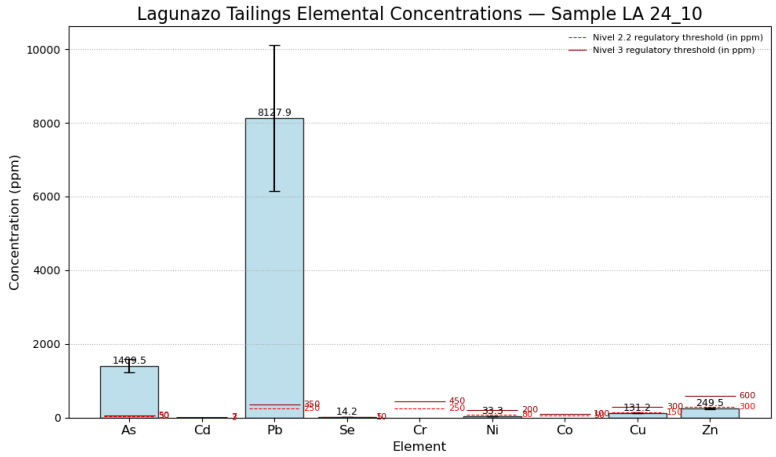



**Figure A.13:** Elemental concentrations for Lagunazo Tailings (sample LA 24-10)

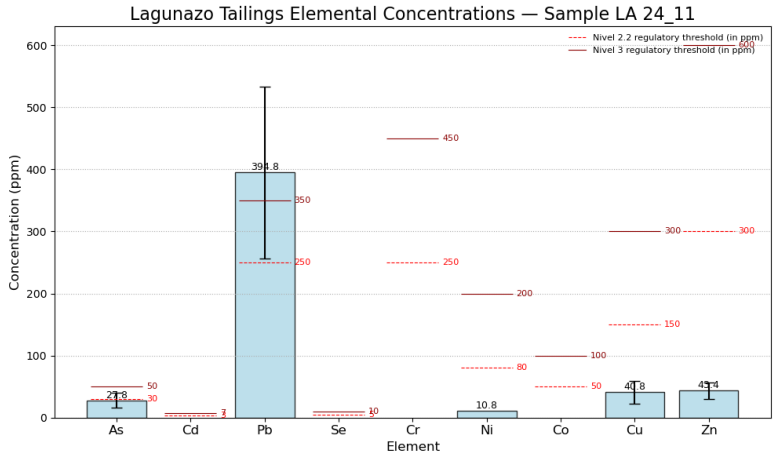



**Figure A.14:** Elemental concentrations for Lagunazo Tailings (sample LA 24-11)

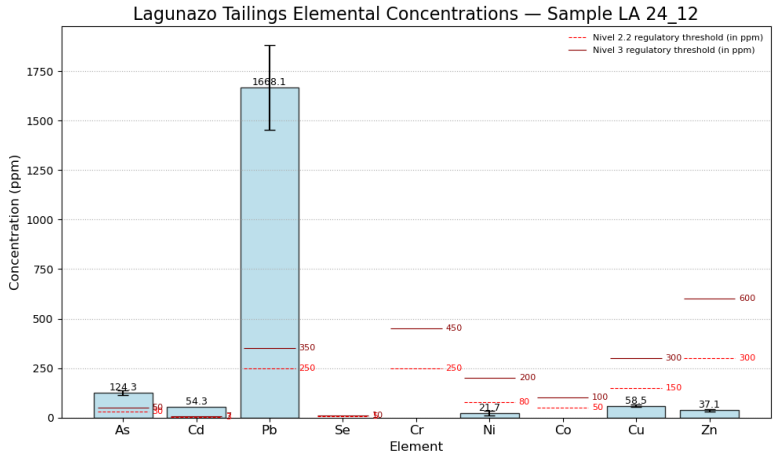



**Figure A.15:** Elemental concentrations for Lagunazo Tailings (sample LA 24-12)

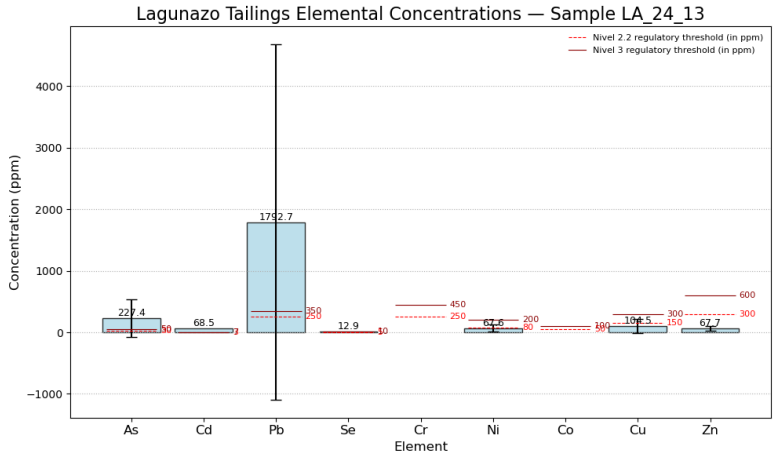



**Figure A.16:** Elemental concentrations for Lagunazo Tailings (sample LA 24-13)

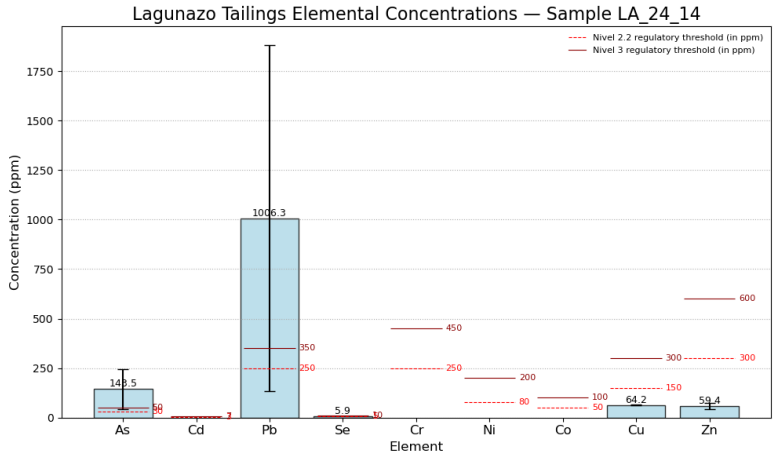



**Figure A.17:** Elemental concentrations for Lagunazo Tailings (sample LA 24-14)

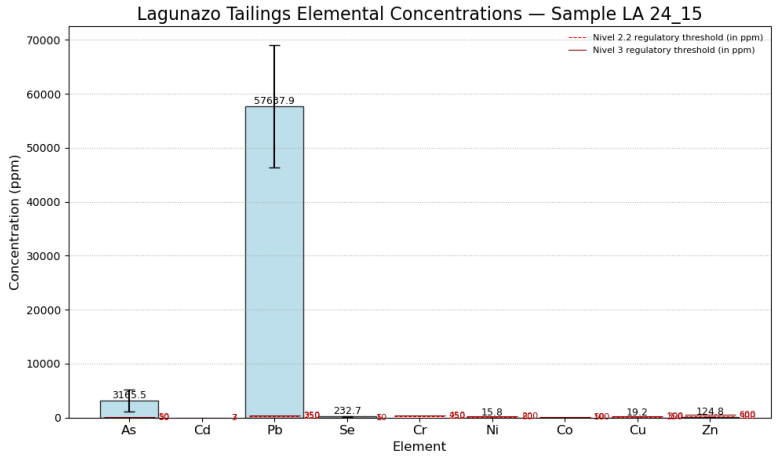



**Figure A.18:** Elemental concentrations for Lagunazo Tailings (sample LA 24-15)

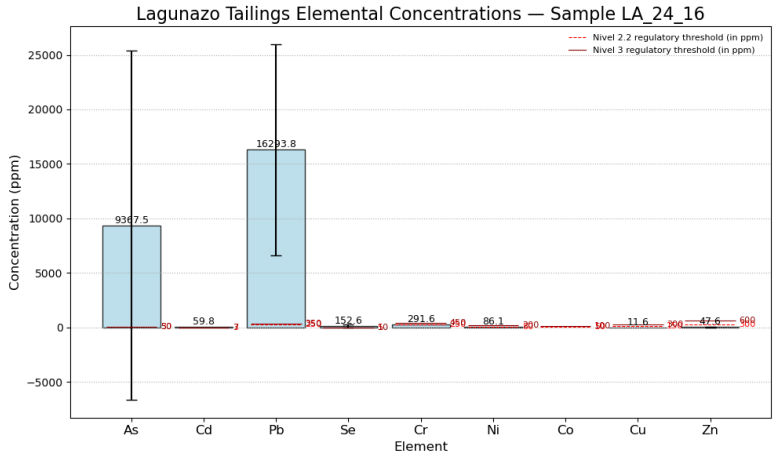



**Figure A.19:** Elemental concentrations for Lagunazo Tailings (sample LA 24-16)

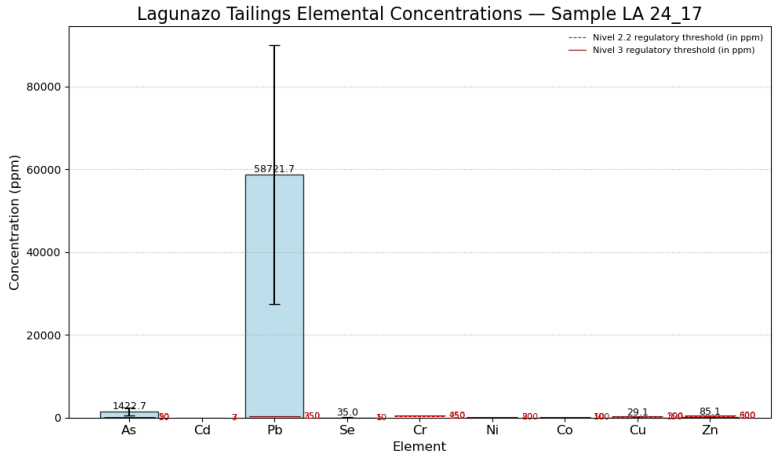



**Figure A.20:** Elemental concentrations for Lagunazo Tailings (sample LA 24-17)

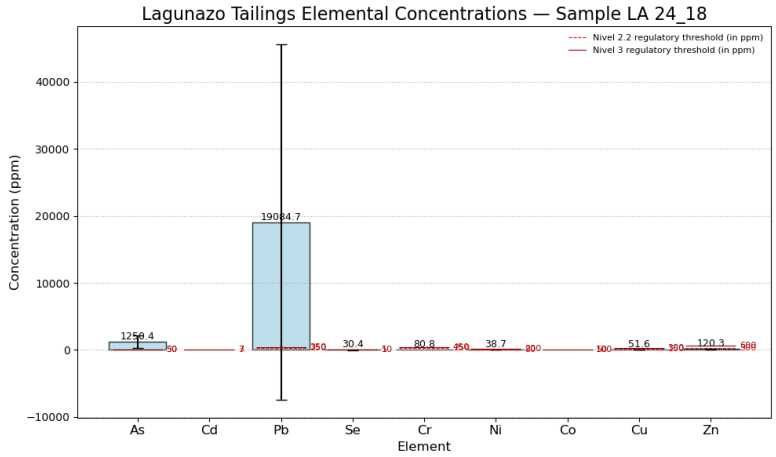



**Figure A.21:** Elemental concentrations for Lagunazo Tailings (sample LA 24-18)

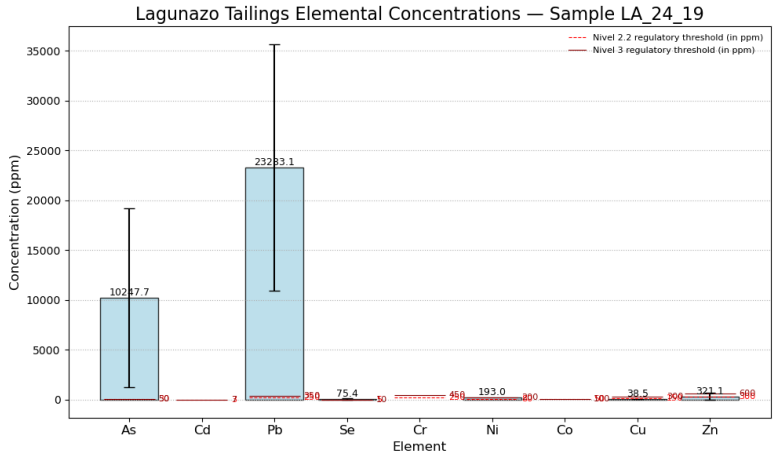



**Figure A.22:** Elemental concentrations for Lagunazo Tailings (sample LA 24-19)

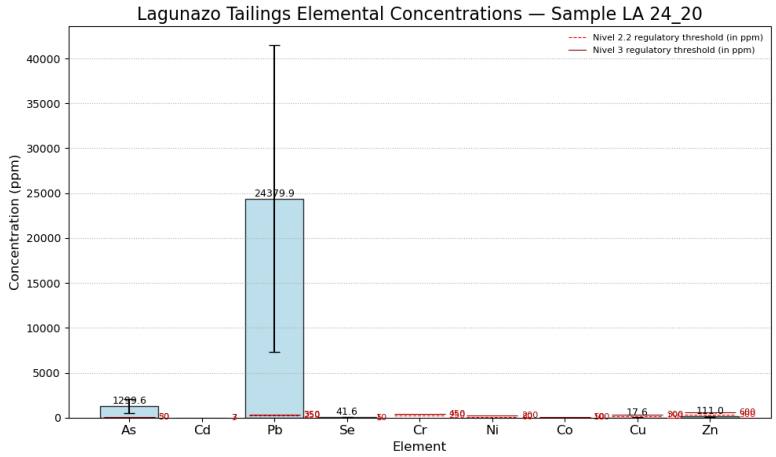



**Figure A.23:** Elemental concentrations for Lagunazo Tailings (sample LA 24-20)

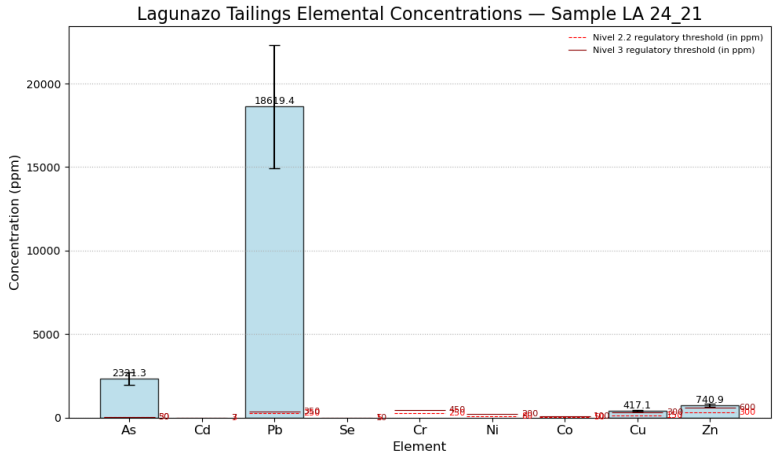



**Figure A.24:** Elemental concentrations for Lagunazo Tailings (sample LA 24-21)

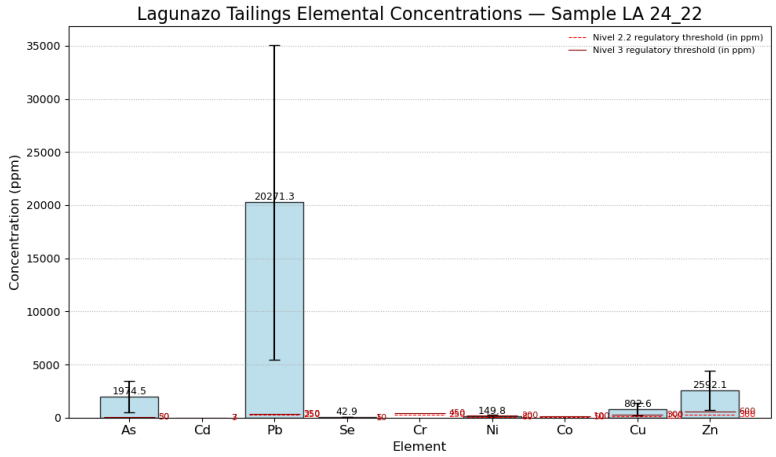



**Figure A.25:** Elemental concentrations for Lagunazo Tailings (sample LA 24-22)

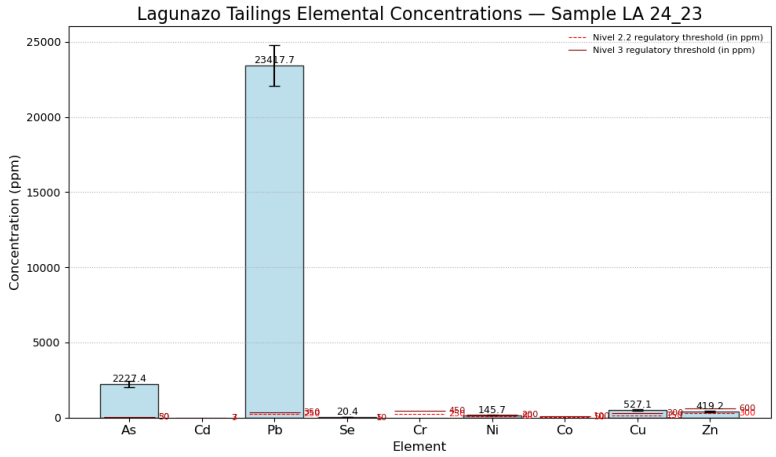



**Figure A.26:** Elemental concentrations for Lagunazo Tailings (sample LA 24-23)

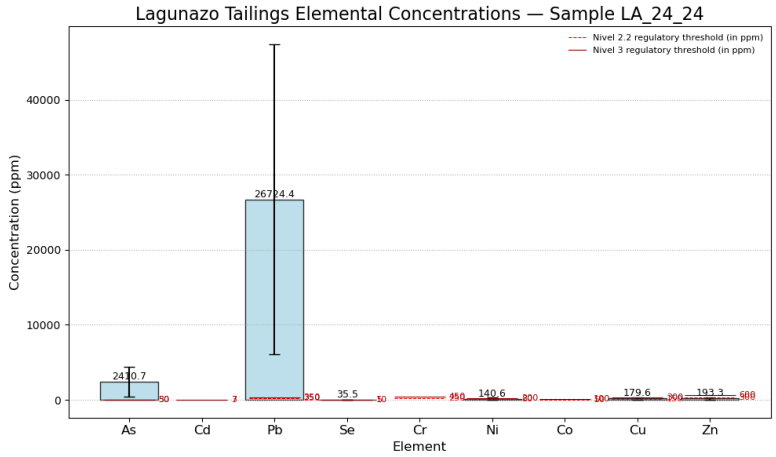



**Figure A.27:** Elemental concentrations for Lagunazo Tailings (sample LA 24-24)

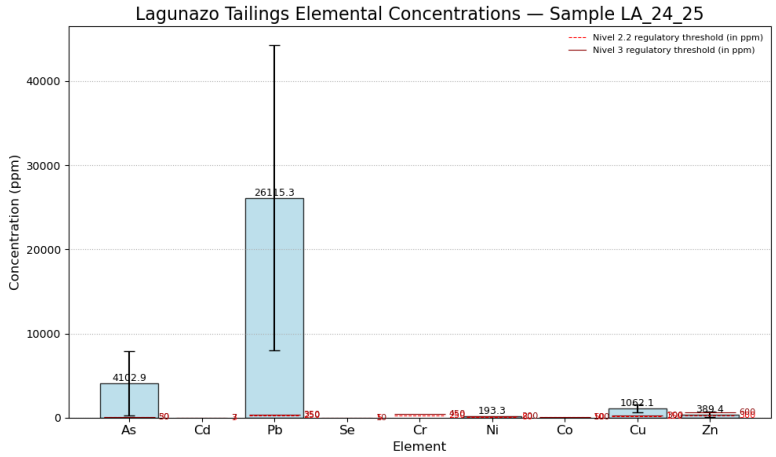



**Figure A.28:** Elemental concentrations for Lagunazo Tailings (sample LA 24-25)

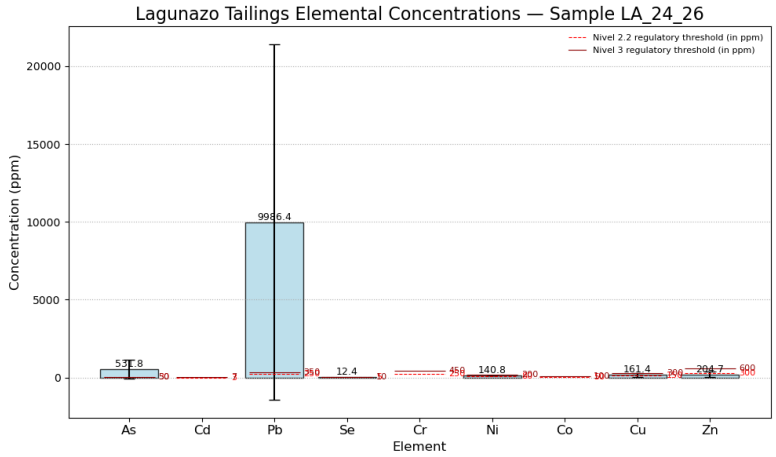



**Figure A.29:** Elemental concentrations for Lagunazo Tailings (sample LA 24-26)

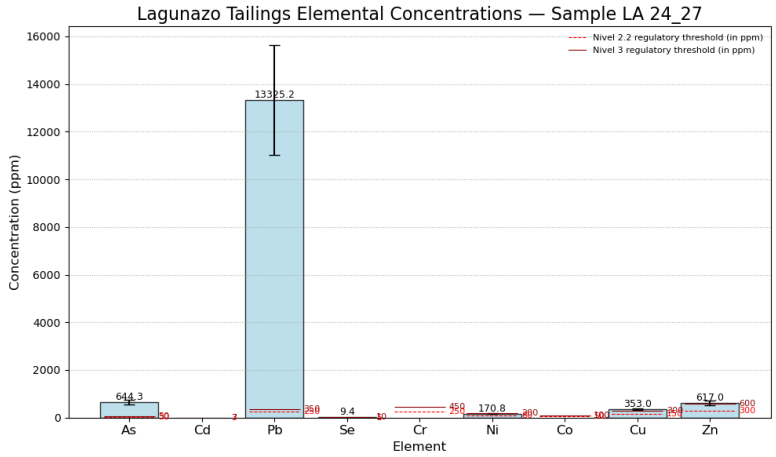



**Figure A.30:** Elemental concentrations for Lagunazo Tailings (sample LA 24-27)

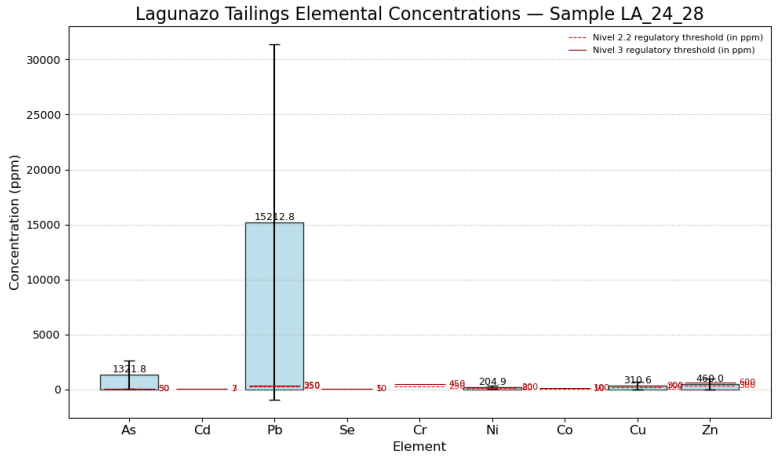



**Figure A.31:** Elemental concentrations for Lagunazo Tailings (sample LA 24-28)

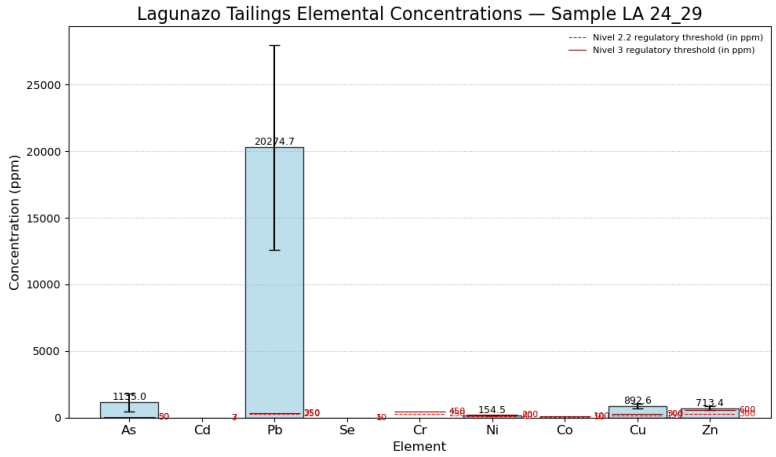



**Figure A.32:** Elemental concentrations for Lagunazo Tailings (sample LA 24-29)

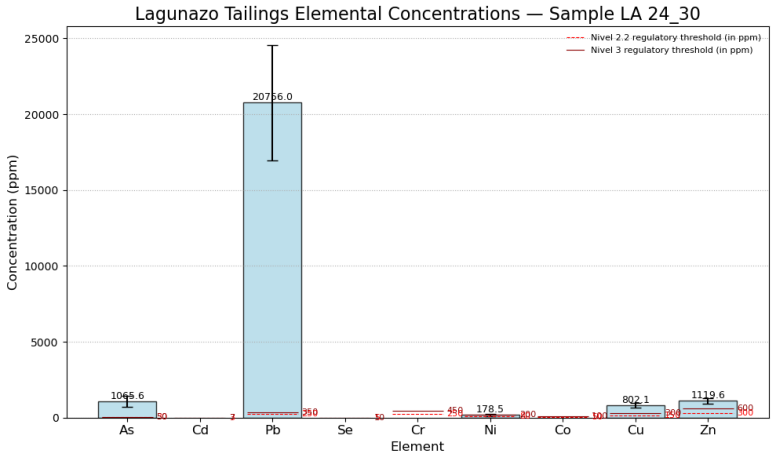



**Figure A.33:** Elemental concentrations for Lagunazo Tailings (sample LA 24-30)

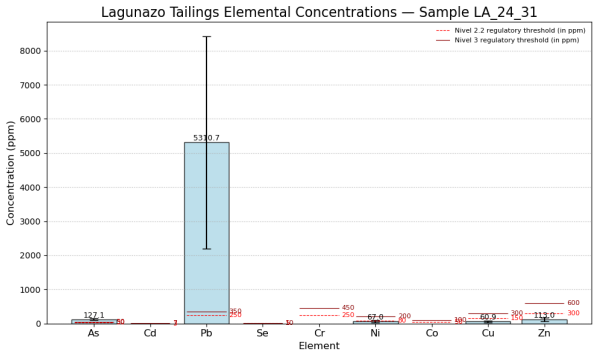



**Figure A.34:** Elemental concentrations for Lagunazo Tailings (sample LA 24-31)

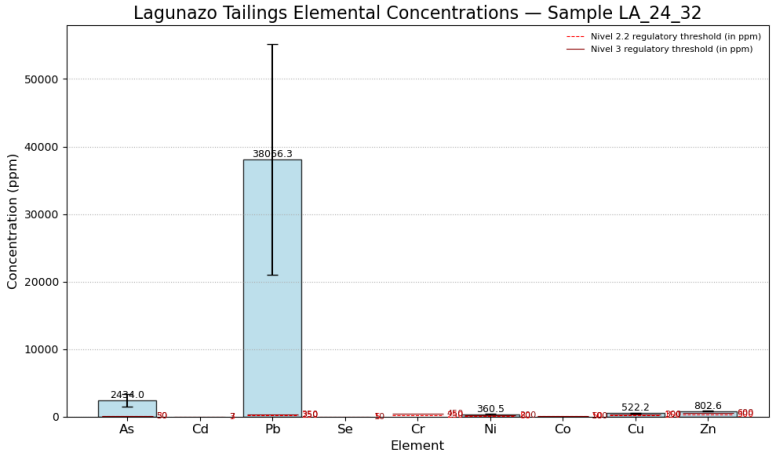



**Figure A.35:** Elemental concentrations for Lagunazo Tailings (sample LA 24-32)

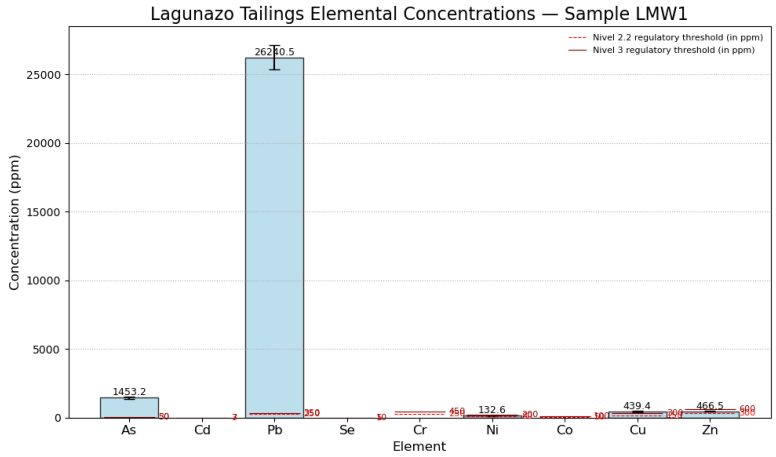



**Figure A.36:** Elemental concentrations for Lagunazo Tailings (sample LMW-1)

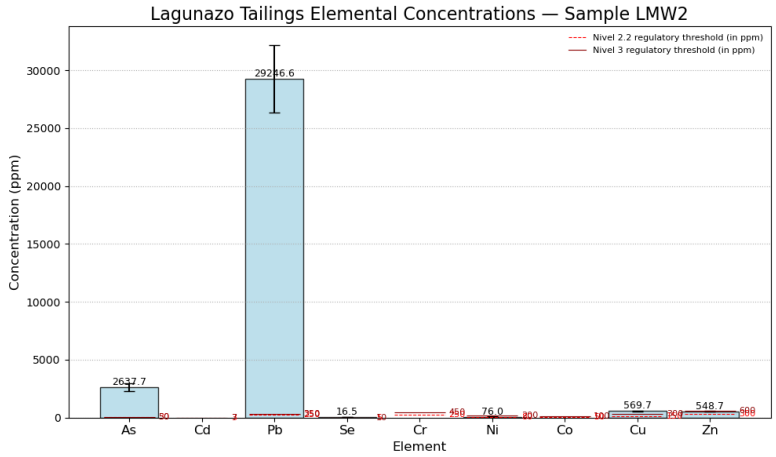



**Figure A.37:** Elemental concentrations for Lagunazo Tailings (sample LMW-2)

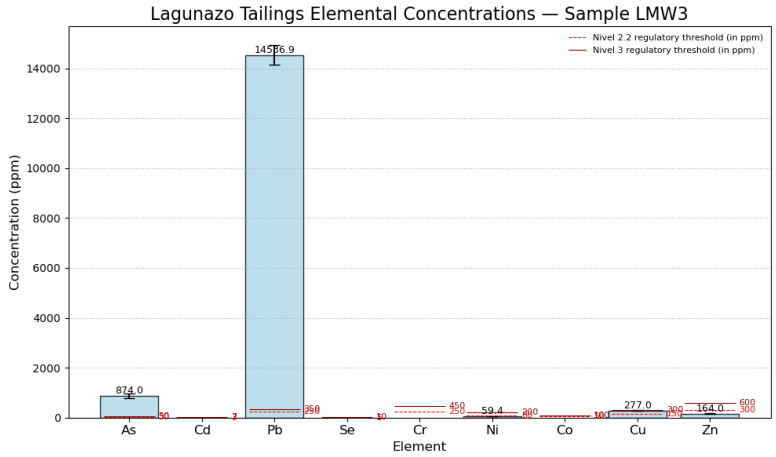



**Figure A.38:** Elemental concentrations for Lagunazo Tailings (sample LMW-3)

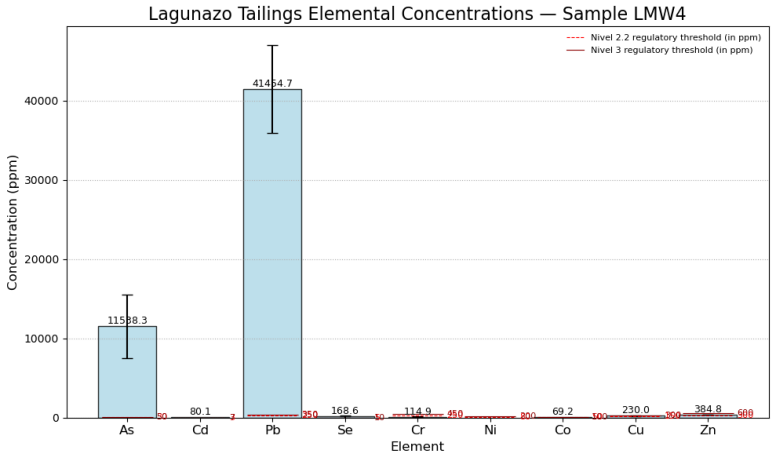



**Figure A.39:** Elemental concentrations for Lagunazo Tailings (sample LMW-4)

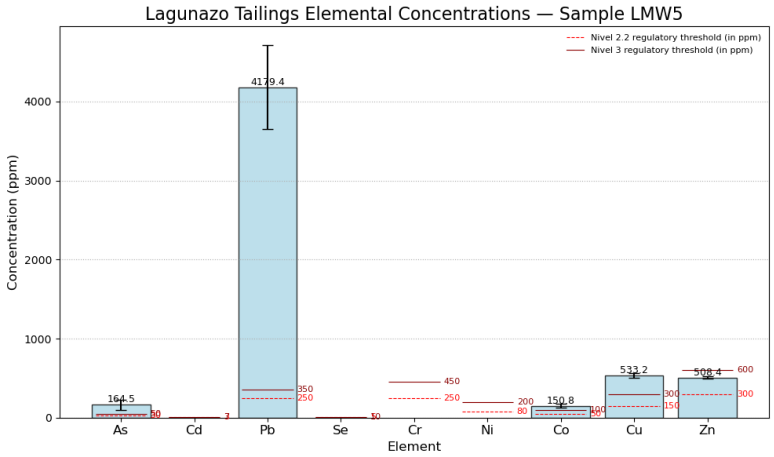



**Figure A.40:** Elemental concentrations for Lagunazo Tailings (sample LMW-5)

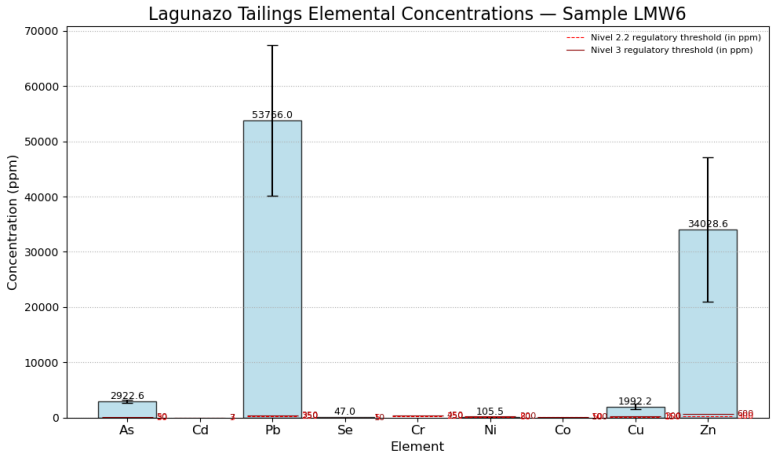



**Figure A.41:** Elemental concentrations for Lagunazo Tailings (sample LMW-6)

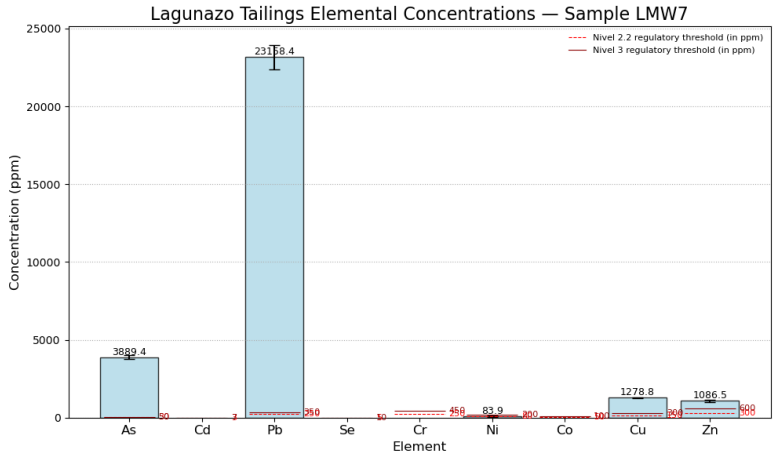



**Figure A.42:** Elemental concentrations for Lagunazo Tailings (sample LMW-7)

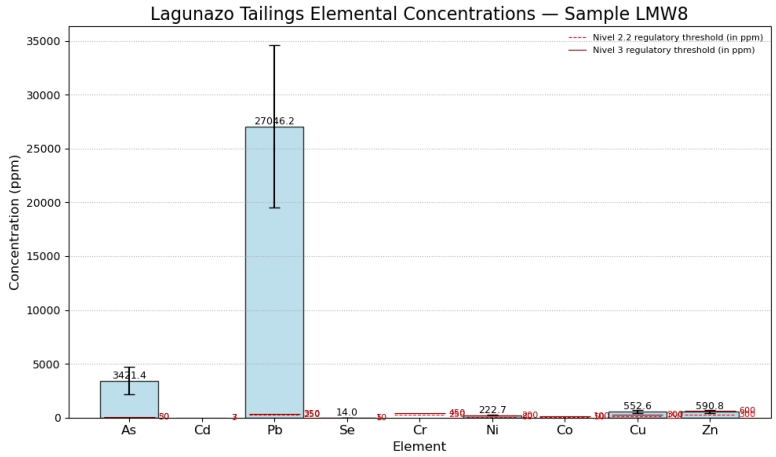



**Figure A.43:** Elemental concentrations for Lagunazo Tailings (sample LMW-8)

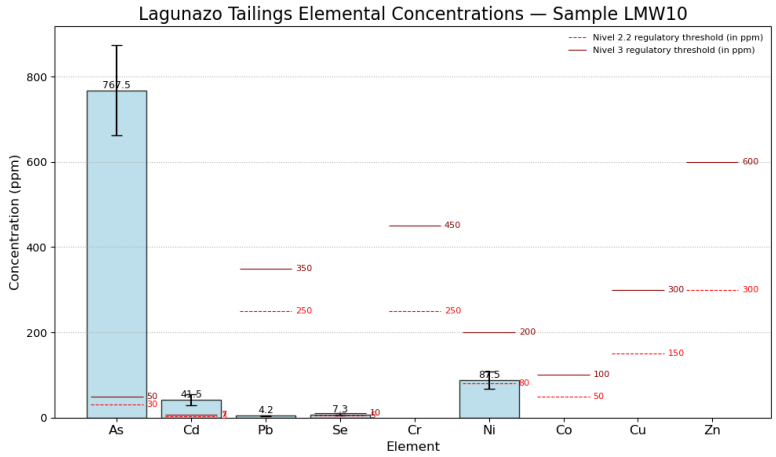



**Figure A.44:** Elemental concentrations for Lagunazo Tailings (sample LMW-10)

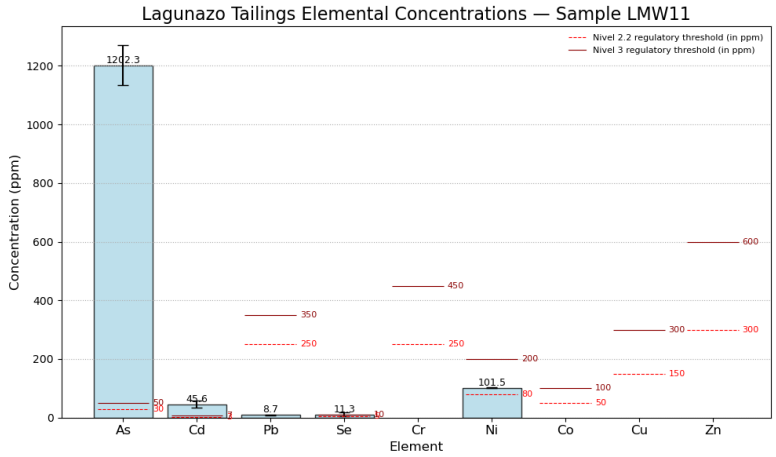



**Figure A.45:** Elemental concentrations for Lagunazo Tailings (sample LMW-11)

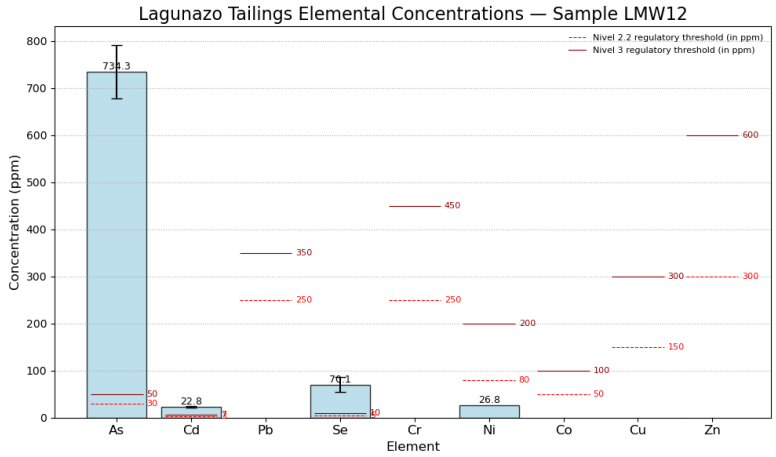



**Figure A.46:** Elemental concentrations for Lagunazo Tailings (sample LMW-12)

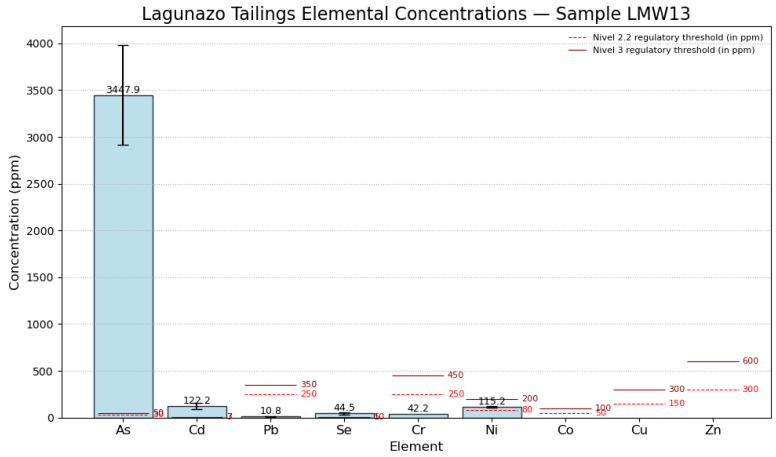



**Figure A.47:** Elemental concentrations for Lagunazo Tailings (sample LMW-13)

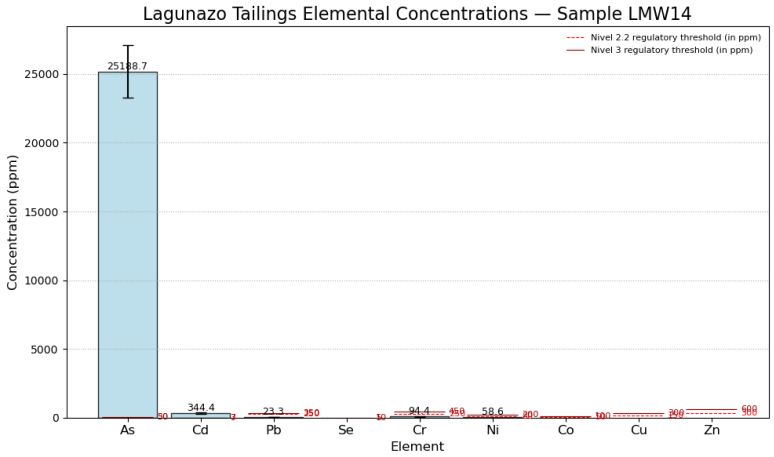



**Figure A.48:** Elemental concentrations for Lagunazo Tailings (sample LMW-14)

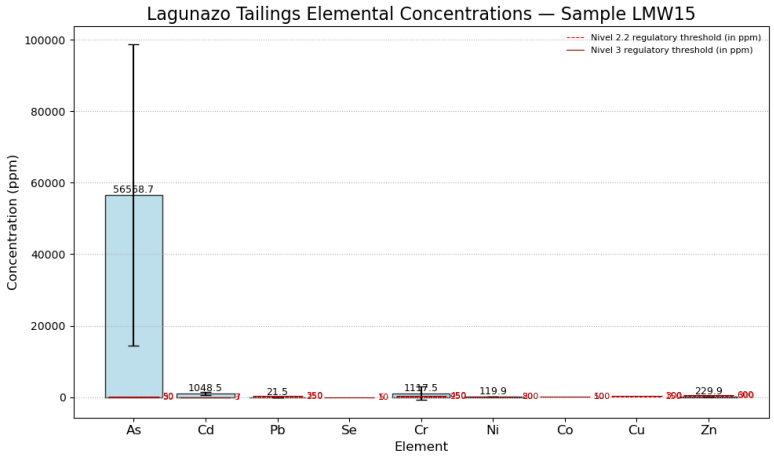



**Figure A.49:** Elemental concentrations for Lagunazo Tailings (sample LMW-15)

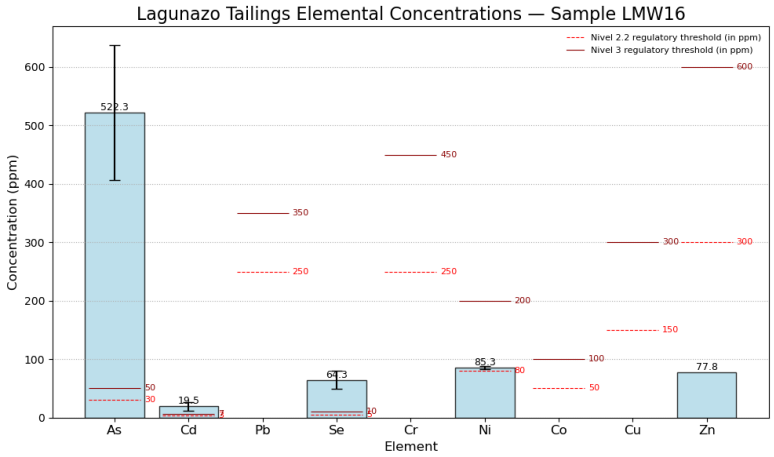



**Figure A.50:** Elemental concentrations for Lagunazo Tailings (sample LMW-16)

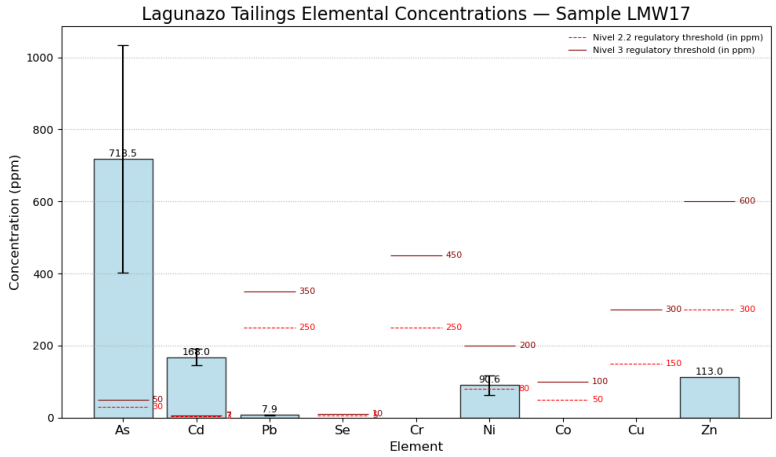



**Figure A.51:** Elemental concentrations for Lagunazo Tailings (sample LMW-17)

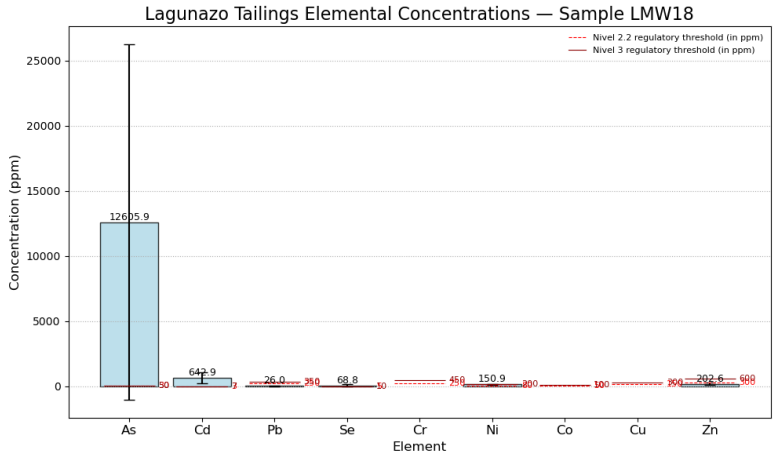



**Figure A.52:** Elemental concentrations for Lagunazo Tailings (sample LMW-18)

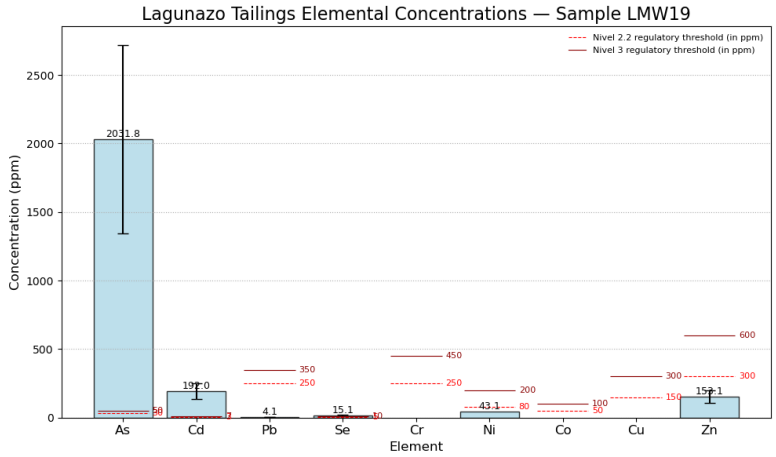



**Figure A.53:** Elemental concentrations for Lagunazo Tailings (sample LMW-19)

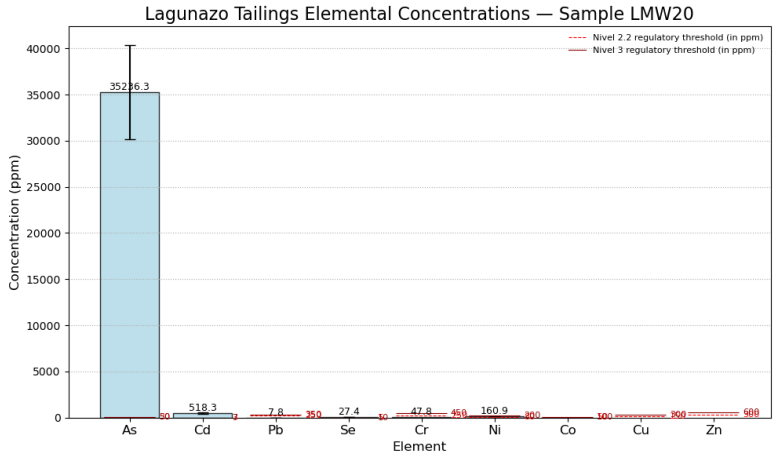



**Figure A.54:** Elemental concentrations for Lagunazo Tailings (sample LMW-20)

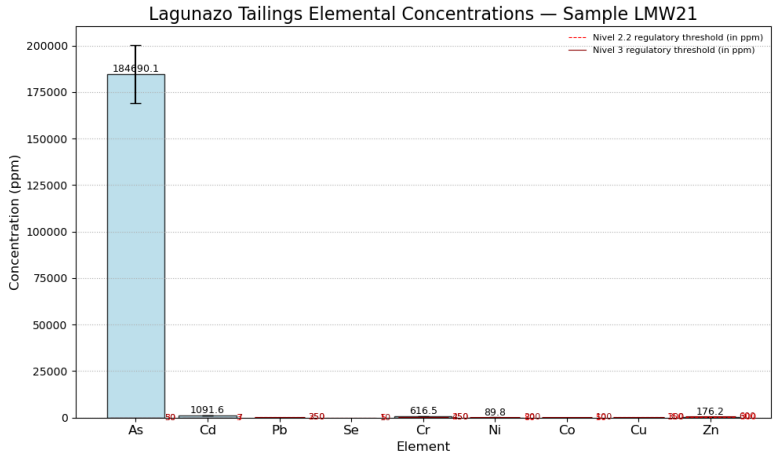



**Figure A.55:** Elemental concentrations for Lagunazo Tailings (sample LMW-21)

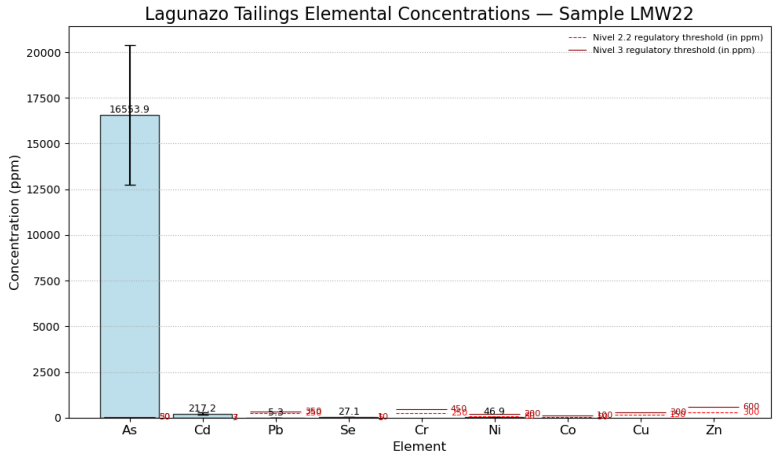



**Figure A.56:** Elemental concentrations for Lagunazo Tailings (sample LMW-22)

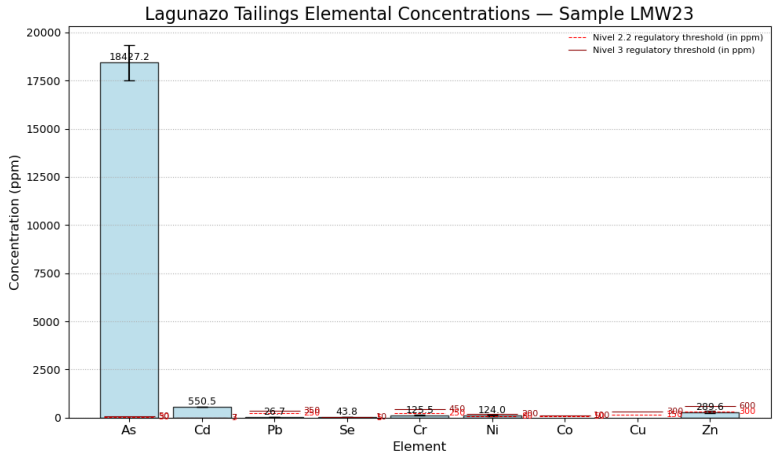



**Figure A.57:** Elemental concentrations for Lagunazo Tailings (sample LMW-23)

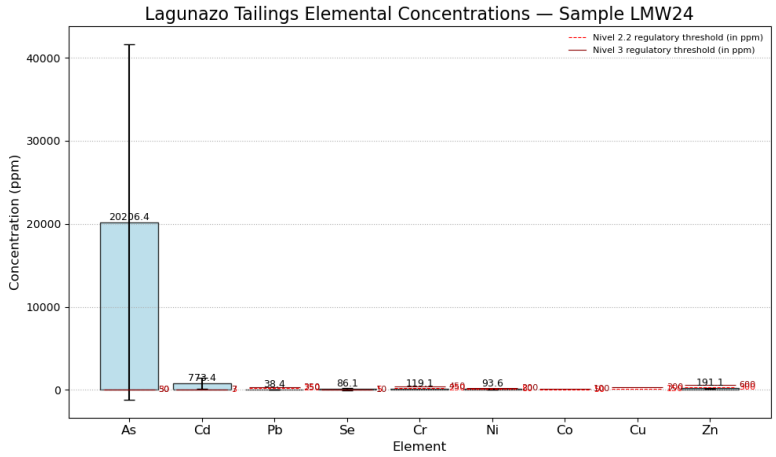



**Figure A.58:** Elemental concentrations for Lagunazo Tailings (sample LMW-24)

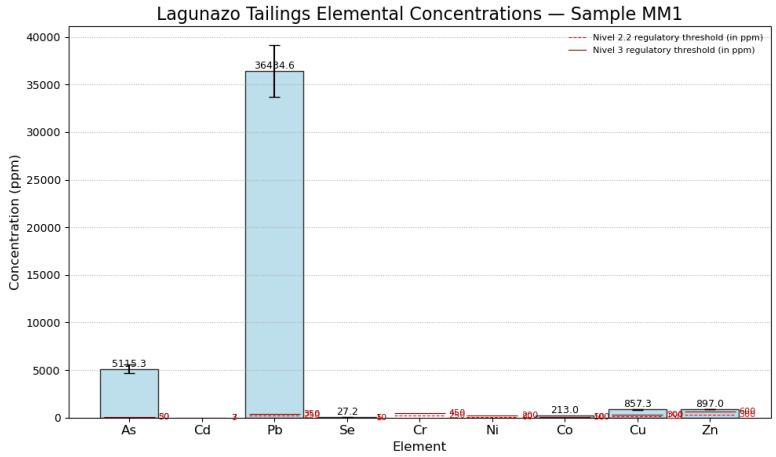



**Figure A.59:** Elemental concentrations for Lagunazo Tailings (sample MM-1)

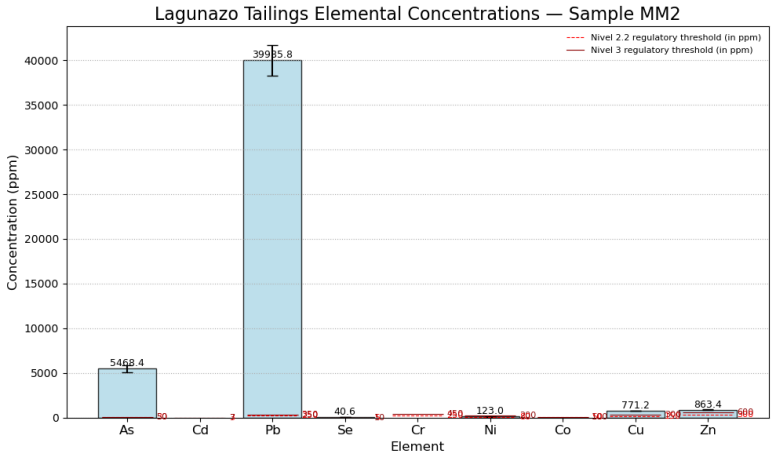



**Figure A.60:** Elemental concentrations for Lagunazo Tailings (MM-2)

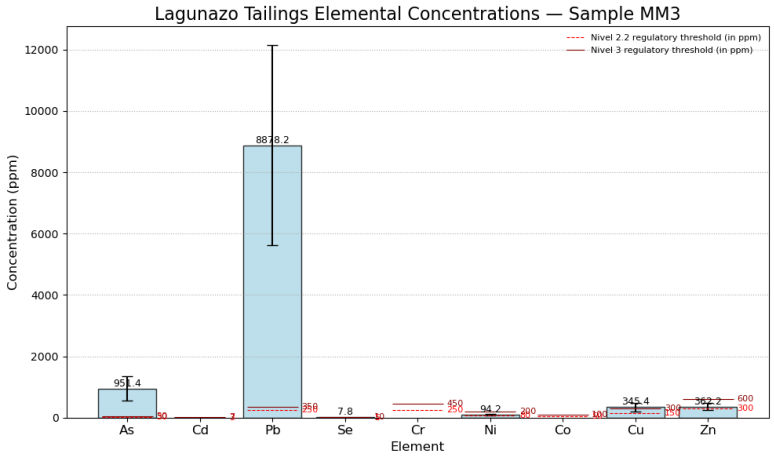



**Figure A.61:** Elemental concentrations for Lagunazo Tailings (MM-3)

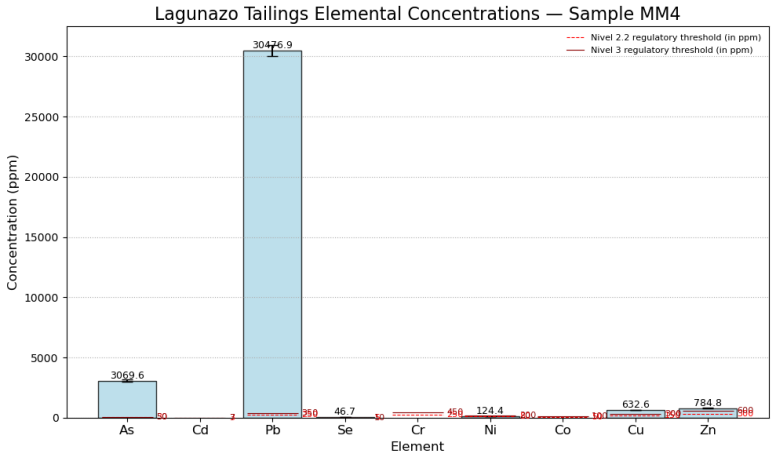



**Figure A.62:** Elemental concentrations for Lagunazo Tailings (MM-4)

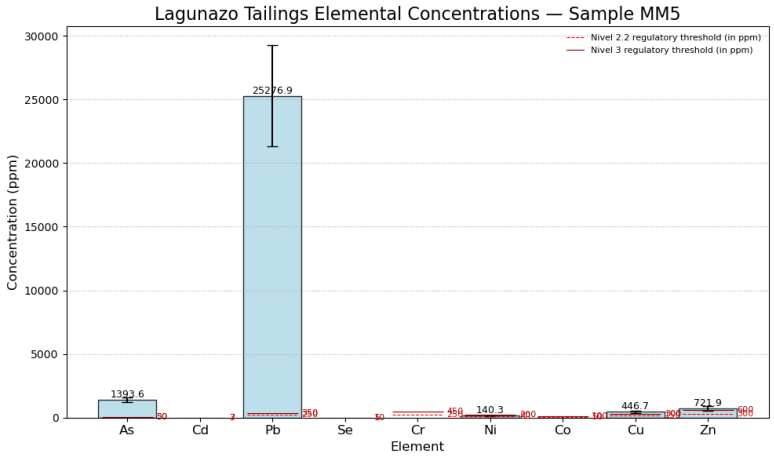



**Figure A.63:** Elemental concentrations for Lagunazo Tailings (MM-5)

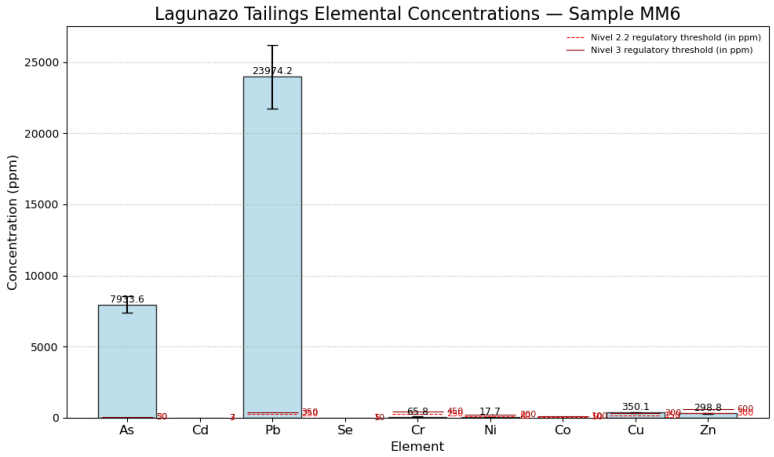



**Figure A.64:** Elemental concentrations for Lagunazo Tailings (MM-6)

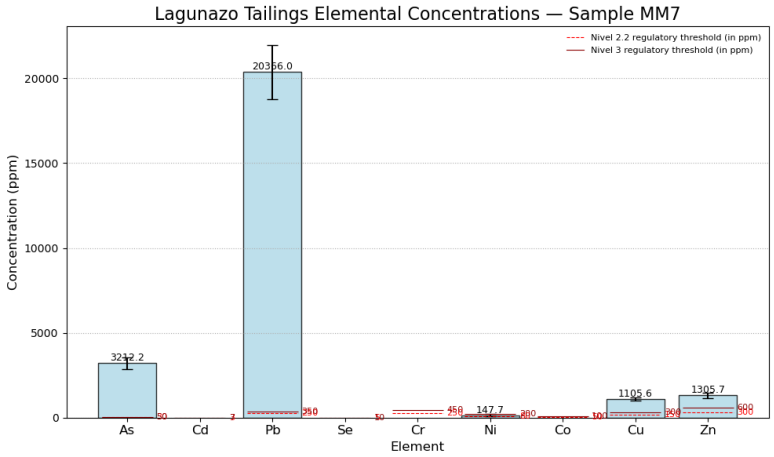



**Figure A.65:** Elemental concentrations for Lagunazo Tailings (MM-7)

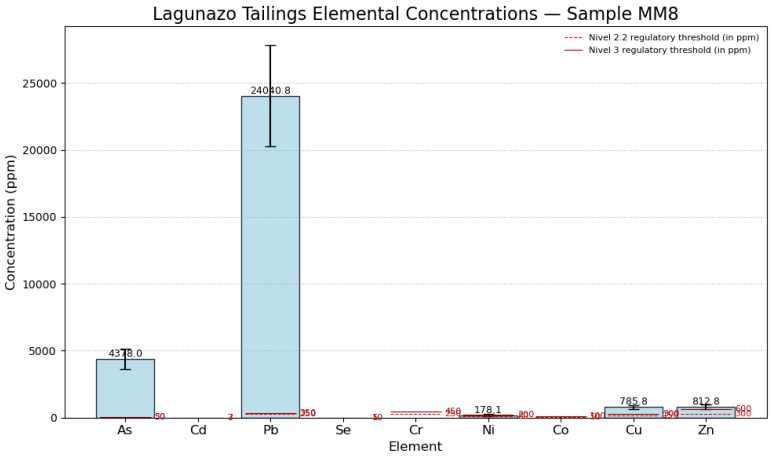



**Figure A.66:** Elemental concentrations for Lagunazo Tailings (MM-8)

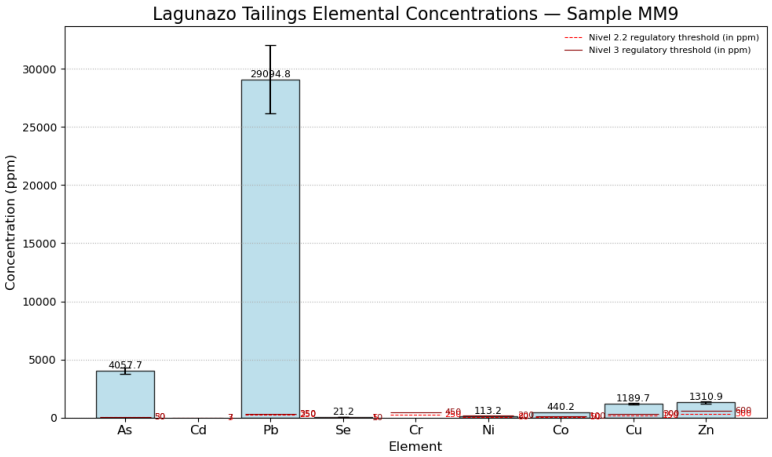



**Figure A.67:** Elemental concentrations for Lagunazo Tailings (MM-9)

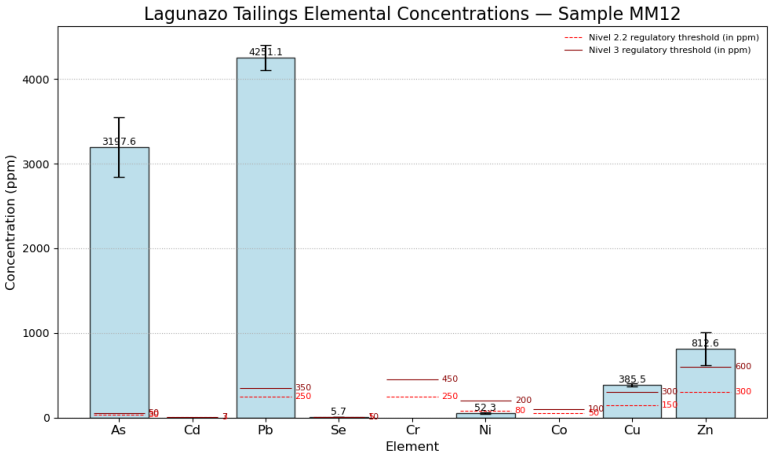



**Figure A.68:** Elemental concentrations for Lagunazo Tailings (MM-12)

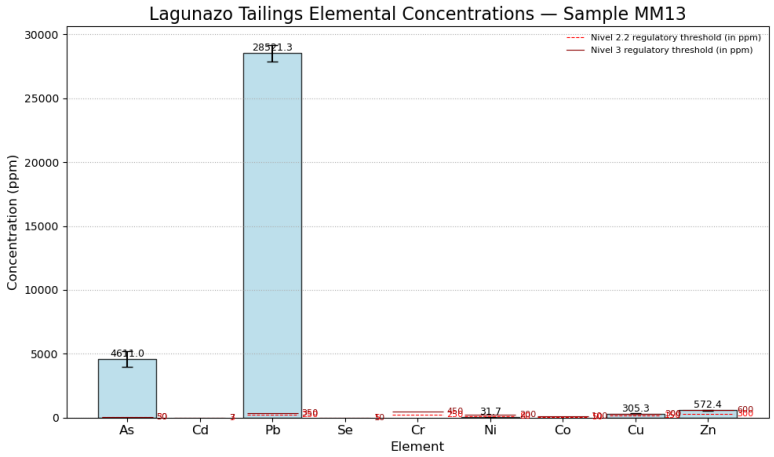



**Figure A.69:** Elemental concentrations for Lagunazo Tailings (MM-13)

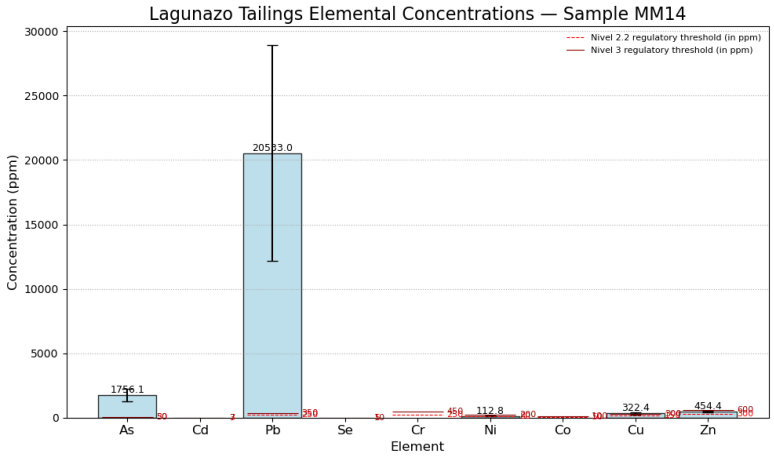



**Figure A.70:** Elemental concentrations for Lagunazo Tailings (MM-14)

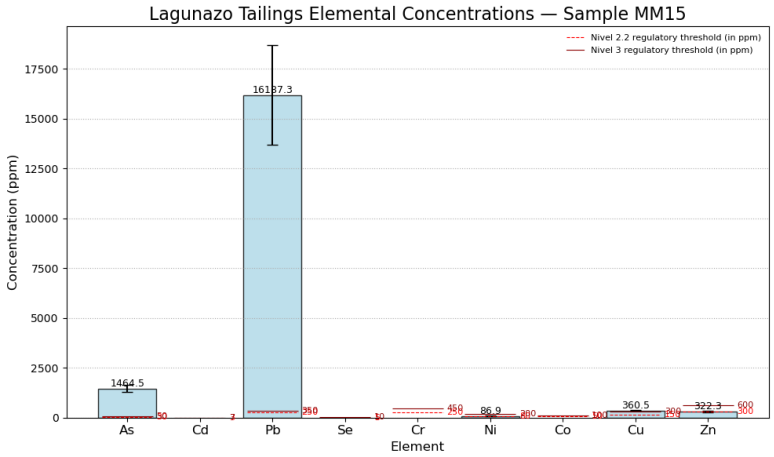



**Figure A.71:** Elemental concentrations for Lagunazo Tailings (MM-15)

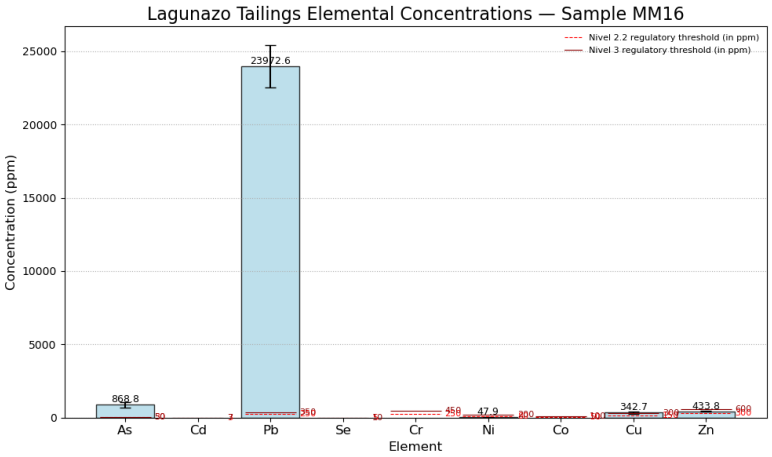



**Figure A.72:** Elemental concentrations for Lagunazo Tailings (MM-16)

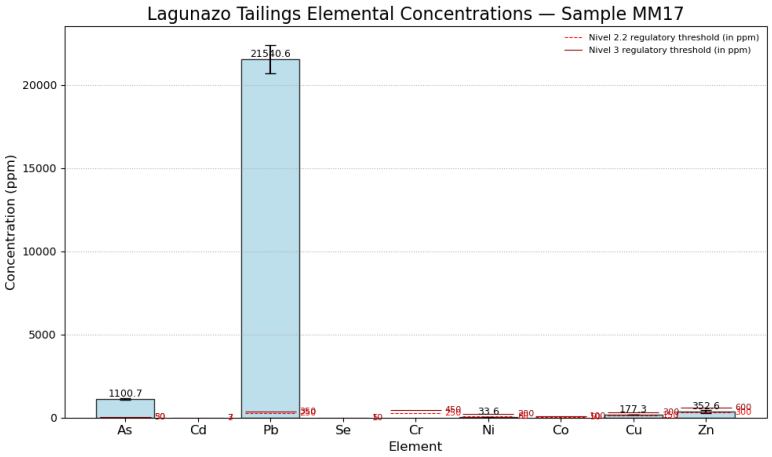



**Figure A.73:** Elemental concentrations for Lagunazo Tailings (MM-17)

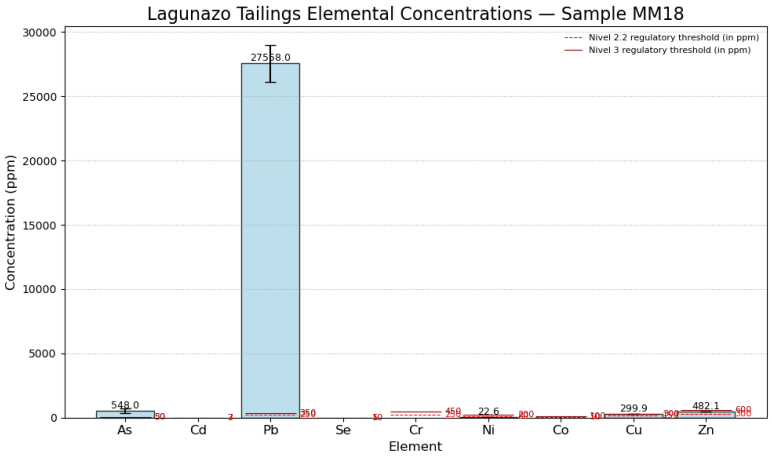



**Figure A.74:** Elemental concentrations for Lagunazo Tailings (MM-18)

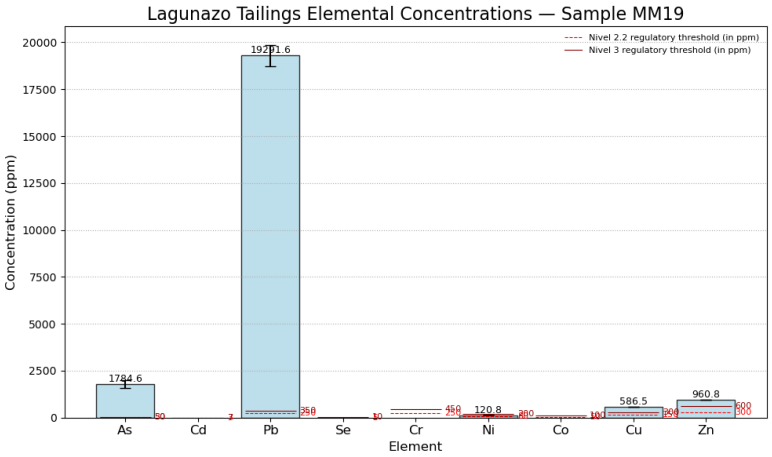



**Figure A.75:** Elemental concentrations for Lagunazo Tailings (MM-19)

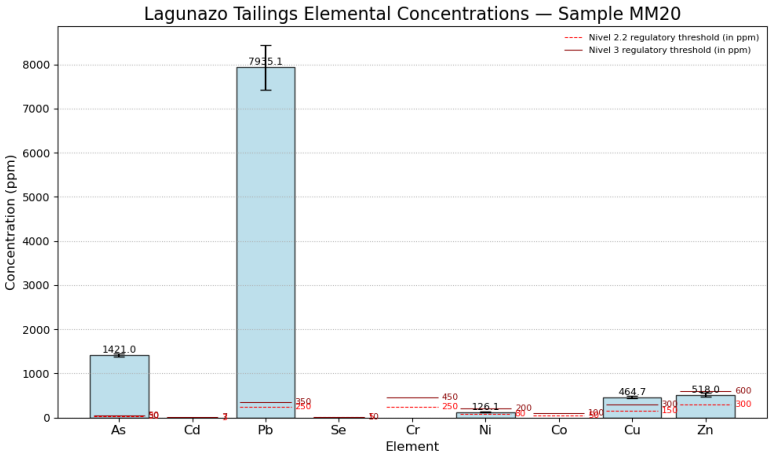



**Figure A.76:** Elemental concentrations for Lagunazo Tailings (MM-20)

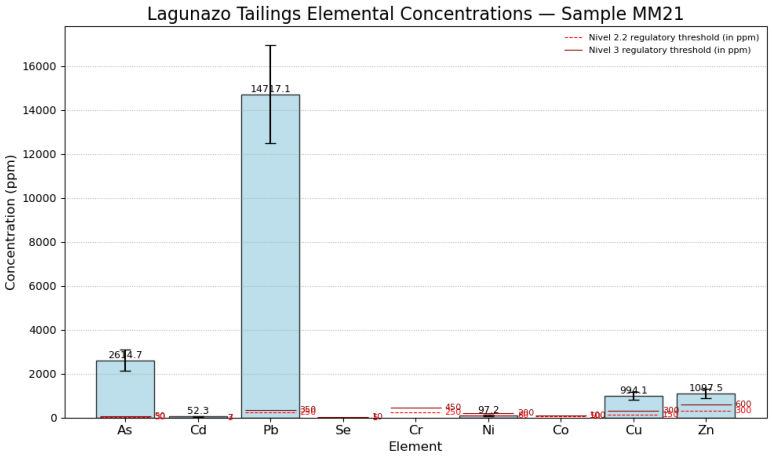



**Figure A.77:** Elemental concentrations for Lagunazo Tailings (MM-21)

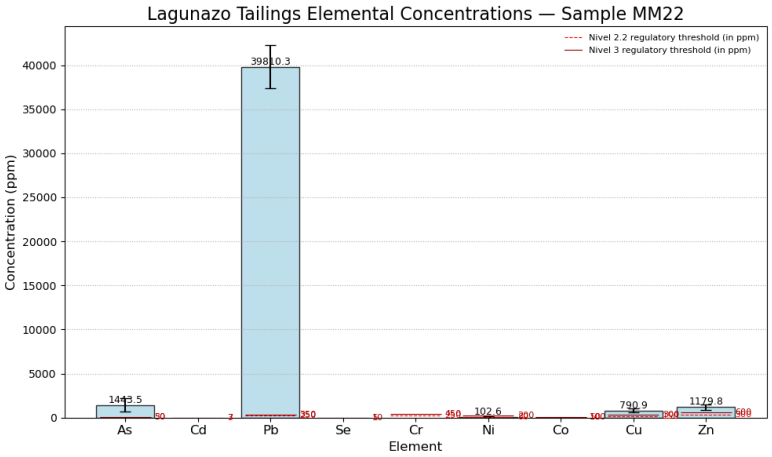



**Figure A.78:** Elemental concentrations for Lagunazo Tailings (MM-22)

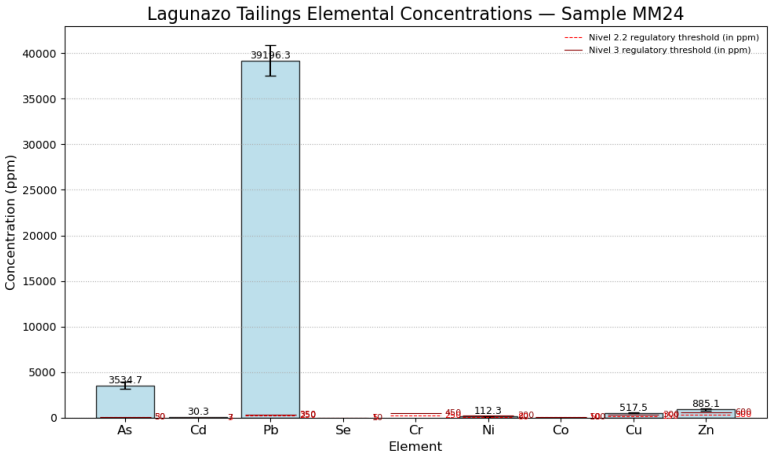



**Figure A.79:** Elemental concentrations for Lagunazo Tailings (MM-24)

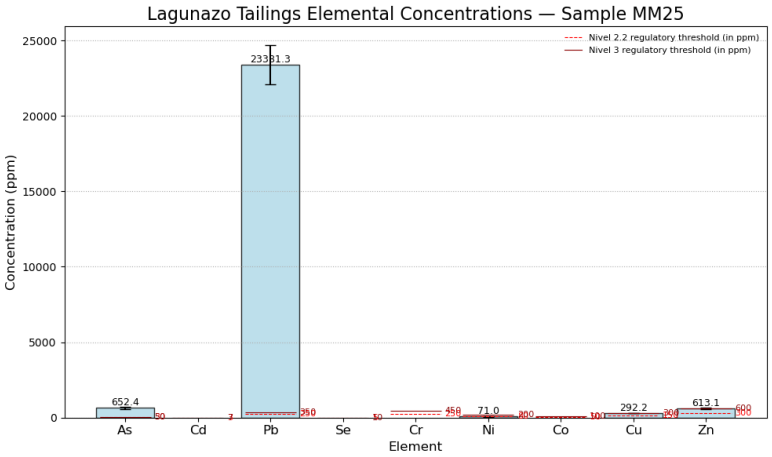



**Figure A.80:** Elemental concentrations for Lagunazo Tailings (MM-25)

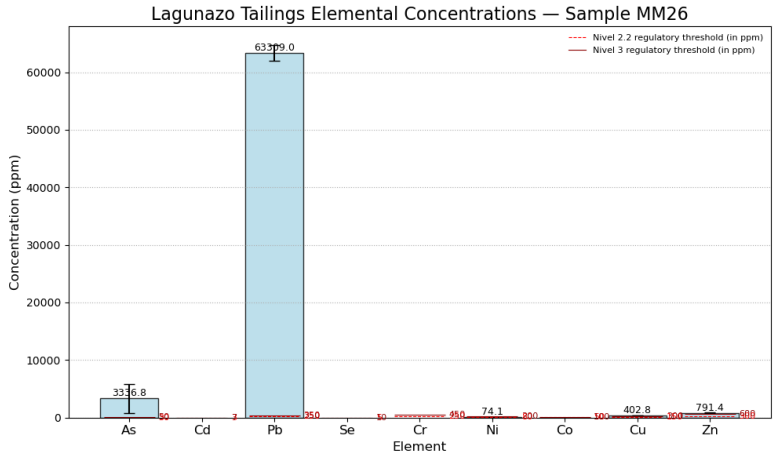



**Figure A.81:** Elemental concentrations for Lagunazo Tailings (MM-26)

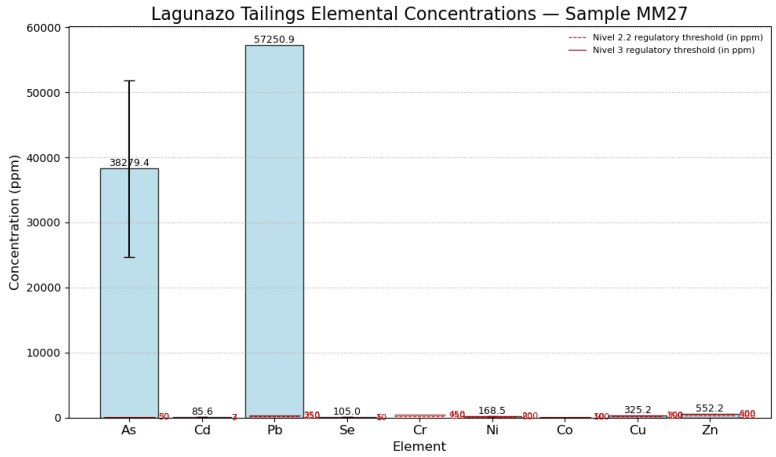



**Figure A.82:** Elemental concentrations for Lagunazo Tailings (MM-27)

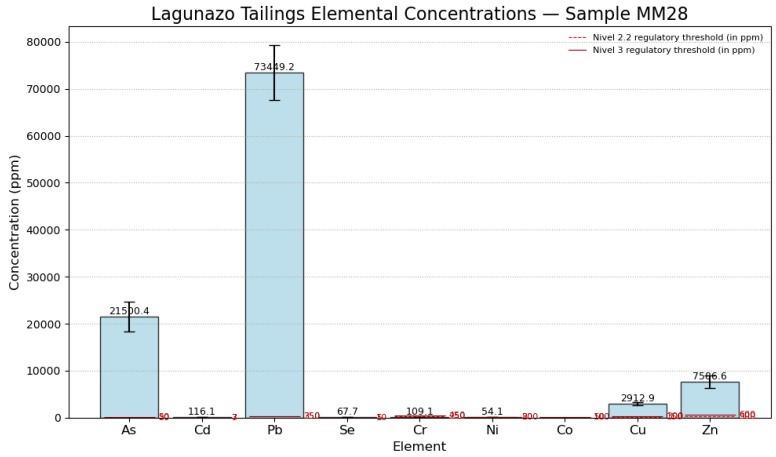



**Figure A.83:** Elemental concentrations for Lagunazo Tailings (MM-28)

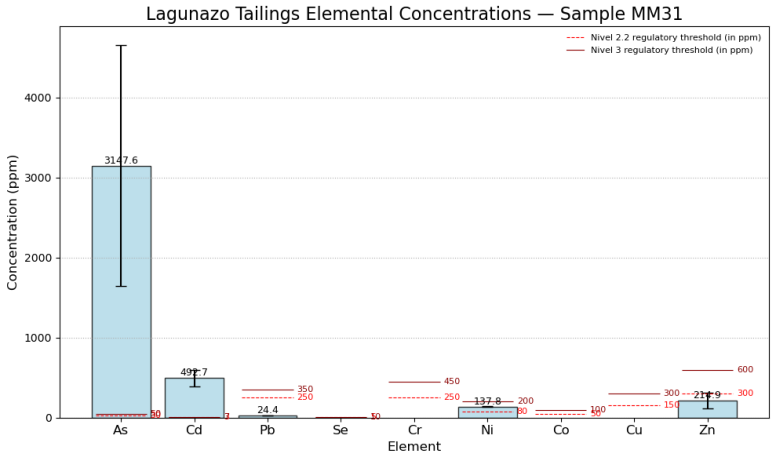



**Figure A.84:** Elemental concentrations for Lagunazo Tailings (MM-31)

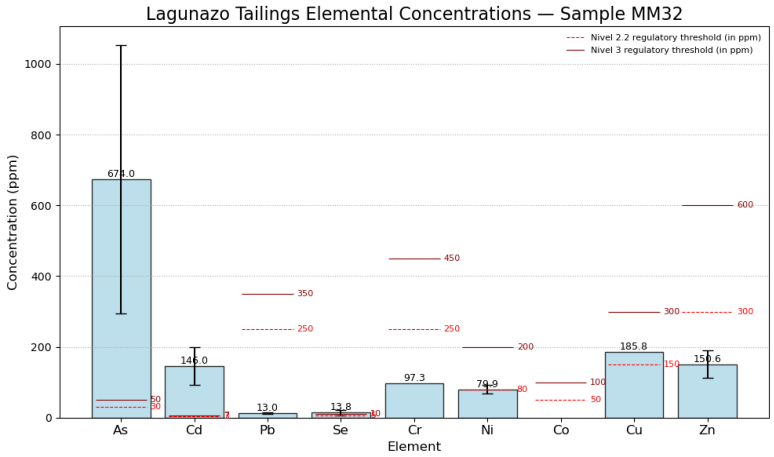



**Figure A.85:** Elemental concentrations for Lagunazo Tailings (MM-32)

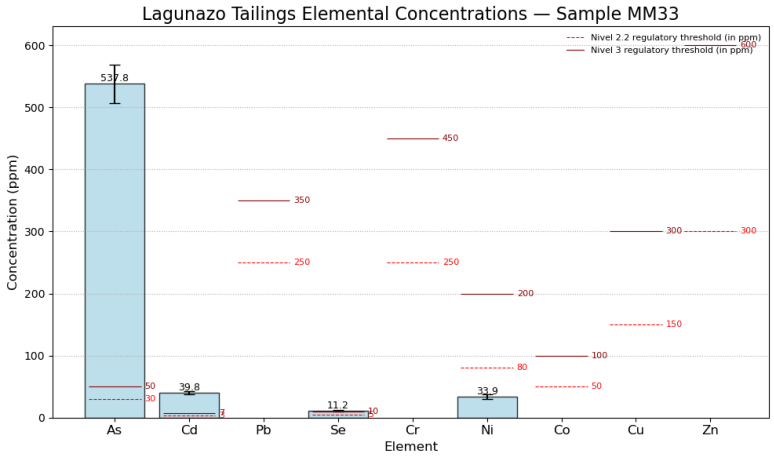



**Figure A.86:** Elemental concentrations for Lagunazo Tailings (MM-33)

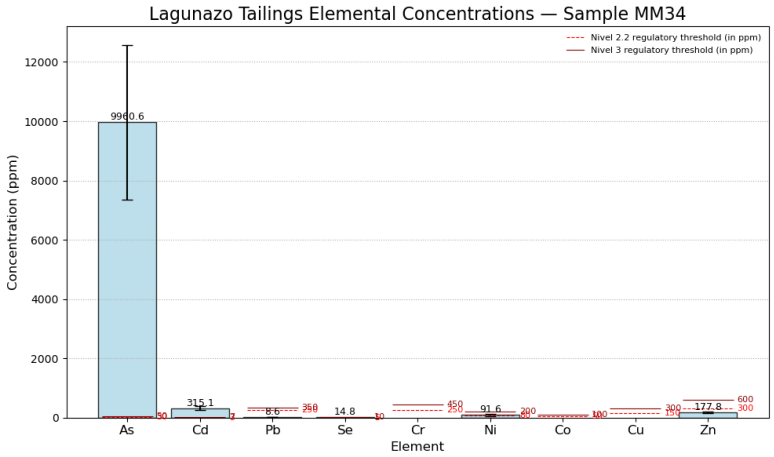



**Figure A.87:** Elemental concentrations for Lagunazo Tailings (MM-34)

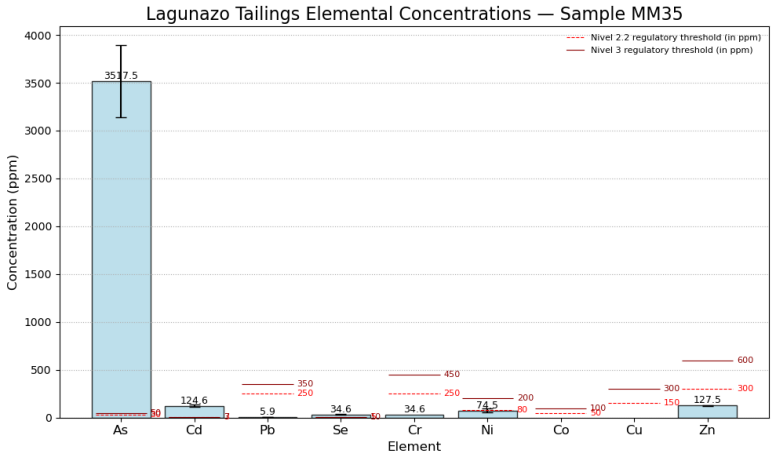



**Figure A.88:** Elemental concentrations for Lagunazo Tailings (MM-35)